Arabidopsis root hair development in adaptation to iron and phosphate supply

D i s s e r t a t i o n

zur Erlangung des akademischen Grades
d o c t o r r e r u m n a t u r a l i u m
(Dr. rer. nat.)
im Fach Biologie

eingereicht an der
Mathematisch-Naturwissenschaftlichen Fakultät I
der Humboldt-Universität zu Berlin

von
Diplom-Biologin Margarete Müller
geboren am 13.7.1973 in Leer

Präsident der Humboldt-Universität zu Berlin
Prof. Dr. Christoph Markschies
Dekan der Mathematisch-Naturwissenschaftlichen Fakultät I
Prof. Dr. Christian Limberg

Gutachter: Prof. Dr. Thomas J. Buckhout
PD Dr. Wolfgang Schmidt

Tag der mündlichen Prüfung: 27. 02. 2007

ABSTRACT

Limitation of immobile nutrients, such as iron (Fe) and phosphate (P), induces the development of additional root hairs that lead to an increase of the absorptive surface of the root. The increased root hair frequency of Fe- and P-deficient Arabidopsis was realized by different strategies. Phosphate-deficient plants increased the number of root hairs while in Fe-starved plants root hairs were branched. The Fe and P starvation responses in plants are thought to be regulated by a systemic signaling mechanism that communicates the nutrient status of the shoot to the root and by a local signaling mechanism that perceives the Fe or P availability in the soil. The influence of local and systemic signals on the respective root hair phenotype was investigated in split-root experiments. This treatment was combined with either a nutrient-sufficient or -deficient shoot. The root hair branching typical of Fe-deficient plants only occured in the presence of both a local and a systemic Fe-deficiency signal. As a consequence, an Fe sufficiency signal acted dominantly to any deficiency signal, independent of its origin. The increased number of root hairs in P-deficient plants, conversely, was activated through either a local or a systemic P deficiency signal. Thus, the P deficiency signal acted dominantly to any sufficiency signal. To determine, which stage of root hair development was influenced by iron and phosphate, mutants with defects in different stages of root hair development were investigated for their root hair phenotype. Mutants affected in the early stages of root hair development, such as specification, displayed marked changes in the number and localization of root hairs. However, the nutritional signal was perceived and translated in this group of mutants. This indicates that the specification genes are involved in the nutrient-sensitive root hair formation, but may not be the direct targets. Early cell characteristics of root hairs in the late meristematic region of the root, like the expression of marker genes, were unaltered in plants adapted to Fe or P deficiency. This suggested the nutritional signal modulates root hair development after these characteristics have been established. Mutants with defects in the later stages of root hair development, such as root hair elongation, showed short or deformed root hairs in the proper position and frequency and were, thus, impaired independent of the Fe or P supply. Thus, the nutritional signal may enter the root hair developmental pathway around the stage of root hair initiation and bulge formation. Finally, six mutants were screened that did not form root hairs under P deficiency but developed normal, when the plants were transferred to P-sufficient medium. One of these mutants, *per2* (*phosphate deficiency root hair defective2*), was characterized phenotypically and genetically. In addition to the impaired root hair growth, the *per2* mutant displayed a constitutively high lateral root number and accumulated an increased amount of anthocyanins under P starvation. Epistatic analysis revealed that *per2* action is independent of early cell specification genes. The *per2* mutation was mapped to a 87.6 kbp region on the upper arm of chromosome 3 containing 19 genes. The *per2* phenotype has not been described before. Thus, *PER2* is a potential new gene involved in root hair development under phosphate deficiency.

ZUSAMMENFASSUNG

Pflanzenwurzeln reagieren auf Phosphat- oder Eisenmangel mit einer vermehrten Wurzelhaarbildung, was eine Vergrößerung der absorptiven Oberfläche bewirkt. Die erhöhte Anzahl an Wurzelhaaren wird dabei auf verschiedene Weise gebildet. Phosphat-defiziente Arabidopsis-Pflanzen erhöhen die Anzahl an Wurzelhaarzellen, während sich unter Eisenmangel verzweigte Wurzelhaare entwickeln. Die Fe- und P-Homöostase wird durch systemische und lokale Signalwege reguliert. Der Einfluss dieser Signale auf die Fe- bzw. P-sensitive Wurzelhaarentwicklung wurde mithilfe von *split-root*-Experimenten untersucht, die mit einem systemischen Mangel- oder Suffizienzsignal kombiniert wurden. Die Verzweigung der Wurzelhaare Fe-defizienter Pflanzen wurde durch ein dominantes Suffizienzsignal reprimiert, unabhängig von seiner lokalen oder systemischen Herkunft. Die Erhöhung der Wurzelhaarzahl bei P-Mangelpflanzen wurde durch ein dominantes Defizienzsignal induziert. Um herauszufinden, welches Entwicklungsstadium von dem jeweiligen Nährstoff beeinflusst wird, wurden Mutanten mit Defekten in frühen und späten Wurzelhaarentwicklungsstadien untersucht. Mutanten mit beeiträchtigter Wurzelhaar-Spezifikation wichen in ihrer Wurzelhaarzahl und –lokalisation vom Wildtyp ab, zeigten aber eine Fe- oder P-sensitive Veränderung. Die Gene aus frühen Entwicklungsstadien sind demnach essentiell für die Reaktion, sind aber nicht das direkte Ziel der Mangelsignale. Frühe Zelleigenschaften in der meristematischen Region waren durch die Eisen- oder Phosphatverfügbarkeit nicht verändert, was darauf hindeutet, dass die Wurzelhaarbildung erst in einem späteren Entwicklungsstadium durch die Nährstoffe beeinflusst wird. Mutanten mit Defekten in späteren Entwicklungsstadien zeigten kurze oder verformte Wurzelhaare unabhängig von der Nährstoffversorgung. Das Fe- oder P-Signal mündet also vor der Wirkung dieser Komponenten in die Wurzelhaarbildung ein. Das heisst, nachdem die korrekte Wurzelhaar-Position und -Anzahl in Anpassung an das Fe- oder P-Angebot festgelegt wurde, werden die Wurzelhaare unter allen Wachstumsbedingungen von einer gemeinsamen Maschinerie elongiert. Zur Identifikation potentiell neuer Gene, die die Wurzelhaarbildung in Anpassung an P-Mangel regulieren, wurden sechs Mutanten isoliert, die keine Wurzelhaare bei P-Mangel bilden, aber nach dem Transfer auf P-suffizientes Medium nicht beeinträchtigt waren. Eine dieser Mutanten, *per2*, wurde phänotypisch und genetisch charakterisiert. Neben der veränderten Wurzelhaarbildung zeigte *per2* auch eine konstitutiv erhöhte Lateralwurzelbildung und eine erhöhte Anthozyan-Akkumulation bei P-Mangel. Laut epistatischen Analysen gehört die *per2* Mutante zu einem Signalweg, der unabhängig von frühen Zellspezifikationsgenen wirkt. Der *per2*-Locus wurde innerhalb eines 87,5 kpb großen Abschnittes auf dem oberen Arm von Chromosom 3 kartiert. Mutanten die einen *per2*-ähnlichen Phänotyp zeigen, wurden bisher nicht beschrieben. Daher handelt es sich bei *PER2* möglicherweise um ein neues Gen, das die Wurzelhaarbildung bei Phosphatmangel reguliert und weitere P-Mangelreaktionen beeinflusst.

TABLE OF CONTENT

INTRODUCTION

A single rye plant possesses a root surface of about 640 square metres (Dittmer 1937). During limitation of immobile nutrients, such as iron (Fe) and phosphate (P), plants increase their root surface by the development of extra root hairs to achieve an improved mobilization and uptake of the respective nutrient. In this work, root hair development adapted to phosphate and iron deficiency has been investigated. In this process, root hair formation is linked to iron and phosphate homeostasis.

1.1 Iron homeostasis in plants

As a transition metal, iron is able to change its oxidation state, making it an important component of biological redox systems such as photosynthesis or the respiratory chain. Although iron is the fourth most abundant element in the lithosphere (http://www.matpack.de/Info/Nuclear/Elements/lithosphere.html), under aerobic conditions it is poorly available for plants, because Fe^{3+} is highly insoluble due to precipitation of iron hydroxide or iron phosphate. In anaerobic environments (e.g. in waterlogged soils) the concentration of the soluble Fe^{2+} increases. When Fe^{2+} is taken up in excess, it is toxic, because it reduces oxygen into superoxide radicals that generate hydrogen peroxide. In the Fenton reaction, hydroxyl radicals are produced. The hydroxyl radicals cause lipid peroxidation and other, non-selective, oxidative damage (Marschner 1995). Thus, in living organisms iron is chelated and its homeostasis underlies a strict regulation (Schmidt 1999, 2003, Hell & Stephan 2003).

Acquisition and uptake of iron from the soil

A visible iron deficiency symptom is an interveinal chlorosis in young leaves, as several steps of chlorophyll synthesis depend on iron (Marschner 1995). For improved iron mobilization and uptake, a variety of physiological and morphological adaptation reactions have evolved. Morphological changes of the root system inducible by a low Fe availability are an enhanced lateral root development and an increased number of root hairs (Moog *et al.* 1995, Pinton *et al.* 1998, Landsberg 1996, Schmidt 1999). Also root tip swellings were observed (Landsberg 1996). In legume or Proteaceen species, proteoid roots, which are dense clusters of short laterals with a high root hair density, develop in response to a low Fe supply (White & Robson 1989, Arahou & Diem 1997). According to López-Bucio *et al.* (2003), the main processes affecting the overall root system architecture are the primary root meristem activity leading to changes in the primary root length, lateral root formation, which increases the exploratory capacity of the root system, and the development of additional root hairs, which increases the surface area of the root. The Fe-deficiency-responsive formation of rhizodermal transfer cells, which have labyrinth-like cell wall inversions, in a variety of species increases the apoplast-symplastic surface area if the root (Kramer *et al*. 1980, Schmidt 1999).

Iron uptake is accompanied by an acidification of the rhizosphere by members of the H^+-ATPase gene family. The lowering of the pH increases iron hydroxide solubility and proton extrusion energizes the membrane for uptake (Marschner 1995, Schmidt 1999, Palmgren 2001). Furthermore, phenolics like piscidic acid and alfafuran, organic acids, mainly citrate and malate, and riboflavin are secreted during Fe starvation. These substances serve as iron chelators, antimicrobial agents, or provide electrons for Fe^{3+} reduction and contribute to iron acquisition (Marschner 1995, Schmidt 1999, Abadía *et al.* 2002, Ae *et al*. 1990, Masaoka *et al*. 1993, Landsberg 1986, Susín *et al*. 1993).

In dicots, Fe depletion induces a reduction-based iron uptake system in the root consisting of a ferric-chelate reductase and a high-affinity iron transporter, referred to as strategy I (Römheld 1987). Strategy II is confined to grasses and is characterized by enhanced release of phytosiderophores, which derive from the precursor nicotianamine (NA) and form stable complexes with Fe^{3+}. These complexes are taken up by a specific transporter identified as the oligopeptide transport protein ZmYS1 (YELLOW STRIPE1; Römheld & Marschner 1986, Curie *et al*. 2001). Strategy I and II are not mutually exclusive since the transporter and the reductase are present also in rice roots (Schmidt 2006).

The gene responsible for the reductase activity in strategy I plants is *FRO2* (*FERRIC-CHELATE REDUCTASE/OXIXASE2*) belonging to the superfamily of flavocytochromes in Arabidopsis and its ortholog *FRO1* in pea (Robinson *et al.* 1999, Waters *et al.* 2002). *FRO1* mRNA is localized in the rhizodermis, cortex, and vascular cylinder of the root and in the mesophyll and parenchyma of the leaf (Waters *et al*. 2002). In Arabidopsis, eight FRO genes exist that are expressed differently in all plant organs and are predicted to function on different subcellular membranes (Mukherjee *et al*. 2006).

The main transporter of strategy I plants is the ZIP metal transporter *IRT1* (*IRON REGULATED TRANSPORTER1*; Eide *et al.* 1996, Eckhardt *et al.* 2001, Cohen *et al*. 2004). *IRT1* and *FRO2* are induced under Fe deficiency and are coregulated (Connolly *et al*. 2003, Vert *et al*. 2003). IRT1 is repressed at the protein level by Fe (Connoly *et al.* 2002). It is localized in the plasmalemma of the rhizodermis, cortex, and anthers (Vert *et al*. 2002).

Iron release into the xylem and long-distance transport through the xylem

After iron has entered the rhizodermis, the main chelator of Fe^{2+} in the symplast is the ubiquitous aminoacid nicotianamine (NA, Hell & Stephan 2003, Stephan *et al.* 1996, von Wirén *et al.* 1999). During Fe starvation, nicotianamine synthase is strongly upregulated in the root (Wintz *et al*. 2003). Radial transport of Fe^{2+}-NA from the rhizodermis to the xylem vessels takes place on a symplasmic route (Stephan *et al.* 1996). Immunolabeling showed that NA is deposited mainly in the vacuoles of root stelar cells (Pich *et al*. 1997). In the iron-overaccumulating pea mutants *brz* (*bronze*) and *dgl* (*degenerated leaflets*), vacuolar NA is increased suggesting a function of NA also in detoxification of excess iron (Pich *et al*. 2001).

Xylem-loading occurs mainly in the xylem parenchyma; it is regulated independently from the uptake into the rhizodermis and cortex (Marschner 1995). Long-distance transport via the xylem occurs as an Fe^{3+}-citrate complex (Tiffin 1966, Pich *et al*. 1994, López-Milán *et al*. 2000), meaning a reoxidation of the iron when released into the xylem. So far, no ferroxidase has been described in higher plants, but Herbik *et al*. (2002) showed that the multicopper ferroxidase-like protein FLP participates in high-affinity iron uptake of *Clamydomonas,* whose iron uptake mechanism involves a reductive step as for strategy I plants (Eckhardt & Buckhout 1998).

Efflux of citrate into the apoplast for Fe^{3+} chelation is catalyzed by FRD3 (FERRIC REDUCTASE DEFECTIVE3), a member of the multidrug and protein efflux family (MATE), which is able to transport citrate (Rogers & Guerinot 2002, Durrett *et al*. 2006). Mutation of *FRD3* leads to ferric iron precipitates in the root vascular cylinder and leaf apoplast and to a decreased iron content within the leaf cells (Delhaize 1996, Green & Rogers 2004). FRD3 functions root-specific and is expressed in the pericycle and the vascular cylinder (Green & Rogers 2004).

The plasma membrane Fe^{2+}-NA transporter AtYSL2 (YELLOW STRIPE-LIKE2) is expressed in the endodermis, pericycle, and most strongly in the xylem parenchyma of the root and shoot (DiDonato *et al*. 2004, Schaaf *et al*. 2005). The function of YSL2 is not entirely clear. Because xylem parenchyma cells play a key role in ion secretion into the xylem and in the reabsorption of ions from the xylem sap along the pathway to the shoot (Marschner 1995), the localization of AtYSL2 indicates a function in one of these processes. AtYSL2 is repressed by Fe deficiency (DiDonato *et al*. 2004, Schaaf *et al*. 2005). The oligopeptide transporter OPT3, which shares sequence similarities with YSL2, is increased in roots of Fe-starved plants. OPT3 transports iron, independent of the presence of NA (Wintz *et al*. 2003).

The natural resistance-associated macrophage protein *NRAMP1* transports Fe^{3+} and is, together with *NRAMP3* and *NRAMP4*, induced in the roots of Fe-deficient Arabidopsis. *NRAMP2* is upregulated under iron sufficient conditions (Curie *et al*. 2000, Thomine *et al*. 2000). NRAMP3 and NRAMP4 are located in the tonoplast of the vascular tissues of roots and shoots suggesting an involvement in long-distance transport (Thomine *et al*. 2003). In the *nramp3nramp4* double mutant, iron is not mobilized from vacuolar globoids, indicating a function of NRAMPs in the export of iron from vacuolar metal pools under iron starvation (Lanquar *et al*. 2005).

The vacuolar iron transporter VIT1 is involved in sequestration of iron into vacuoles. *VIT1* is expressed throughout the plant independent of the iron availability but most strongly in seeds. In wildtype embryos, iron is concentrated in the provascular strands of the cotyledons, hypocotyls, and radicle, which is abolished in *vit1* (Kim *et al*. 2006).

Iron uptake by leaf cells, iron storage, and phloem-transport into sink organs

After the iron has reached the leaf apoplast, uptake by leaf cells depends on the reduction of iron, most likely catalyzed by members of the FRO family (Mukherje *et al*. 2006). Also photoreduction has been observed (Brown *et al.* 1979). Chelation of Fe^{2+} by NA within the leaf cells is supported by the fact that the NA-deficient tomato mutant *chloronerva* reveals iron precipitates along the veins and a permanent interveinal chlorosis rescued by exogenous NA application (Scholz 1989). The chlorosis indicates a lack of mobile iron within the intercostal mesophyll. Cloning of *chloronerva* revealed that the mutated gene encodes nicotianamine synthase (Ling *et al*. 1999).

About 80% of the leaf iron is located in the chloroplasts (Smith 1984). The major iron storage component in the plant is the protein phytoferritin (Briat *et al*. 1999). Ferritin has ferroxidase activity and consists of a hollow sphere containing an iron phosphate core (Wade *et al*. 1993, van Wuytswinkel *et al*. 1995, Harrison & Arosio 1996). Ferritin accumulates mainly in the non-green plastids of roots and shoots and is induced by iron excess (Lobréaux & Briat 1991). The transmembrane protein PIC1 (PERMEASE IN THE INNER ENVELOPE OF CHLOROPLASTS1) is located in the plastids and mediates iron transport. *pic1* mutants only grow heterotrophically and are chlorotic and dwarf, indicating that PIC1 may be important for iron transport into the plastids (Duy *et al*. 2006).

Translocation of iron from the leaf cells to sink organs depends on symplastic transport via plasmodesmata and the phloem, since meristems and newly developing organs do not have complete xylem structures (Hell & Stephan 2003). Evidence for the symplastic iron transport was provided by Zhang *et al*. (1995), as radioactive iron fed to the xylem did not directly reach the shoot apex but after remobilization from older leaves.

In the phloem sap, iron is predominantly in the Fe^{3+} state (Maas *et al*. 1988), meaning a further oxidation of the iron when released into the phloem. As an iron chelator involved in long-distance transport via the phloem, the small iron transport protein ITP belonging to the family of dehydrins has been isolated. ITP specifically binds Fe^{3+} in *vitro* and transports iron in *vivo* (Krüger *et al*. 2002). The iron in sink organs like beech nuts and young growing tissues is again in the form of Fe^{2+}-NA (Kristensen & Larsen 1974, Stephan *et al*. 1990, 1994, Pich *et al*. 1994). Thus, phloem unloading of Fe^{3+}-ITP to Fe^{2+}-NA must involve iron reduction. Possible candidates catalyzing this process are members of the FRO gene family (Mukherjee *et al*. 2006).

The Fe^{2+}-NA transporter *AtYSL1* is expressed in the xylem parenchyma of leaves, pollen, and in young silique parts (Le Jean *et al*. 2005). The seeds of the *ysl1* mutant contain less iron and nicotianamine. Thus, YSL1 seems to be crucial for iron loading into sink organs. Hell and Stephan (2003) speculated that NA could have a shuttle function in phloem unloading. In pea seeds, ferritin is the major iron storage component (Marentes & Grusak 1998). Figure 1 summarizes the path of iron through dicotyl plants.

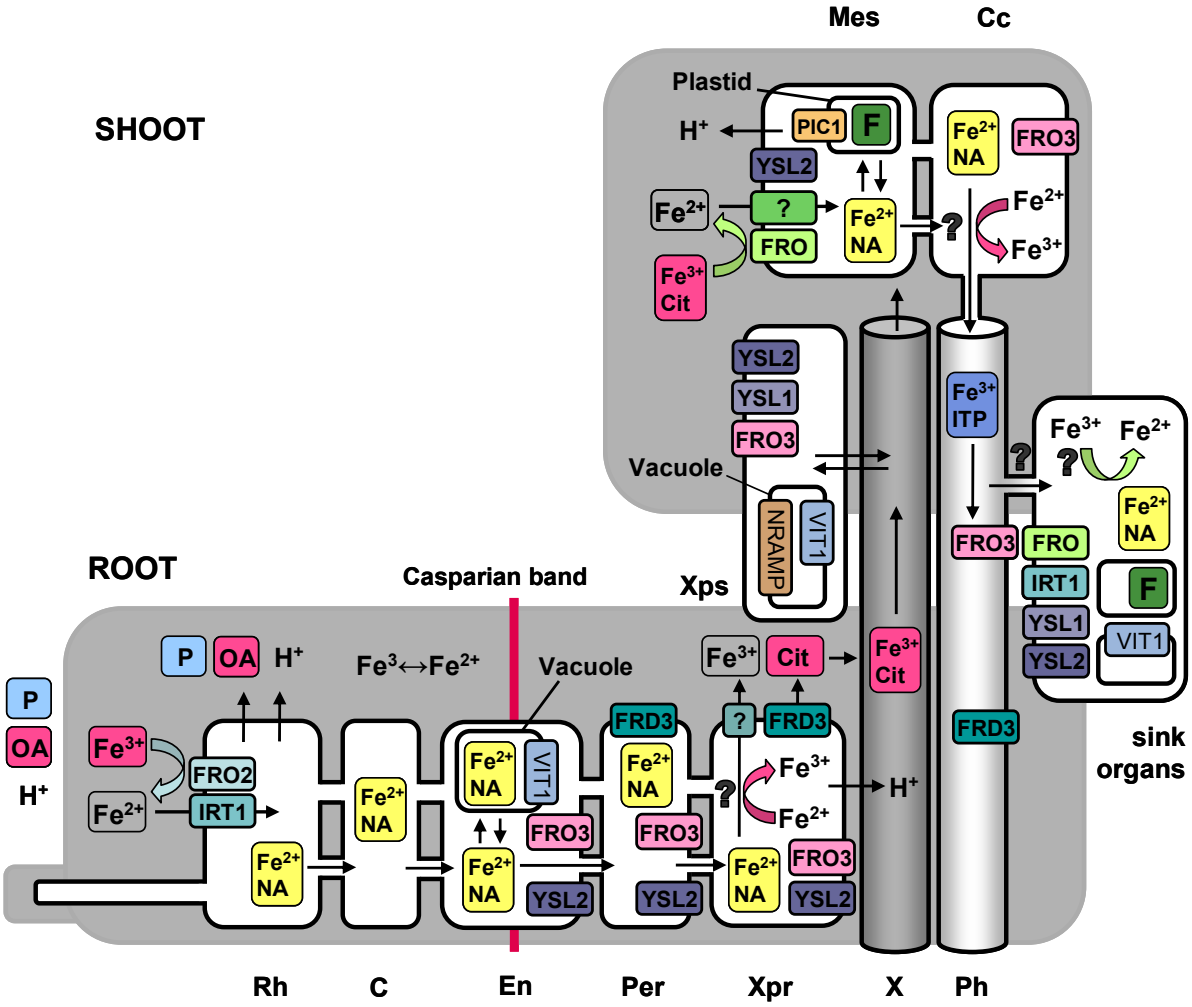

Figure 1: A model for iron transport through dicotyl plants. The apoplast is marked in grey, the symplast in white. Iron uptake starts in the rhizodermis (Rh). The Fe^{3+} ions are mobilized by the secretion of phenolics (P), organic acids (OA), and protons (H^+) into the rhizosphere. Free or chelated iron diffuses or precipitates within the apoplastic space and is detained by the casparian band. Uptake into the rhizodermal cells takes place after reduction of Fe^{3+} chelates by FRO2 through IRT1. Inside the root cells, iron is chelated by NA and reaches the cortical (C), endodermal (En), pericycle (Per) and xylem parenchyma cells of the root (Xpr) via the symplastic way through plasmodesmata. NA accumulates in the vacuoles of the endodermis. VIT1 mediates iron sequestration into vacuoles. Xylem loading is mainly accomplished by the xylem parenchyma. The main iron transport species within the xylem is Fe^{3+} citrate. A prerequisite for xylem transport of iron is the excretion of citrate (Cit) into the apoplast catalyzed by FRD3. For the reoxidation of iron during the transfer from Fe^{2+}-NA towards Fe^{3+} citrate, no molecular component has been identified so far. It is not clear, whether the iron is oxidized before or after release into the apoplast. *FRO3* and *YSL2* are induced in the endodermis, pericycle, and the xylem parenchyma cells of root (Xpr) and shoot (Xps), but their function is unknown. From their localization, a role in xylem loading or exchange processes along the pathway to the shoot could be assumed. The vacuolar metal transporter NRAMP also occurs in the shoot xylem parenchyma and may be involved in the remobilization of iron from vacuolar iron pools. After release of Fe^{3+} citrate into the leaf apoplast, iron uptake by the leaf cells again depends on *FRO* action. An acidification of the apoplast is also important. The symplastic transport within the leaf cells again occurs as Fe^{2+}-NA. Transport into plastids is mediated by PIC1. The main iron storage component in plastdis is ferritin that has ferroxidase activity. Phloem transport towards sink organs mainly occurs in the Fe^{3+} state, probably bound to ITP. Phloem parenchyma is not shown; it expresses *FRD3* and *FRO3*. The loading of iron into sink organs is not well understood. A function of Fe^{2+}-NA as the transport form within the cells would comprise a further reduction step catalyzed by *FRO* gene family members. IRT1, YSL1, and YSL2 are found in sink organs. An important iron storage component within seeds beneath NA is ferritin.

Regulation of iron homeostasis

An important mediator regulating the strategy I and the morphological adaptations to Fe deficiency is the bHLH protein FER, also designated as FRU (FER-LIKE REGULATOR OF IRON UPTAKE) or FIT (FE-DEFICIENCY INDUCED TRANSCRIPTION FACTOR, Jacoby *et al*. 2004, Colangelo & Gueriot 2004). *FER* was initially cloned from tomato (Ling *et al*. 2002). The *fer* mutant is chlorotic and fails to induce ferric-chelate reductase activity or *FRO2* and *IRT1* transcription (Brown *et al*. 1971, Ling *et al*. 2002). Homozygous *fru* or *fit* knock-outs of Arabidopsis reveal the same phenotype and have reduced iron content (Jacoby *et al*. 2004, Colangelo & Guerinot 2004). The expression of 72 out of 179 iron-regulated genes depend on FIT (Colangelo & Guerinot 2004). Grafting experiments revealed that *FER* acts root-specific (Brown *et al*. 1971). In the late meristematic region of tomato roots, FER is located in the nucleus of the rhizodermis and outer cortical cell layers. In the mature root hair zone FER transcripts were found in the vascular cylinder between the xylem and the phloem poles (Brumbarova & Bauer 2005, Ling *et al*. 2002). In Arabidopsis, *FRU* shows a similar expression pattern (Jacoby *et al*. 2004). This implies that in addition to controlling the uptake from the soil, *FER/FRU/FIT* also might regulate xylem-loading or long-distance transport within the root. FER/FRU/FIT shows highest expression in response to iron deficiency at the transcriptional and posttranscriptional level and is down-regulated at generous iron supply (Jacoby *et al*. 2004, Colangelo & Guerinot 2004, Brumbarova & Bauer 2005). Since *FER/FRU/FIT* is controlled by iron, the iron status is sensed upstream of FER action (Brumbarova & Bauer 2005). *FIT* overexpressers had no obvious phenotype, which led Colangelo & Guerinot (2004) to conclude the protein levels are not altered in these lines or an additional factor is necessary for regulation of the target genes.

Auxin and ethylene are assumed to be involved in the iron-deficiency-responsive induction of transfer cells and extra root hairs, because application of either hormone mimics the morphological Fe-deficiency phenotype, and Fe starvation increases the synthesis of auxin and ethylene (Landsberg 1984, 1996, Schmidt & Bartels 1996, Schmidt *et al*. 2000, Römheld & Marschner 1986, Romera *et al*. 1999). Pharmacological inhibition of ethylene synthesis or action represses the Fe stress syndrome (Romera & Alcántara 1994). Auxin transport inhibitors or ethylene inhibitors suppress root hair development of iron sufficient or deficient Arabidopsis. Auxin- or ethylene-insensitive mutants were not able to produce root hairs in the presence or absence of Fe (Schmidt & Schikora 2001). Because auxin can enhance ethylene production, it is supposed the impact of auxin on the morphological Fe deficiency responses could be mediated through ethylene (Yu & Yang 1979, Kim *et al*. 1992, Romera *et al*. 2006).

Linking of iron homeostasis to the homeostasis of other nutrients

In Fe-starved Arabidopsis, Thimm *et al*. (2001) showed a transcriptional induction of several primary metabolism enzymes. α-amylase and glycolysis enzymes are upregulated in the

shoot, whereas citrate cycle, respiration, and fermentation are induced in the root, indicating that triosephosphates are mobilized beyond photosynthesis yield in the shoot and are sent towards the root to supply the need for energy and reduction equivalents. Anaplerotic sequences are increased in the root fitting with the excretion of organic acids (Thimm *et al*. 2001).

Several components involved in iron homeostasis also bind other transition metals as listed in Table 1. Therefore, iron homeostasis is linked with the homeostasis of other transition metals.

Table 1: Affinity of several components involved in iron homeostasis to divalent metals other than iron.

Component	Substrates	Reference
FRO	Fe, Cu, Mn	Norvell *et al*. 1993, Welch *et al*. 1993
IRT1	Fe, Zn, Mn, Co, Cd	Rogers *et al*. 2000
NRAMP	Fe, Cu, Zn, Mn	Thomine *et al*. 2000, 2003
NA	Fe, Zn, Mn, Cd	Stephan *et al*. 1996
YS1	Fe, Cu, Zn, Mn, Ni, Cd	Schaaf *et al*. 2004
PIC1	Fe, Cu	Duy *et al*. 2006
VIT1	Fe, Mn	Kim *et al*. 2006

Phosphate strongly chelates iron, in the soil as well as in the plant (Marschner 1995). To that effect, phosphate starvation increases iron accumulation involving ferritin expression, which marks iron excess. High phosphate supply induces *IRT1* transcription normally induced by iron deficiency. This interaction leads to a mutual impact of iron and phosphate homeostasis (Hirsch *et al*. 2006).

1.2 Phosphate homeostasis in plants

Phosphate is required in the range of 0.3-0.5% of the plant dry matter for optimal growth. In cells, it occurs as phosphate ester or an anhydride bond, which are stable, but can also easy be hydrolysed. These properties make phosphate be an important structural element in nucleic acids and phospholipids and play a central role in energy metabolism and regulatory phosphorylation. The high phosphate demand of plant cells stands in contrast to the low P availability of the most soils. Although abundant, phosphate is highly immobile because of strong interactions with Fe, Ca, Al, and organic compounds (Marschner 1995, Raghothama 1999). Therefore, plants have evolved various strategies for P acquisition from the soil and internal remobilization of phosphate (Raghothama 1999, Raghothama & Karthikeyan 2005, Poirier & Bucher 2002, Franco-Zorrilla *et al*. 2004, Hammond *et al*. 2004, Ticconi & Abel 2004).

Acquisition of phosphate from the soil

In more than 80% of all land plants, phosphate acquisition by roots is accomplished by mycorrhiza, a symbiosis formed by plant roots with soil fungi from the order Glomeromycota. The fungus provides the plant with nutrients from the soil, mainly phosphate, in exchange for photosynthetic carbohydrates (Karandashov & Bucher 2004). The fungal mycelium increases the explored soil volume. In non-mycorrhizal plants, extension of P depletion zones is closely related to root hair length, whereas in mycorrhizal plants, P depletion zones by far exceed the root hair cylinder (Marschner 1995). Based on fossil data, mycorrhiza is even thought to be a precondition for colonization of land by the first terrestrial plants (Karandashov & Bucher 2004, Wellmann *et al*. 2003).

Apart from mycorrhiza, an improved soil exploration is achieved by restructuring root system architecture. Under phosphate starvation, root biomass increases, thereby, in relation to the shoot, which is consistent with the transport carbohydrate and phosphate from the shoot towards the root (Marschner 1995, Jeschke *et al*. 1996, 1997, Raghothama 1999, Forde & Lorenzo 2001). In P-starved Arabidopsis, primary root growth is reduced caused by a shift from an indeterminate to a determinate developmental program due to loss of meristematic cells (Williamson *et al*. 2001, Linkohr *et al*. 2002, Sánchez-Calderón *et al*. 2005). Primary root growth inhibition is accompanied by an increase in the number and length of laterals (Bates & Lynch 1996, Williamson *et al*. 2001, Linkohr *et al*. 2002). Nacry *et al*. (2005) observed contrasting effects of P starvation on lateral root formation with a strong inhibition of primordia initiation combined with a marked stimulation of their activation. The latter was also described by López-Bucio *et al*. (2005). In bean, soybean, and pea, adventitious rooting occurs. In addition, the angle of the root growth becomes more horizontal representing a gravitropic response. The production of this shallower root system under P stress is termed 'topsoil foraging', since P availability is normally highest near the soil surface (Bonser *et al*. 1996, Lynch & Brown 2001). Using a geometric model, Ge *et al*. (2001) calculated a reduction of inter-root competition within the same plant by topsoil foraging.

In P-deficient rape, spinach, tomato, Arabidopsis, and barley, the root surface is increased by the formation of additional root hairs that are also elongated (Foehse & Jungk 1983, Bates & Lynch 1996, Gahoonia & Nielsen 1997). In addition, root hairs of P-starved plants initiate closer to the meristem (Ma *et al*. 2003). Phosphate-sensitive root hair elongation is the result of both, an increased growth rate and growth duration (Bates & Lynch 1996). Root hairs are the major site of phosphate uptake (Gahoonia & Nielson 1998). Arabidopsis mutants with short or no root hairs revealed a lower P accumulation under P limitation than wildtype plants (Bates & Lynch 2000). Phosphate efficient Arabidopsis accessions have more and longer root hairs and higher root penetration abilities than inefficient types indicating the importance of explorative root morphology for P acquisition (Narang *et al*. 2000). Also the development of transfer cells under P shortage has been described (Schikora & Schmidt 2002). A massive

increase of the root surface area is achieved by the development of cluster (proteoid) roots in Proteaceae, legumes, and other families (Lamont 2003).

Cluster roots exudate high amounts of citrate, malate, and oxalate, which exchange phosphate from Fe, Al, and Ca salts (Gardner *et al*. 1983, Grierson 1992). Excretion of organic acids for P acquisition also occurs in species without cluster root formation (Lipton *et al*. 1987). For refilling the citrate cycle, phospho*enol*pyruvate carboxylase is induced (Pilbeam *et al*. 1993, Johnson *et al*. 1996). The importance of citrate exudation is demonstrated in Arabidopsis overexpressing citrate synthase that shows an improved growth under P limitation (Koyama *et al*. 2000). Phosphate-efficient Arabidopsis accessions secret more organic acids than inefficient ones (Narang *et al*. 2000). A phosphate starvation-inducible MATE is suggested as a potential candidate for organic acid secretion (Vance *et al*. 2003).

Piscidic acid and alfafuran are secreted for solubilization of P from iron salts (Marschner 1995). Under P limitation, the rhizosphere is acidified, which is attributed to the H^+-ATPase activity. The pH decrease can dissolve P from Ca phosphate and is important for phosphate uptake (Moorby *et al*. 1988, Yan *et al*. 2002).

To mobilize P from organic components, hydrolytic enzymes are secreted into the rhizosphere. Among these are acid phosphatases with low substrate specifity that are induced by P deficiency (Ueki 1978, Lefebvre *et al*. 1990, Duff *et al*. 1991). Acid phosphatase enzyme activity is correlated with synthesis of acid phosphatase mRNA and protein (del Pozo *et al*. 1999, Miller *et al*. 2001). In addition, phosphate is remobilized within P-deficient plants, which is achieved by induction of at least one specific intracellular phosphatase in the vacuole (Duff *et al*. 1991). In Arabidopsis, three purple acid phosphatases are inducible by low P (del Pozo *et al*. 1999, Li *et al*. 2002).

Further hydrolytic enzymes induced upon P starvation are extracellular RNases (Nürnberger *et al*. 1990, Löffler *et al*. 1992). The RNase genes *RNS1* and *RNS2* are upregulated in P-deficient Arabidopsis, but also during senescence. From putative signal sequences, excretion into the extracellular matrix and rhizosphere for P mobilization from the soil and recycling within the plant is presumed (Taylor *et al*. 1993, Bariola *et al*. 1994). An extracellular cyclic nucleotide phosphodiesterase together with the other nucleolytic enzymes enables the complete utilization of P from nucleotides (Abel *et al*. 2000). Arabidopsis grown with DNA as the only P source showed normal biomass production, indicating an excretion of DNase (Chen *et al*. 2000).

Phosphate transport

Phosphate uptake is driven by a proton gradient generated through activity of an H^+-ATPase and takes place as proton symport (Ullrich-Eberius *et al*. 1984, Sakano 1990, Muchhal *et al*. 1997). In plants, phosphate transporters are grouped into three families, Pht1, Pht2, and Pht3 (Rausch & Bucher 2002). They belong to major facilitator superfamily, which occurs

ubiquitously and transports small solutes along chemiosmotic gradients (Raghothama 1999, Pao *et al*. 1998). High-affinity phosphate transporters (Pht1) have been identified in many species (Muchhal *et al*. 1996, Smith *et al*. 1997, Kai *et al*. 1997, Leggewie *et al*. 1997). The Pht1 family in Arabidopsis consist of nine members that are differentially expressed in root and shoot tissues (Mudge *et al*. 2002). Pht1;1-4 are induced by low P in the rhizodermis, preferentially in root hairs, and in the cortex. Pht1;1 and Pht1;4 play a significant role in P acquisition since the *pht1;1pht1;4* double mutants show a 75% reduction in P uptake capacity even under sufficient P supply (Shin *et al*. 2004). The Pht1 high-affinity transporters take up phosphate from the apoplast into the symplast during acquisition from low-P soil as well as during long-distance transport, uptake into leaf cells, and remobilization processes within the plant in the course of the life-cycle and under P limitation (Mudge *et al*. 2002). Intracellular trafficking of Pht1 towards the plasma membrane is regulated by PHF1 (PHOSPHATE TRASPORTER TRAFFIC FACILITATOR1), which is localized in the endoplasmatic reticulum and related to SEC12 proteins of the early secretory pathway. PHF1 enables the endoplasmatic reticulum exit of Pht1 and is induced by P starvation (González *et al*. 2005).

Pht2;1 of Arabidopsis is a low-affinity phosphate transporter. It is mainly expressed in green tissues irrespective of the P status of the shoot. Its ortholog in potato is also transcribed in roots and tubers (Daram *et al*. 1999, Rausch *et al*. 2004). Pht2 was detected in the inner chloroplast membrane (Ferro *et al*. 2002, Rausch *et al*. 2004). It is expressed in the leaf cells, most strongly in the vasculature and pericycle of root and shoot, but also in flowers, siliques, and seeds, and it is induced by light. Thus, Pht2 is under the control of developmental signals, light, and sink strength (Rausch *et al*. 2004). Members of the Pht3 family are deduced to be mitochondrial P transporters (Rausch & Bucher 2002, Kiiskinen *et al*. 1997, Takabatake *et al*. 1999).

Xylem loading of phosphate and distribution within the plant

The concentration of inorganic phosphate in the cytoplasm of root cells is generally low. After uptake into rhizodermis and cortex, P is quickly incorporated into organic molecules. When the P availability is high, the phosphate content of the vacuoles increases. Release into the xylem occurs again as free phosphate (Marschner 1995).

An Arabidopsis mutant defective in xylem loading is *pho1*. It reveals reduced phosphate content in the shoot along with increased anthocyanin production while root P concentration is slightly elevated. P uptake into hypocotyls of derooted *pho1* plants is not impaired (Poirier *et al*. 1991). PHO1 is a transmembrane protein that shows highest sequence homology with the Rcm1 mammalian cell surface receptor for retroviruses and with the Syg1 protein from yeast involved in the mating pheromone signal transduction pathway (Hamburger *et al*. 2002). Syg1 interacts with the heterotrimeric G protein complex (Spain *et al*. 1995). *PHO1* is expressed in the mature vascular system of the root and lower hypocotyl, where it is most

pronounced in pericycle and xylem parenchyma cells (Hamburger *et al*. 2002). Evidence for P transport by PHO1 is lacking. Thus, PHO1 may be is a subunit of a multisubunit transporter or it may influence P export into the xylem indirectly (Hamburger *et al*. 2002).

The principle transport form of P in the xylem is inorganic phosphate, and the P concentration in the xylem sap is constant, independent of the P supply (Bieleski 1973, Mimura *et al*. 1996 Jeschke *et al*. 1997). The cytoplasmic P content of the leaf cells remains unaffected by the P availability while vacuolar P is exhausted under P deficiency, which coincides with the apoplastic P concentration (Mimura *et al*. 1996).

The main pathway for P distribution is the phloem. Phosphate moves quickly from the xylem to the phloem and is very mobile within the plant so that an individual P atom can make several circuits through the organism (Bieleski 1973).

Metabolic adaptations to P shortage

In addition to mobilization of P by intracellular nucleases and phosphatases, phosphate is released from phospho*enol*pyruvate (Poirier & Bucher 2002, Hammond *et al*. 2004). Starch is synthesized in the leaves (Foyer & Spencer 1986, Fredeen *et al*. 1989, Ciereszko *et al*. 2001). The conversion of triose phosphate into starch leads to a release of P within the chloroplast (Poirier & Bucher 2002). Membrane phospholipids are replaced with non-phosphorus galactolipids and sulfolipids (Poirier & Bucher 2002, Hammond *et al*. 2004). During P starvation, the portion of P translocated from the shoots to the roots is increased (Drew & Saker 1984, Jeschke *et al*. 1996, 1997).

If the intracellular P concentration is low, ATP synthesis through photosynthetic and respiratory electron flow is limited. Plants acclimatize with structural re-assembly of the photosynthetic apparatus and the use of alternative oxidase pathway. Also several key enzymes of the Calvin Cycle are inhibited. In addition, metabolic adaptation responses are induced that bypass ATP- and P-dependent enzymes of the glycolysis by using pyrophosphate or forbearing phosphorylation steps (Poirier & Bucher 2002).

Phosphate starvation leads to an increased anthocyanin synthesis. As anthocyanins absorb UV light, they could protect nucleic acids from UV radiation during P-limited photosynthesis (Poirier & Bucher 2002, Hammond *et al*. 2004).

Integration of local and systemic signals by the PHR1/PHO2/At4 pathway

The physiological and morphological phosphate deficiency responses in plants are thought to be differentially controlled by a systemic signaling mechanism communicating the P status of the leaf cells to the root and by a local signaling mechanism perceiving the P availability in the soil. Split root experiments and replenishment studies showed that root hair elongation is induced by local P deprivation regardless of P status of the plant (Bates & Lynch 1996). Primary root growth slows down when the root tip grows from a P-depleted environment into

a P-rich segment and shows a further growth reduction when again reaching a P-depleted zone. This indicates an interaction of local and systemic signals in regulating primary root meristem activity. Lateral root density was not affected by heterogeneously supplied phosphate, whereas lateral root elongation was greatly reduced outside a P-rich patch (Linkohr *et al*. 2002). Transcription of the high-affinity transporters *LePT1* and *LePT2* in the roots is systemically repressed in split-root experiments (Liu *et al*. 1998). If Arabidopsis plants are resupplied after P limitation, transcript levels of high-affinity transporters and other P starvation-inducible genes decline rapidly indicating a local response (Müller *et al*. 2004).

The gene *Mt4* from *Medicago* is strongly induced in the roots following phosphate starvation and is downregulated by phosphate fertilization or infection with mycorrhiza (Burleigh & Harrison 1997). As *Mt4*-like genes, *TPSI1* (*TOMATO PHOSPHATE STARVATION-INDUCED1*), *AtIPS1* (*INDUCED BY PHOSPHATE STARVATION1*), *At4*, and *OsPI1* (*PHOSPHATE LIMITATION-INDUCIBLE1*) have been identified (Liu *et al*. 1997, Burleigh & Harrison 1999, Martín *et al*. 2000, Wasaki *et al*. 2003). In split-root plants, *Mt4* is systemically repressed.

In a mutant screen for plants with impaired *AtIPS1* reporter gene activity, the MYB-CC protein PHR1 (PHOSPHATE STARVATION RESPONSE1) has been identified. The *phr1* mutant does not accumulate anthocyanin under P depletion and reveals reduced expression of *At4*, acid phosphatase (*AtACP5*), ribonuclease (*RNS1*), and phosphate transporter (*AtPt1*). Root hairs are not altered in the mutant (Rubio *et al*. 2001). *PHR1* is homologous to *PSR1* (*PHOSPHORUS STARVATION RESPONSE1*) from *Chlamydomonas*; both are localized in the nucleus. PSR1 level is strongly increased upon P starvation, whereas PHR1 is only moderately induced under low P conditions (Rubio *et al*. 2001, Wykoff *et al*. 1999). PHR1 binds as a dimer to an imperfect palindromic sequence in the promoter regions of *AtIPS1*, *AtIPS3*, *At4*, *Mt4*, *TPSI1*, *AtACP5*, *PAP1*, *RNS1*, and *AtPT1* (Rubio *et al*. 2001).

The *pho2* mutant overaccumulates phosphate in the leaves, while root P concentration stays normal (Delhaize & Randall 1995). The P accumulation in the shoot is a result of an increased uptake rate, increased translocation from the root to the shoot, and an impaired remobilization from the shoot to the root. Grafting experiments revealed that *pho2* acts root-specific in causing the high P content of the shoot. The increased uptake rate of *pho2* disappeared when the shoot was removed. Thus, PHO2 might be involved in long-distance signaling (Dong *et al*. 1998, Bari *et al*. 2006). *PHO2* encodes a ubiquitin-conjugating E2 enzyme (Chiou *et al*. 2006, Aung *et al*. 2006, Bari *et al*. 2006).

The miRNA399 is strongly induced by low P in roots and most prominently in shoots. The primary transcripts of miRNA399 decrease rapidly after re-addition of P. This response is highly specific to P. The target of miRNA399 is the 5' UTR of an ubiquitin-conjugating E2 enzyme (*UBC24*), which is an allel of *PHO2* (Sunkar & Zhu 2004, Fujii *et al*. 2005, Chiou *et al*. 2006, Bari *et al*. 2006). E2 proteins are part of the ubiquitin-proteasome pathway tagging

proteins for degradation (Ciechanover 1998, Hellmann & Estelle 2002). Transgenic plants that overexpress *UBC24* without the 5' UTR show less induction of *AtPT1* and less inhibition of primary root growth. Lateral root density and expression of *At4* and *RNS1* were not altered (Fujii *et al*. 2005).

Overexpression of miRNA399 leads to downregulation of *UBC24/PHO2*, which resembles the *pho2/ubc24* phenotype (Fujii *et al*. 2005, Chiou *et al*. 2006, Aung *et al*. 2006).

From these results it is hypothesized that the abundance of PHO2 in high P conditions leads to a direct or indirect downregulation of high-affinity uptake systems preventing overload. Upon P starvation, *PHO2* is posttranscriptionally downregulated by miRNA399 whereby repression of P uptake is alleviated. In addition, a component controlling the internal P concentration of shoot cells or the translocation from the shoot to the root seems to be modified by PHO2 (Dong *et al*. 1998, Chiou *et al*. 2006, Bari *et al*. 2006). PHO2 orthologs with miRNA399 binding sites were found in many angiosperms, but not in *Physcomitrella patens* or *C. reinhardtii*, indicating the system is conserved in vascular plants and may have originated during the evolution of higher plants (Bari *et al*. 2006).

Expression of 21 P starvation-inducible genes affected in *pho2* is also altered in *phr1*. The high primary transcript level of miRNA399 in P-deficient plants is impaired in *phr1*, and the PHR1 *cis*-element is found upstream of the miRNA399s, placing PHR1 superior to miRNA399 and its posttranscriptional modification of *PHO2* (Bari *et al*. 2006).

Also *At4*, *AtIPS*, *At4.1*, and *At4.2* possess miRNA399 binding sites. Thus, in addition to the strong transcriptional induction of the *At4*-like genes in response to P deprivation, also a posttranscriptional control by miRNA399 may occur. *At4* is expressed in the endodermis and vascular tissues of P-starved roots and after prolonged P depletion also in the cortex and epidermis (Shin *et al*. 2006). *AtIPS1* expression, in contrast, is found throughout the plant (Martín *et al*. 2000). Loss of *at4* function impacts the allocation of P from the shoots to the roots leading to an increased P content in the shoot, but in contrast to *pho2*, re-allocation occurs only under P starvation and the uptake rate into the root is not altered in *at4* (Shin *et al*. 2006).

Phosphate-deficient *siz1* plants show an enhanced primary root growth inhibition, extensive lateral root and root hair development, increased root/shoot ratio, and higher anthocyanin accumulation, even though intracellular P levels are similar to the wildtype. Transcript abundance of *Pht1;4* and acid phosphatase is higher in *siz1*; *AtIPS1* and *AtRNS1* are lower. AtSIZ1 is a small ubiquitin-like modifier (SUMO) E3 ligase. From its sequence an involvement in chromatin organisation and ligase activity are predicted, which is consistent with SIZ1 localization in the nucleus. A sumoylation target of SIZ1 is PHR1. Thus, SIZ1 is an important positive and negative upstream regulator of P starvation responses. *SIZ1* mRNA is more abundant in roots than in shoots and is only slightly responsive to P deprivation (Miura *et al*. 2005).

Further regulators of Pstarvation responses

The phospholipase Dζ2 is induced in roots and shoots upon P starvation. The *pldζ2* mutant shows reduced phospholipid hydrolysis under limiting P conditions. Although the root meristem is disorganized in *pldζ2*, leading to a decreased primary root length and root hairs developing closer to the apex, PLDζ2 is suggested to have a metabolic rather than a regulative function (Cruz-Ramírez *et al*. 2006).

The bHLH protein OsPTF1 is induced in P-deficient roots and constitutively expressed in shoots. Overexpressing lines show higher root length and surface area resulting in increased P uptake rates in P-limited conditions. One-hundred-fifty-eight genes related to metabolism, nutrient transport, and regulation are significantly changed in the overexpressers, of which almost all have E-box elements in their promoters as typical binding sites for bHLH transcription factors (Yi *et al*. 2005).

In *pdr2* (*P_i deficiency response2*), primary root growth inhibition and lateral root development is enhanced under low P conditions. The primary root and newly formed laterals subsequently lose meristem activity followed by the development of secondary and tertiary laterals, respectively, together leading to a small stunted root system. Anthocyanin and starch accumulation and P starvation-inducible gene expression are enhanced in P-deficient *pdr2*. Phosphate content is higher in *pdr2* grown without P and lower when supplied with DNA as a phophate source. Meristem function can be restored by Phi indicating *pdr2* disrupts sensing of low external P availability (Ticconi *et al*. 2004). The *pdr2* phenotype is reminiscent of the experiment of Torrey (1950), in which removal of the primary root tip resulted in an increase of laterals. Ablation of root cap cells inhibits primary root growth while lateral root development is stimulated. This implies an involvement of the root cap cells in the signaling system that alters root system architecture (Tsugeki & Fedoroff 1999).

The *lpi1* and *lpi2* (*low phosphorus insensitive*) mutants fail to inhibit primary root growth under P starvation. Root hair density is lower, whereas root hair elongation and anthocyanin accumulation are unaffected. Expression of *AtPT1*, *AtPT2*, *PAP1*, *ACP5*, and *IPS1* is reduced. *lpi2* fails to increase the number of laterals in low P conditions, whereas the reaction in *lpi1* is normal (Sánchez-Calderón *et al*. 2006).

QTL analysis of low P grown Arabidopsis RILS (Bay-0 x Shahdara) revealed three loci involved in reduction of primary root growth. The locus *LPR1* is not involved in increasing root hair number or length, anthocyanin accumulation, acid phosphatase excretion, or Pht1;4 induction (Reymond *et al*. 2006).

Involvement of hormones in the regulation of phosphate homeostasis

Cytokinin favours shoot growth while inhibiting lateral root formation. A decrease in the content of cytokinin has been associated with P deficiency (Salama & Wareing 1979, Horgan

& Wareing 1980). Exogenously supplied cytokinin counteracts the root growth stimulation induced by low P (Kuiper 1988, Kuiper *et al*. 1988). The phosphate starvation inducible genes *AtIPS1*, *At4*, *AtACP5*, and *AtPT1* are downregulated after cytokinin treatment, and anthocyanin accumulation is decreased. However, the increase in the root hair number and length was unaffected by the hormone (Martín *et al*. 2000, Franco-Zorrilla *et al*. 2002). The *cre1* (*cytokinin response1*) mutant displays reduced sensitivity of *AtIPS1* reporter gene activity to cytokinin repression. Also the cytokinin-dependent repression of *At4*, *AtACP5*, and *AtPT1* and of anthocyanin accumulation is reduced in P-deficient *cre1*, and lateral root formation is not inhibited (Franco-Zorrilla *et al*. 2002). *CRE1* is allelic to the cytokinin receptor kinase *WOL/AHK4* (WOODEN LEG/ARABIDOPSIS HISTIDINE KINASE4). *CRE1* is downregulated by P starvation and induced by cytokinins (Mähönen *et al*. 2000, Inoue *et al*. 2001, Suzuki *et al*. 2001, Franco-Zorrilla *et al*. 2002).

Auxin treatment inhibits primary root growth and promotes lateral root initiation by activation of the cell cycle in xylem pericycle cells, which is blocked by inhibition of auxin transport (Evans *et al*. 1994, Casimiro *et al*. 2001, Himanen *et al*. 2002). Auxin-resistant mutants show decreased primary root growth inhibition in response to auxin and reveal a reduced number of laterals (Evans *et al*. 1994, Hobbie & Estelle 1995). Inhibition of acropetal auxin transport or removing the shoot also inhibits lateral root formation (Reed *et al*. 1998). The involvement of auxin in remodelling root system architecture adapted to P starvation is controversial. Williamson *et al*. (2001) suggested auxin is not involved in primary root growth reduction and increased lateral root formation of P-deficient plants, because auxin-resistant mutants reacted in the same manner as the wildtype. However, *iaa28* did not respond to the stimulatory effect of low P on lateral root and root hair formation. Treatments of high and low P-grown wildtype plants with auxin and auxin antagonists resulted in an altered sensitivity of P-starved plants to the hormone with respect to primary root growth and lateral root development (López-Bucio *et al*. 2002). Nacry *et al*. (2005) measured a significantly increased auxin concentration in the primary root and short laterals of P-starved plants along with increased activity of the auxin-responsive reporter *DR5-GUS*. The authors concluded auxin redistribution is altered in the root of P-deficient plants. Cluster root formation in P-sufficient lupin was increased by foliar application of auxin and reduced in P-deficient plants by auxin transport inhibitors (Gilbert *et al*. 2000).

Auxin and ethylene promote root hair elongation, as auxin- or ethylene-resistant mutants have no or shorter root hairs; treatment of these mutants or wildtype plants with auxin or an ethylene precursor significantly increases root hair length (Wilson *et al*. 1990, Pitts *et al*. 1998). As with the role of auxin in remodelling root architecture, the role of auxin and ethylene in root hair development during adaption to the P supply is also controversial. An involvement of auxin in the root hair elongation under P deficiency is suggested by Bates and Lynch (1996), because this process was inhibited by blocking auxin transport. Schmidt and Schikora (2001) found that the auxin-resistant mutants *axr1* and *axr2*, and the ethylene-

insensitive mutant *ein2* are not able to produce root hairs under sufficient nutrient supply or Fe deprivation, whereas root hairs of P-deficient plants develop normally, which is in support of inhibitor studies. These authors suggest that root hair formation in adaption to P limitation is regulated independently from root hair development in sufficient or Fe-starved plants and apparently does not require auxin or ethylene. Also Ma *et al*. (2001a) observed no significant effect of ethylene inhibitors on root hair development of P-starved plants. In contrast, Zhang *et al*. (2003) and He *et al*. (2005) observed an inhibition of P stress-induced root hairs and a reduced response of ethylene-insensitive mutants to P limitation assuming an interacting effect of ethylene and phosphate signaling on root hair development.

1.3 Root hair development

Root hairs are tubular outgrowths of root epidermal cells that serve in water and nutrient uptake. They are the primary site of infection of rhizobia. Root hairs evolved 400 million years ago within the lineage of tracheophyta, indicating an important role for root hairs in the adaptation of land plants (Peterson 1992). Different stages of root hair development are defined. These stages are root hair specification, initiation, bulge formation, and tip growth (Schiefelbein & Somerville 1990, Dolan *et al*. 1994).

Root hair specification

In the rhizodermis of crucifers like Arabidopsis, root hair cells are formed in a position dependent pattern. Only those epidermal cells located over the clefs of two underlying cortical cells develop a root hair, which is called the hair position (H position). Epidermal cells with contact to only one cortical cell become a non-hair cell, which is typically the non-hair position (N position). If the epidermis is separated from the cortex, root hairs develop in nearly all rhizodermal cells (Bünning 1951, Dolan *et al*. 1994). An arrangement of H and N cell files is also observed in other Brassicales as well as in Caryophyllales, Malpighiales, Rosales, Myrtales, Cornales, Ericales, Solanales, Lamiales, and Boraginaceae (Dolan 2006, Kim *et al*. 2006). First differences between H and N cells are visible in the late meristematic region, where H cells show a more intense cytoplasmic staining, shorter cells that undergo a higher rate of cell division, and a delay in vacuolization relative to cell elongation (Dolan *et al*. 1994, Galway *et al*. 1994, Berger *et al*. 1998a). Laser ablation experiments have shown that it is positional information not cell lineage that defines cell fate (Berger *et al*. 1998b).

Two opposing pathways determine the development of H and N cells in the late meristematic region and are assumed to act by lateral inhibition with feedback (Lee & Schiefelbein 1999, Bernhardt *et al*. 2005, Schiefelbein & Lee 2006). In the first pathway, a transcription factor complex specifies the non-hair cell fate in the N position. This complex includes the MYB class transcriptional regulator WER (WEREWOLF), which possesses a DNA binding as well as a putative transcriptional activation domain, two bHLH transcription factors GL3

(GLABRA3) and EGL3 (ENHANCER OF GLABRA3) that act in a partially redundant manner, and TTG1 (TRANSPARENT TESTA GLABRA1) containing a WD40 domain involved in protein-protein interaction (Galway *et al*. 1994, Walker *et al*. 1999, Lee & Schiefelbein 1999, Bernhardt *et al*. 2003). This complex induces the expression of the homeodomain protein *GL2* (*GLABRA2*) in the N position as WER recognizes a MYB binding site within the *GL2* promoter (Hung *et al*. 1998, Lee & Schiefelbein 1999, Koshino-Kimura *et al*. 2005). GL2 inhibits root hair development since the *gl2* mutant develops root hairs in the N position (Masucci *et al*. 1996). The gene *CAPRICE* (*CPC*) also contains a MYB binding site and is likewise transcribed in the N position through positive regulation by the WER/TTG/GL3/EGL3 complex. *CPC* encodes a small MYB protein without transcriptional activation domain that is able to move from the N cells to the neighboring H cells, probably via plasmodesmata (Wada *et al*. 1997, 2002, Lee & Schiefelbein 2002, Kurata *et al*. 2005). In the H position, CPC acts as a negative regulator of *WER* and its own expression, and, in addition, it replaces WER in the transcription factor complex described above by binding to the bHLH proteins (Lee & Schiefelbein 1999, Koshino-Kimura *et al*. 2005). Because CPC lacks the transcriptional activation domain, this alternatively composed complex inhibits *GL2* expression in the H position, thus specifying the hair fate. As a feedback loop, CPC induces *GL3/EGL3* in the H position. The proteins are transported towards the N position, where their expression is blocked by *WER*. In addition, *GL3* and *EGL3* also inhibit their own transcription in the N position (Bernhardt *et al*. 2003, 2005).

Pharmacological inhibition of histone deacetylase affects the position-dependent expression of *WER*, *CPC*, *GL2*, and root hair pattern. Mutation of the histone deacetylase *HDA18*, which is expressed in all root tissues, leads to a randomized patterning of *WER* expression and root hair occurrence suggesting an involvement in transcriptional regulation of cell specification genes after the positional cues have been perceived (Xu *et al*. 2005).

Another regulation level for the expression of *GL2* in the N position is chromatin remodelling. Around the *GL2* locus in N cells, chromatin is in an 'open' conformation, and it is 'closed' in H cells. CPC is required to establish the 'closed' state in the H position, but neither GL2 nor cell fate specification is required for the 'open' conformation. The chromatin state is reset at mitosis and is respecified during the following G1 phase according to the underlying positional information (Costa & Shaw 2006).

The *erh1* and *erh3* mutants (*ectopic root hair*) have additional root hairs and show a denser cytoplasmic staining also in N cells (Schneider *et al*. 1997). In *erh3*, the orientation of cell walls is abnormally oblique in all tissues of the root tip. Microtubules reorganization is delayed in the *erh3* allele *fra2* (*fragile fibre2*) and cell wall biosynthesis disturbed. The activity of ERH3 is required for both, hair and non-hair cells. The expression pattern of *GL2* is altered in *erh3* as well as the occurrence of lateral root cap, endodermis, and cortical markers. *ERH3* codes for a katanin-p60 protein expressed throughout the whole plant. As

katanin-p60 proteins sever microtubules; ERH3 may act either directly by microtubule disruption or by a katanin-dependent cell wall biosynthetic process that incorporates molecules conferring the positional information spatially into the cell wall (Burk *et al*. 2001, Webb *et al*. 2002).

The positional information is likely to be perceived by SCM (SCRAMBLED), a receptor-like kinase expressed in all tissues of the developing root except the root cap. SCM is necessary for the position-dependent pattern of *WER*, *CPC*, and *GL2*. In *scm* mutants, root hairs are distributed randomly. The cell division rates in H and N position are altered indicating that early cell characteristics are affected. SCM is predicted to possess a signal sequence for secretion, an extracellular leucine-rich repeat typically participating in protein-protein interactions, and an intracellular kinase domain (Kwak *et al*. 2005).

The root hairless mutants *rhl1*, *rhl2*, and *rhl3* do not reveal a denser cytoplasmic staining or delay in vacuolization in any epidermal cell in the late meristematic region. In addition, the *rhl* mutants are dwarf and their nucleolus is deformed. RHL1, RHL2, and RHL3 are subunits of the topoisomerase VI complex important for ploidy-dependent cell growth. Thus, endoreduplication is important for root hair development. According to double mutant analysis, this process is independent of *GL2* action (Schneider *et al*. 1997, 1998, Sugimoto-Shirasu *et al*. 2005).

Epidermal cell polarity and root hair initiation

After specification, the rhizodermal cells elongate, and then root hairs are initiated near the apical end of the cell towards the root tip. Root hair initiation is, therefore, linked with epidermal cell polarity (Schiefelbein & Somerville 1990, Dolan *et al*. 1994, Grebe 2004). Establishment of cell polarity bases on vesicle trafficking. An important mediator of this process in Arabidopsis is the ArfGTPase ARF1 (ADP-RIBOSYLATION FACTOR1), which is localized in Golgi membranes and endocytic vesicles (Donaldson *et al*. 1992a, Xu & Scheres 2005). ArfGTPases are involved in membrane trafficking. They recruit cytosolic coat proteins to the sites of vesicle budding (Vernoud *et al*. 2003). In ARF1 mutants, root hairs develop more basally and additional root hairs derive from one trichoblast (Xu & Scheres 2005). Treatment with the vesicle transport inhibitor brefeldin A (BFA) causes basal shifting of root hair initiation (Grebe *et al*. 2002, Xu & Scheres 2005). BFA inhibits Arf GEF (ARF-guanosine exchange factor), which regulates ArfGTPase by catalyzing the guanine nucleotide exchange (Donaldson *et al*. 1992b, Helms & Rothman 1992). Weak mutant alleles of the Arf GEF GNOM also display a basal shift of root hair emergence (Steinmann *et al*. 1999, Fischer *et al*. 2006).

Pharmacological and mutant analyses suggest an involvement of auxin and ethylene in polar root hair initiation (Masucci & Schiefelbein 1994, Grebe *et al*. 2002). Auxin may, thereby,

induce root hair initiation through an increased ethylene production (Cho & Cosgrove 2002). Auxin and ethylene act downstream of *GL2* expression (Masucci & Schiefelbein 1996).

The auxin influx carrier AUX1 (AUXIN-RESISTANT1) is localized at the apical and basal ends of epidermal cells. This localization is abolished by BFA and, conversely, AUX1 is required for BFA-sensitive vesicle trafficking. The *aux1* mutation causes a basal shift of root hair initiation (Grebe *et al*. 2002). Polar root hair localization is, moreover, mediated by combined activity of AUX1, EIN2, and GNOM. In the triple mutant, the auxin gradient is abolished and the root hair initiation site is displaced, namely stronger than in the single mutants. Locally applied auxin can coordinate root hair positioning (Fischer *et al*. 2006). Also the localization of PIN2 (PIN-FORMED2), an auxin efflux carrier, is a potential target of ARF1 action in the rhizodermis (Xu & Scheres 2005). PIN2 localizes in the late meristematic and elongation zone at the basal rhizodermal plasma membranes (Müller *et al*. 1998). However, *pin2*, *pin2pin1*, or *pin2pin4pin7* mutants do not show alterations in root hair polarity indicating that the epidermal cell polarity does not rely on PIN function (Fischer *et al*. 2006).

A further component important for polar root hair initiation is RHD6. The *rhd6* mutant reveals very few root hairs that emerge more basally. When treated with auxin or the ethylene precursor ACC, root hair number is increased in *rhd6* (Masucci & Schiefelbein 1994).

Root hair initiation and bulge formation

Polar localization of RopGTPases specifies the site of root hair outgrowth. Rops are plant specific RhoGTPases that are key regulators of the actin cytoskeleton. Expression of constitutively active Rop2, Rop4, and Rop6 abolishes polar root hair formation. Rops localize at the sites of root hair emergence before bulge formation and remain at the tips of elongating root hairs until growth ceases. This localization is sensitive to BFA treatment (Zheng & Yang 2000, Molendijk *et al*. 2001, Jones *et al*. 2002, Vernoud *et al*. 2003). Rop2 recruitment depends on ARF1 action and on the combined activity of AUX1, EIN2, and GNOM (Xu & Scheres 2005, Fischer *et al*. 2006). As targets of Rop action in developing root hairs, the plasma membrane-bound NADPH oxidase complex and the actin binding protein profilin involved in actin organization have been suggested (Molendijk *et al*. 2001, Jones *et al*. 2002, Vernoud *et al*. 2003).

The RhoGTPase GDP dissociation inhibitor (RhoGDI) SCN1 (SUPERCENTIPEDE1) is involved in regulating the localization of Rop2. The *scn1* mutant has multiple tip-growing sites that do not elongate. RhoGDIs regulate RhoGTPases by sequestering them in the cytosol and inhibiting the dissociation of GDP from the GTPases. SCN1/AtRhoGDI1 interacts with Rop4 and Rop6. This interaction is weakened in *scn1* and Rop2 mislocalized (Carol *et al*. 2005, DerMardirossian & Bokoch 2005, Bischoff *et al*. 2000, Vernoud *et al*. 2003).

SCN1 belongs to a mechanism that focuses the production of reactive oxygen species (ROS) catalyzed by the NADPH oxidase RHD2 (ROOT HAIR DEFECTIVE2) to root hair tips (Carol *et al*. 2005, Foreman *et al*. 2003). ROS are essential for root hair elongation as they stimulate hyperpolarization-activated Ca^{2+} channels in the apex of growing root hairs. The resulting influx of extracellular Ca^{2+} leading to a tip-focussed Ca^{2+} gradient is required for root hair tip growth (Foreman *et al*. 2003, Véry & Davies 2000, Wymer *et al*. 1997, Schiefelbein *et al*. 1992). The local influx of Ca^{2+} does not precede bulge formation suggesting Ca^{2+} does not trigger root hair initiation. In the *rhd2* mutant, which initiates root hair bulges that do not elongate, no ROS are produced and no tip-focussed Ca^{2+} gradient is established (Schiefelbein & Somerville 1990, Foreman *et al*. 2003, Wymer *et al*. 1997). Differences in the transcriptomes of *rhd2* and the wildtype comprise 606 genes that are higher expressed in the wildtype and 313 genes that are higher in *rhd2* (Jones *et al*. 2006).

ACTIN2 and is essential for bulge site selection and tip growth. The *der1* (*deformed root hairs1*) mutation in the *ACTIN2* gene causes a basal shift of root hair outgrowth and short or deformed root hairs (Ringli *et al*. 2002).

Polar root hair initiation is possibly regulated by phospholipid signaling, since ectopic expression of PLDζ1 leads to mislocalization of root hair initiation sites. Root hairs are deformed and are also formed in non-hair cells. PLDζ1 is repressed by GL2, a negative regulator of root hair development (Ohashi *et al*. 2003).

Sterol biosynthesis is required for establishment of epidermal cell polarity. Mutation of enzymes belonging to the sterol synthesis pathway, like *smt1* (*sterol methyltransferase1*) or *hydra2* defective in sterol C14 reductase, leads to a randomized root hair initiation over the apical-basal axis of trichoblasts and to the development of multiple and branched root hairs. Sterols can act in lipid rafts, which are sterol-rich regions of plasma membrane important for polarity determination (Willemsen *et al*. 2003, Souter *et al*. 2002).

The *S*-acyl transferase TIP1 is important for root hair initiation and tip growth (Hemsley *et al*. 2005, Parker *et al*. 2000). The *tip1* mutant has short root hairs that are often branched (Schiefelbein *et al*. 1993, Ryan *et al*. 1998). *S*-acylation is a reversible protein modification that promotes association with membranes (Yalovsky *et al*. 1999). Acylation has been implicated in protein sorting into lipid rafts (Bagnat & Simons 2002). Yeast *S*-acyl transferase localizes to the Golgi apparatus and the late endosome (Harada *et al*. 2003). Potential targets of TIP1 are Rops, G proteins, phospholipases, or calcium-dependent protein kinases (CDPKs). TIP1 could regulate vesicle traffic by directing proteins to a discrete area of the membrane (Hemsley *et al*. 2005).

Local acidification of the cell wall is required for root hair initiation. Its prevention stops the initiation process. The acidification is present from the first morphological indications of bulge formation and maintains until tip growth begins (Bibikova *et al*. 1998). Expansins accumulate in the developing root hair bulges (Baluška *et al*. 2000). Expansins are

extracellular proteins that regulate plant cell enlargement by inducing relaxation and extension of cells at an acidic pH optimum (McQueen-Mason *et al*. 1992, Cosgrove 2000). The expansin genes *EXP7* and *EXP18* are expressed in root hair cells during the initiation and elongation state and are localized at the emerging root hair tip. In *rhd6*, *EXP7* and *EXP18* expression is blocked suggesting RHD6 is a positive regulator of the two expansin genes (Cho & Cosgrove 2002). *EXP7* and *EXP18* expression is also lower in *rhd2* (Jones *et al*. 2006).

Root hair initiation is accompanied by an increase in xyloglucan endotransglycosylase (XET) activity at the site of the future bulge formation, which is lowered in *rhd2*. As XETs cleave and rejoin xyloglucan chains, XET could locally loosen the cell wall leading to turgor-mediated bulge formation. XET localization is independent of the actin cytoskeleton (Vissenberg *et al*. 2001, Jones *et al*. 2006).

Root hair tip growth

Auxin is also involved in root hair elongation. Mutation in the K^+ transporter TRH1 prevents root hair tip growth, which can be rescued by the application of auxin. Also multiple initiation sites are observed in *trh1*. Although TRH1 has K^+ transport activity, this phenotype is independent of the external K^+ concentration (Rigas *et al*. 2001, Desbrosses *et al*. 2003). TRH1 accelerates auxin efflux in Arabidopsis root segments and yeast. TRH1 is expressed in the root cap and the lateral root cap. It is suggested that TRH1 assists in basipetal auxin transport in the columella providing an auxin concentration in the rhizodermis adequate for root hair development (Vincente-Agullo *et al*. 2004). Ectopic expression of the auxin effluxer PIN3 or of PID (PINOID), a kinase positively activating auxin efflux, in root hair cells inhibits root hair elongation underlining the importance of auxin for root hair tip growth (Lee & Cho 2006).

During root hair tip growth, vesicles containing cell wall material are secreted by exocytosis at the apical zone of the growing tip. The resulting membrane surplus is compensated by endocytosis in the subapical zone. The mechanism regulating the directional secretion to the tip must involve a continuous re-localization towards the advancing tip. This process is regulated by a network of small GTPases, Ca^{2+}, phospholipids, ROS, protein kinases, and the cytoskeleton. Multiple feedback loops allow the growing tip to maintain itself (Hepler *et al*. 2001, Dolan & Davies 2004, Šamaj *et al*. 2004, 2006, Cole & Fowler 2006).

The microtubules cytoskeleton is important for regulating the direction of root hair tip growth. By placing proteins that serve as spatial cues to the expanding tip, microtubules may determine the site where exocytosis takes place (Bibikova et al. 1999, Sieberer *et al*. 2005). The actin cytoskeleton is fundamental for polarized growth during root hair development. It is responsible for the motility of vesicles and organelles (Hepler *et al*. 2001).

ARF1 is involved in the regulation of membrane trafficking during root hair tip growth. Mutation in the ArfGAP (ArfGTPase-activating protein) RPA (ROOT AND POLLEN

ARFGAP), which regulates ARF1 by catalyzing GTP hydrolysis, leads to short and deformed root hairs. RPA is localized at the Golgi system (Song *et al*. 2006, Vernoud *et al*. 2003).

Mutation in the small G protein RHD3 causes short wavy root hairs and a reduced cell expansion also other tissues (Wang *et al*. 1997, Schiefelbein & Somerville 1990, Hu *et al*. 2003). *rhd3* reveals a striking reduction in vacuole size and an abnormally high number of secretory vesicles concentrated in the subapical region of the root hairs (Galway *et al*. 1997). RHD3 is required for vesicle trafficking from the ER to the Golgi, ER organisation, and membrane transport from the plasma membrane to the vacuole (Zheng *et al*. 2004). RHD3 is essential for actin organization and cell wall biosynthesis; cell wall thickness is dramatically reduced in *rhd3* (Hu *et al*. 2003). RHD3 acts downstream of auxin, ethylene, and RHD2 (Wang *et al*. 1997, Schiefelbein & Somerville 1990).

The exocyst is an oligomeric protein crucial for the specification of vesicle docking and fusion during exocytosis (Eliás *et al*. 2003). In the maize *rth1* (*roothairless1*) mutant, which is defective in a homolog of the SEC3 exocyst subunit, root hair bulges fail to elongate (Wen *et al*. 2005). Mutation in the Arabidopsis *EXO70A1* gene, a family member of another putative exocyst subunit, also stops root hair development after bulge formation. In analogy with yeast and mammals, an interaction of EXO70A1 with Rabs or Rops, e. g. Rop2, has been suggested (Synek *et al*. 2006).

Localization of the RabGTPase RabA4b at the tips of growing root hairs is correlated with tip growth. RabA4b is associated with vesicles distinct from the *trans*-Golgi network. RabA4b localization depends on the actin cytoskeleton and on *RHD2*, *RHD3*, and *RHD4* action (Preuss *et al*. 2004). RabA4b interacts with the phosphatidylinositol-4-kinase PI-4Kβ1. PI-4Kβ1 interacts with the Ca^{2+} sensor AtCBL1. Thus, RabA4b recruitment of PI-4Kβ1 could result in Ca^{2+}-dependent generation of phosphatidylinositol-4-phosphate (PIP) at a tip-localized membrane compartment (Preuss *et al*. 2006). The actin binding protein profilin and its ligand phosphatidylinositol-4,5-bisphosphate (PIP_2) accumulate at the tips of bulges and growing root hairs (Braun *et al*. 1999). Installation of the actin-based tip growth machinery requires profilin action and occurs after expansin-associated bulge formation (Baluška *et al*. 2000).

The PI transfer protein (PITP) COW1 (CAN OF WORMS1) is important for root hair elongation. It is localized in epidermal cells and in the central cylinder of the meristematic, elongation, and root hair zone (Böhme *et al*. 2004). The COW1 homolog AtSfh1p enriches along the plasma membrane at the growing tip. Dysfunction impairs PIP2 accumulation at the tip, leads to Ca^{2+} influxes all along the root surface, causes defects in the actin cytoskeleton, and disorganizes microtubule networks in the root hair. AtSfh1p could generate PIP2 landmarks that couple to components of the actin cytoskeleton (Vincent *et al*. 2005, Hsuan & Cockcroft 2001). In yeast and humans, PITPs are involved in PLC and PLD signaling. PITP

presents PI to PI-4-kinase, thereby increasing PIP_2. PIP_2 is cleaved by PLC to generate IP_3. In addition, PIP2 has been shown to potentiate PLD activity (Spiegel *et al*. 1996).

Expression of the IP_3 phosphatase *MRH3* and of the two predicted GPI-anchored proteins *MRH4* and *MRH5* is suppressed in *rhd2*. The proteins could act in lipid rafts, as is the case in mammals (Jones *et al*. 2006).

PLDs produce phosphatidic acid (PA). In Arabidopsis, PA activates the phosphoinosite-dependent kinase PDK1 by specific binding, which, in turn, stimulates AGC2, a cAMP/cGMP-dependent kinase C. AGC2 localizes to the root hair tip and to the nucleus. The *agc2* mutant displays reduced root hair length (Anthony *et al*. 2004).

MtCDPK1 is important for root hair tip growth. In the aberrant root hairs of RNAi plants, ROS production at the tip is abolished and the actin cytoskeleton disorganized (Ivashuta *et al*. 2005).

In the Arabidopsis *oxi1* (*oxidative signal-inducible1*) mutant, root hair length is reduced. OXI1 is a protein kinase induced by H_2O_2 that is required for the H_2O_2-dependent activation of the mitogen-activated protein kinases (MAPKs) MPK3 and MPK6 (Rentel *et al*. 2004). The alfalfa MPK6 homologue SIMK (stress-induced MAPK) shows an actin-dependent localization in the tips of growing root hairs (Šamaj *et al*. 2002).

Root hairs of *rhd4* are short and deformed and have localized cell wall thickenings. *rhd2* is epistatic to *rhd4* (Schiefelbein & Somerville 1990, Galway *et al*. 1999).

Cell wall components involved in root hair tip growth

The cell wall is a crucial determinant for cell shape. Without it, the protoplast forms a sphere. It is a rigid but pliable structure that confers protection and cell cohesion and is important for communication between cells. The cell wall consists of a cellulose-xyloglucan network that is embedded in a matrix of pectic polysaccharides. During cell growth, cellulose is synthesized at the plasma membrane, whilst the other components are synthesized in the endomembrane system and released by exocytosis into the matrix (Carpita & Gibeaut 1993). Mutation in the cellulose-like synthase gene *CSLD3*/*KOJAK* (*KJK*) gene leads to inhibition of root hair tip growth and to leakage of cytoplasm at the root hair tip (Wang *et al*. 2001). *CSLD3*/*KJK* is expressed preferentially in root hair cells. Its location on the ER indicates the gene is required for the synthesis of noncellulose wall material. *kjk* is epistatic to *cow1* and acts independent of *tip1*, *rhd2*, *rhd3*, and *rhd4* (Favery *et al*. 2001).

The *rhd1*/*reb1* (*root hair defective1*/*root epidermal bulger1*) mutant develops large bulges at the base of the root hairs; root hair length is normal. RHD1/REB1 encodes an UDP-D-glucose 4-epimerase that is required for the galactosylation of xyloglucan and type II arabinogalactan, which are components of the pectin matrix and of cell wall proteins (Schiefelbein & Somerville 1990, Seifert *et al*. 2002).

Structural proteins form an independent structure-determining network within the extracellular matrix that assists in proper cell wall assembly (Cassab 1998). Hydroxyproline-rich glycoproteins of the extensin and arabinogalactan protein (AGP) families representing cell wall structural proteins amount a large proportion among the genes, whose expression is lowered in *rhd2* (Jones *et al*. 2006). The two extensin-like genes *Dif10* und *Dif54* are specifically expressed in root hairs (Bucher *et al*. 1997). The proline-rich cell wall structural protein PRP3 is expressed in root hair cells of the root hair zone, which depends on correct localization of *GL2* expression and on GL2 function (Bernhardt & Tierney 2000). *AGP30* is induced in atrichoblasts of the late meristematic region. This pattern does not depend on localization and function of GL2. In the root hair zone, AGP30 appears in the cortex, endodermis, and vasculature. Expression of *AGP30* is regulated by abscisic acid and ethylene. The complementary expression pattern of *PRP3* and *AGP30* indicates a role of the two proteins in determining the extracellular matrix structure specifically for hair and non-hair cells (van Hengel *et al*. 2004).

A possible regulator of proper cell wall assembly is the chimeric leucine-rich repeat/extensin protein LRX1 localized in the wall of root hairs. The *lrx1* mutant develops root hairs that frequently abort, swell, or branch due to an aberrant cell wall structure. LRX are involved in protein-protein or ligand-protein interaction and might play a role in connecting the cell wall with the plasma membrane by anchoring target proteins (Baumberger *et al*. 2001, Cassab 1998). An enhancer of *lrx1*, *enl1*, is affected in the *ACTIN2* gene (Diet *et al*. 2004). *rhd2* is epistatic to *lrx1* and *LRX1* expression lowered in *rhd2*. *tip1* is also epistatic to *lrx1*, whereas *rhd3* and *rhd4* act parallel (Baumberger *et al*. 2003, Jones *et al*. 2006). The repressor of the *lrx1* mutation, *rol1*, compensates for the absence of *LRX1*. ROL1 is involved in rhamnose biosynthesis, a major component of pectin, suggesting structural changes in the cell wall cause suppression of the *lrx1* mutant phenotype (Diet *et al*. 2006). *EXP7*, *EXP18*, *CSLD*/*KJK PRP3*, *LRX1*, and *LRX2* contain a root hair-specific *cis*-element (RHE), which is conserved across angiosperms. This transcriptional module acts downstream of cell-fate determining pathways regulating the position-dependent root hair development like in Arabidopsis or the position–independent root hair development occurring in other species (Kim *et al*. 2006).

1.4 Aim of the work

Both iron and phosphate deficiency lead to an increase in the number of root hairs. First evidence for a differential regulation of iron- and phosphate-related root hair development was provided by Schmidt and Schikora (2001). In this work, an examination was conducted to identify further differences that may exist between root hairs of iron- and phosphate-deficient Arabidopsis plants. To this end, different approaches were used.

To find out, if the iron- or phosphate-sensitive root hair development was under local or systemic control, split root experiments were conducted that were combined with a sufficient or deficient shoot.

To determine, which stage of root hair development was influenced by iron and phosphate, mutants with defects in different stages of the root hair developmental pathway were investigated for their root hair patterning and root hair phenotype.

Finally, to identify potentially novel genes involved in root hair formation in adaptation to P starvation, mutants were screened that did not develop root hairs under P-deficient conditions but appeared normal, when the plants were transferred to P-sufficient medium. The phenotype of one mutant was examined in further detail and the mutated locus was isolated by map-based cloning.

2 MATERIALS AND METHODS

2.1 Plant material

The *Arabidopsis thaliana* wildtype Col-0 was used in the experiments. In addition, the following genotypes were investigated (Table 2).

Table 2: Genotypes of the mutants used in the experiment.

Mutant	Accession	Kind of mutagenesis	Plant age (d) in Ref.	Reference
frd3-1	Col	point mutation	not determined	Rogers & Guerinot 2002
pho1-2	Col	EMS	not determined	Delhaize & Randall 1995
rhl1	Ws	T-DNA (Feldmann 1991)	3	Schneider *et al*. 1997
rhl2-1	Col	EMS	3	Schneider *et al*. 1997
rhl3-1	Col	EMS	3	Schneider *et al*. 1997
erh1	Ler	fast neutrons	3	Schneider *et al*. 1997
erh3	Col	EMS	3	Schneider *et al*. 1997
wer	Col	EMS	4	Lee & Schiefelbein 1999
cpc	Ws	T-DNA	not determined	Wada *et al*. 1997
ttg	Ler	EMS	5-6	Galway *et al*. 1994
gl2-1	Ler	fast neutrons	4-5	Masucci *et al*. 1996
rhd6	Col	T-DNA (Feldmann & Marks 1987)	5	Masucci & Schiefelbein 1996
trh1	Ws	T-DNA	3	Rigas *et al*. 2001
tip1-2	Col	X-ray	3-5	Ryan *et al*. 1998
rhd2	Col	EMS	4	Schiefelbein & Somerville 1990
rhd3	Col	EMS	4	Schiefelbein & Somerville 1990
rhd4	Col	EMS	4	Schiefelbein & Somerville 1990
kjk	Ler	EMS	3-4	Favery *et al*. 2001

csld	Ws	T-DNA (Feldmann 1991)	4-7	Wang *et al*. 2001
rhd1	Col	EMS	4	Schiefelbein & Somerville 1990
lrx	Col	En-1 (Wisman *et al*. 1998)	4	Baumberger *et al*. 2001

The GL2-GUS lines were provided by J. Schiefelbein and the CPC-GUS lines by T. Wada.

2.2 Growth conditions

Plants were grown in a growth chamber on agar medium as described by Estelle and Somerville (1987). The medium was composed of (mM): KNO_3 (5), $Ca(NO_3)_2$ (2), $MgSO_4$ (2), KH_2PO_4 (2.5), and (µM): $MnCl_2$ (14), H_3BO_3 (70), $ZnSO_4$ (1), $CuSO_4$ (0.5), Na_2MoO_4 (0.2), $CoCl_2$ (0.01), NaCl (10), and 40 µM FeEDTA. Sucrose (44 mM) and 5 mM MES (2-[N-morpholino]ethanesulfonic acid) were included, and the pH was adjusted to 5.5. The medium was solidified with 0.6% (w/v) agar for horizontal and 0.8% for vertical culture (Fluka, Taufkirchen, Germany). The seeds of all genotypes were surface-sterilized by immersion in 5% (v/v) NaOCl for 5 min and 96% ethanol for 7 min, followed by four rinses in sterile water. Seeds were placed onto Petri dishes containing agar medium and kept for 3 d at 4°C in the dark, before the plates were transferred to a growth chamber. The *rhl*, *wer*, *ttg*, *gl2*, *cpc*, *erh*, *rhd*, *trh1*, *lrx*, *tip1*, and *kjk* mutants were grown at 21°C in continuous light (50µE, Philips TLD Double Flux 115 W/33 RS lamps, Eindhoven, The Netherlands). All other plants were cultivated at 21°C in a 12 h photoperiod with a light intensity of 175 µE (Philips TLD 58W/840 and alternating 58W/830 lamps, Hamburg, Germany).

For investigation of root hair patterning, differential cytoplasmic staining, and analysis of GUS plants, twelve-day-old plants were transferred to fresh agar medium (control plants), medium without FeEDTA and with 100 µM 3-(2-pyridyl)-5,6-diphenyl-1,2,4-triazine sulphonate (FerroZine®, Serva, Heidelberg, Germany; -Fe plants), or without P (-P plants). Five plants were placed per Petri dish. The lower concentration of K due to the absence of KH_2PO_4 in the -P medium was compensated for by the addition of 2.5 mM KCl. Plants were analyzed 7 days after transplantation. The Mutants from the root hair developmental pathway were analyzed after 9 days. The medium containing phosphite was obtained by replacing KH_2PO_4 with a freshly prepared filter-sterilized stock solution of potassium phosphite (Fluka, Taufkirchen, Germany) after autoclaving.

For the split-root experiments, the Col-0 wildtype and the *frd3-1* and *pho1-2* mutants were sown and transplanted to fresh control medium as described above. The root system of 25-day-old plants was then washed in Fe- or P-free nutrient solution and was divided into two nearly equal parts. One-half of the root system was grown on Fe- or P-deficient agar medium and the other half on sufficient medium (+/-Fe or +/-P plants). Two plants were placed per Petri dish. As controls, plant roots were split on divided plates containing medium either with or without Fe or P (+/+ or -/- plants). Root hair patterning was investigated two and seven

days after splitting. The root system of the *frd3-1* mutant was split on +/-Fe, +/+Fe and -/-Fe plates, the *pho1-2* mutant on +/-P, +/+P and -/-P media. Both mutants were analyzed after seven days.

For ICP, *per2* and Col-0 plants were cultured on Petri dishes and in aerated liquid culture. The liquid culture medium was composed of (mM): KNO_3 (3), $MgSO_4$ (0.5), $CaCl_2$ (1.5), K_2SO_4 (1.5), NaH_2PO_4 (0.5), (µM): H_3BO_3 (25), $MnSO_4$ (1), $ZnSO_4$ (0.5), $(NH_4)_6Mo_7O_{24}$ (0.05), $CuSO_4$ (0.3), and 40 µM FeEDTA. Plants were precultured for 32 d; the culture medium was changed weekly. The plants were then grown for one week in medium without NaH_2PO_4 (-P) and control medium (+P). One-half of the plants were replenished with 0.5 mM NaH_2PO_4 and harvested after two days. Five plants were used per genotype and treatment. The climate conditions were 21°C and a 10 h photoperiod at 300 µE (Planstar 400W Osram, Munich, Germany).

Plant material for DNA analysis, crossings, and production of seeds was grown in potting soil (GS-90 fein, Einheitserde-Werkverband, Sinntal-Jossa, Germany) mixed with vermiculite in a 1:1 ratio and supplemented with Lizentan® Combigranulat (Bayer, Monheim, Germany) according to the manufacturer's instructions. Light conditions were a 12 h photoperiod with alternating Master HPI-T+ and SON-T Green Power lamps (400 W, Philips, Hamburg, Germany).

2.3 Hand-cut sections, counting of root hairs, and photography

Root hair patterns were analyzed in cross-sections of 10 root apical segments collected from 10 different plants per genotype and treatment. The apical first cm of the root tip was excised, washed in 0.5 µM $CaSO_4$ and fixed in a 3% agarose solution. Hand-cut sections from the root hair zone were stained with 0.05% toluidine blue (Hoyer Merck, Darmstadt, Germany) in 10 mM natrium acetate pH or 0.1% Calcofluor White Fluorescent Brighterner 28 (Sigma, Munich, Germany) (http://www.lsa.umich.edu/mcdb1/faculty/schiefel/lab/protocols.html). One cell layer each was analyzed using a Zeiss Axioskop2 plus microscope (Zeiss, Jena, Germany). The number of cortical and epidermal cells and root hairs in H and N position as well as branched root hairs was counted in five sections per root segment. In *csld* mutant, root hair frequency was estimated in apical segments of 20 roots in the 2nd mm behind the apex under the Stemi 2000-CS stereomicroscope (Zeiss, Jena, Germany) in the dark field by counting the bulges. Statistical significance of differences between mean values was determined using Students *t*-test. Two experimental repetitions were not significantly different and were, therefore, combined into one value. Micrographs and dark field photos were recorded with a Nikon Coolpix 990 digital camera. Photographs of whole plants were taken with a Nikon D 70 mirror reflex camera.

2.4 GUS assay, histology, and differential cytoplasmic staining

For the detection of GUS activity, the roots were submerged in substrate solution consisting of 100 µM sodium phosphate, pH 7.0, containing 0.1% Triton-X-100, 1 mM X-Gluc (5-brom-4-chloro-3-indolyl-β-D-glucopyranoside), 10 mM EDTA, and 1 mM $K_3Fe(CN)_6$. The reaction time of the GL2-GUS plants was 60 min. CPC-GUS plants were stained for 7 h.

To localize GUS activity in H and N cells, microtome sections of plastic-embedded tissues were prepared. The embedding procedure was conducted at 4°C. Stained roots were fixed overnight in 50 mM sodium phosphate, pH 7.0, containing 2% glutaraldhyde. After rinsing in the respective buffer for 15 min, the tissue was dehydrated in a graded ethanol series of 10, 20, 40, 60, 80, 90, and 95% (v/v) for 10 min each and two times in 100% ethanol for 30 min. The tissue was infiltrated with pure LR White (London Resin Co. Ltd., London, GB) followed by one change of LR White for 1 h each and one change overnight. The root segments were placed into gelatine capsules (Plano, Wetzlar, Germany) and polymerized at 60°C for 14 h. Transverse sections (4 µm) cut with a Microm HM 355 microtome using 45° glass knives were mounted on slides and covered with Roti®-Histokitt (Roth, Karlsruhe, Germany). Sections were examined in a Zeiss Axiophot photomicroscope by bright-field microscopy and photographed with a Nikon D1 digital camera. The images were processed with Adobe Photoshop software to enhance the differential signals detected in epidermal cells. The patterning of GUS activity was investigated with images of four sections per root and six roots per genotype and treatment.

For detection of the differential cytoplasmic staining, wildtype roots were embedded and cut as described above and stained with toluidine blue.

2.5 Cryo-SEM

For cryo-SEM root tips were fixed on the probe plate with carbon adhesive and frozen in liquid nitrogen at -175°C. After sublimation at -95°C in an Oxford-Cryochamber-/Transfersystem CTS 1500C roots were observed in a Hitachi S-3200N scanning electron microscope.

2.6 Ferric-chelate reductase activity

The ferric-chelate reductase activity was measured with intact roots in the growth medium described above without sucrose and agar containing 0.5 mM FeEDTA and 0.5 mM FerroZine®. Five individual experiments with 10 plants per treatment (+/+Fe, -/-Fe, +/-Fe) were conducted.

2.7 Mutant screening

For the mutant screening and analysis, seeds were sown directly on medium without P and analyzed after 14 days. Mutants were screened that do not develop root hairs on P-deficient medium but form normal root hairs after transfer to P-sufficient medium. The roots were observed in the dark field with the Stemi 2000-CS stereomicroscope (Zeiss, Jena, Germany). A population of 39,266 EMS-mutagenized M2 plants (Col-0, Lehle seeds) and 31,326 M2 plants from a T-DNA mutant population (Ws, 1st 49 of 100 Feldmann pools, NASC stock code N3115, set N2606-N2628) were screened. Two-hundred-five M3 lines of putative mutants from the EMS screening and 13 M3 lines of putative mutants from the T-DNA screening were re-analyzed for the described phenotype. About 100 plants per line were investigated.

2.8 Crossing and analysis of double mutants

The *per2* mutant was backcrossed to Col-0, and mapping populations with C24, Cvi, Ler, and Nd were prepared. Double mutants were generated with *gl2-1* and *erh3*. Reziprocal crosses were made. From five 5-week-old plants of each genotype, all secondary inflorescences were excised, and the meristem of the primary inflorescence and flowers with white petals was removed. From 5-6 remaining buds, all anthers were removed. After two days, unwantedly fertilized flowers were removed and the absence of anthers in remaining flowers was checked. The stigma was pollinated with anthers from the respective father genotype. F1 plants were self-pollinated to obtain F2 progeny. Phenotypical analysis of double mutants was conducted with about 800 F2 plants.

2.9 Map-based cloning

Low resolution mapping of the *per2* mutation was performed by linkage analysis with the SNP marker set described by Törjek *et al*. (2003). One-hundred-thirteen F2 plants from a mapping population with C24, which displayed the *per2* root hair phenotype, were analyzed with the markers MASC03658, MASC02577, MASC06086, MASC05857, MASC05386, MASC02947, MASC04279, MASC05045, MASC09219, MASC02820, MASC05208, MASC03154, MASC09207, MASC04317, and MASC04576 spanning the whole genome and with MASC03898, MASC02999, MASC05312, MASC03344, MASC02841, and MASC04516 from the upper arm of chromosome 3. Recombination frequencies were transformed into genetic map distances (D) using the Kosambi function. Fine mapping was performed with 987 F2 plants exhibiting the *per2* phenotype from a mapping population with Cvi. Plants that had a recombination event between MASC04279 and MASC02841 were analyzed with a higher marker density in that region. SNPs were obtained from TAIR and by

sequence comparisons of intergenic regions from Col-0 and Cvi. The phenotype of the recombinant lines was again checked in the F3.

2.10 DNA-isolation

About 50 mg leaf material were harvested into 12x96 collection microtubes (Qiagen, Hilden, Germany), which were cooled with liquid N_2 and disrupted 2 min in the Retsch mill (Retsch, Haan, Germany) at a frequency of 20/s. The powder was mixed with 8 mM Tris, pH 8.0, containing 400 mM NaCl, 40 mM EDTA, and 2% SDS and incubated at 60°C for 20 min. After precipitation with 200 µl 3 M potassium acetate, pH 4.8 at 4°C for 10 min, proteins were removed by centrifugation at 5,600 g for 10 min. The supernatant was transferred to fresh collection microtubes and the DNA was precipitated by mixing with 40 µl 3 M sodium acetate, pH 5.2 for 30 sec. After centrifugation, the DNA pellet was washed with 200 µl 70% ethanol and dried for 10 min at 60°C. The DNA was resolved in 150 µl 10 mM Tris/HCl, pH 8.0, containing 1 mM EDTA and heated for 5 min at 60°C. One µl 100 mg/ml RNase (Marcherey-Nagel, Düren, Germany) was added and incubated at 37°C for 10 min. DNA was precipitated with 15 µl 3 M sodium acetate, pH 5.2, and 300 µl 96% ethanol and washed with 200 µl 70% ethanol. After drying for 20 min at 60°C, the DNA was resolved in 150 µl 10 mM Tris/HCl, pH 8.0, containing 1 mM EDTA. DNA for the fine mapping was isolated with the DNeasy 96 Plant Kit (Qiagen, Hilden, Germany) according to the manufacturer's instructions. The DNA quality was checked by electrophoresis in a 1% agarose gel containing 40 mM Tris/acetate, pH 8.5, 1 mM EDTA, and 0.01 µl/ml ethidiumbromide (Fluka, Taufkirchen, Germany). Ten µl DNA solution were mixed with 5 µl loading buffer composed of 25% glycerin containing xylene cyanol (Sigma, Munich, Germany) and bromphenol blue (Aldrich, Munich, Germany). Electrophoresis was run at 90 mV.

2.11 PCR, SNaPshot analysis, and sequencing

SNPs were detected with primer extension using the SNaPshot method. For this, 200-400 bp DNA fragments containing the respective SNP were amplified. Primers were designed using the Primer 3 program (http://frodo.wi.mit.edu/cgi-bin/primer3/primer3_www.cgi#PRIMER_SEQUENCE_INPUT). PCR was conducted in a 12.5 µl reaction mixture containing 1.5 µl of the DNA solution, 10 mM Tris/HCl pH 9.0, 2 mM $MgCl_2$, 0.8 mM dNTPs (Qbiogene, MP Biomedicals, Germany), 0.5 nM primers, and 0.75 U Taq DNA-polymerase (OptiTaq, roboklon, Berlin, Germany). The cycling conditions were 94°C for 2 min, 40 cycles of 94°C for 10 s, 55°C for 30 s, 72°C for 1 min, and 2 min termination at 72°C. Five µl of the PCR product was electrophoretically checked in a 2.5% agarose gel as described above.

For sequenzing, 500-600 bp fragments were amplified. PCR was performed as described above. Sequencing was done by Martin Meixner (Services in Molecular Biology, Berlin, Germany). SNPs were identified by using Sequencher software.

Primers for low resolution mapping were used according to Törjek *et al*. (2003). Primers (5'→3') for high-resolution mapping are listed in Table 3 and primers for sequencing in Table 4.

Table 3: Primers for SNaPshot analysis

Marker	Forward primer	Reverse primer	SNaPshot primer
K13E13[1]	acattcgttcatcacaagctcg	actctccattaggcccatcaagg	agactctacggttggttgcgga
MVI11[1]	catcccggttcataccattc	caatccacccatttgcttct	gcgaaaacgcgatgaggaaagtga
MMB12[1]	tcccaagctgccataaactc	caaactagcccccgtcatta	agcaccaccacgagcaccca
MQC12[2]	tcgataaccgatcagggcgt	acatttgtcgacacccctggagt	catatgctcgctgtgttctttg
MQC12-1[2]	attgcgggagacactgaaat	gagatgggcatgctaaaacc	actgaaatcagtgaaggacatt
K10D20-7.16[2]	tcttgtgttttcttgtcatcgtg	ccccagatcccaagtgtgta	taaccacaaactgttttgagc
K10D20f[2]	agcagctccccacaaattac	tttcgatagaagctgaaacaaga	ttacatgtctccatcattgac
F3H11-1r[2]	caaaaatccgcctccttaca	atgagaatcgcgggataaca	agaatcgcgggataacaatact
F3H11-7.22[2]	ggggaaaatcattgatagtgct	tgagagtatgggaccattgc	ttcacgtcgatgataacctat
M0E17-3[2]	gctcctcttgggtttatgtgg	gccattgagattttgatagcac	tggtatgactttaaggagaag
M0E17-2f[2]	tgattctttaccccaaaactgaa	cgaaacttggatcagcaaaa	tgtgattccttggttatctac
MFD22[2]	tcttagaaacacgcatcagacc	cctcggatacataatgcatcagc	cggatacataatgcatcagcat
MSA6[2]	gtatcgcttcaaacccaagtcca	tgcagaaatgacaagcccct	cattaacgctctaatattgtt
MIL23[1]	agaatgtgaaggcttggtctg	accgttaccgcatccggttca	gatgtgcatgaagctagagctat
MKA23[1]	ctattctcccactgggtctg	tggcatgttgatacctgagca	gacaagggtttccacgaaatgc

[1] The source of SNP is NASC SNP database (http://www2.mpiz-koeln.mpg.de/masc/search_masc_snps.php), [2] The source of SNP is this work

Table 4: Primers for sequencing

Fragment	Forward primer	Reverse primer
MQC12	gggtgcctttcactgatgtt	gcattatattggggcttgga
K10D20-7.157as	gtaaaaattccccgcctagc	tgtcaatatgtcatcatcatcagaa
K10D20-7.157bs	tcctctaatgcgaaatgtatgc	aaaaatggaggacaagccttaac
K10D20-7.16s	tgtacacaatgcggttgtca	aaagcatttttgggtctcca
K10D20	cgagaacgtggaccgactat	cgcctcacacagttgcttag
K10D20-2	atccgatgtcagtggtgtga	gacgccatctcattggtttt
F3H11-1	gtggccaatgtgggttttac	tatggcccacaatggttttt
F3H11-2	tggattttggctcgagattc	cgacaacatcatttggcttg
F3H11-7.22s	tcatgggaatggcattgata	aaccggaggaggcttaacat
F-F3H11/M0E17	cattgtggttgctggttttg	ttgcattgaatcctccatga
M0E17-1	taagccaaaatggaggaacg	gtacgaggaagcgagcaagt

M0E17-2	attcgatgcggttctacgtc	ttgaatgatcccgagaaagg
M0E17-3	cgaagagatcaaaccggaag	taacgttctcgtcgcttgtg
M0E17-4	ctcgaagtgcacgcatgtat	atccttgattgccgatcttg
MFD22	gtgcagcatttgaagggttt	tcattgctgccattgttgat
MSA6	tctcgaacaatgtgtgtttgc	tgcagaacatgggttaaacg
At3g20500-1	gcgtcgcaaaagcctataaa	caggaccaaatgaatctaaaaaca
At3g20500-2	tgaagaaaacattgatgcttga	catccacggccttacacttg
At3g20500-3	ccaggggatctatcgtatgc	cagccatcatttcatcacctt
At3g20500-4i	aggctgatctctcgaaggtg	ccactctggtgacggatctt
At3g20500-5	tcacacttacggtgcagttg	tgtcacattcgttgaaccatc
At3g20510-1	tccttttgaacattactcacattagg	cccagatcgctaaaaaggaa
At3g20510-2	agtgttcttgccattgattga	gcgttatgacaaccgcatt
At3g20510-3	tcgctggttatatcagtctcaaa	ttcagatgagtttcagtcacca
At3g20530-1i	atcattcttctttttaaggtttcaat	tttgcatcaatgcagtctttg
At3g20530-1.1	tgatccctttggattcgag	tgttccggggtttctatctg
At3g20530-2	aaagaagcgaggcgtatttg	gccgcaactttcattcttgt
At3g20530-3	gcgcggaacaagaagaag	acattgctgctactgcaagc
At3g20530-4i	aggcgagtccattgttcaaa	gccattgctctatgacaaacc
At3g20555-1	tcgtctataatattggcgtacact	aagccgcttgtaacgtcgta
At3g20590-1	tgactttgccagtcagttgg	tgagatccagcctgaaaacc
At3g20590-2	tttctccaccatcaacacga	gcaaaagttgaaatcaaacacc
At3g20600-1	tcaaccaatcagcaaaccaa	ctgaaaacagccgatccatt
At3g20600-2	aagccgctaaacaaccagac	tttccccatttgaacggtta
At3g20610-1	ccggttattgtaccatgccta	accgcttgaataaccgtctg
At3g20610-2	ccacacgtatcaacaactcctc	cacatgcatcaaaccaaagc

2.12 Anthocyanin measurement

Anthocyanin absorption of 20-day-old plants from vertical culture was measured. Leaf material (10-50 mg from 2-4 plants) was homogenized with a RZR 2020 homogenisator (Heidolph, Schwabach, Germany) in 1.5 ml of a mixture of propanol:HCl:H_2O (18:1:81) and extracted in boiling water for 1.5 min. After centrifugation at 16,400 g for 10 min, the extinction of the supernatant was measured at $\lambda = 535$ nm in a Novaspect II spectro photometer (Pharmacia, Freiburg, Germany). Four replicas were performed and the experiment repeated once. One representative experiment is shown.

2.13 Inductively coupled plasma emission spectroscopy (ICP)

For elemental analysis material from roots, shoots, and seeds was dried for 7 d at 60°C and then ground to powder. Material (50-100 mg) was weight into Teflon vessels and 1 ml HNO_3 (Suprapur, Merck, Darmstadt, Germany) and 0.5 ml Millipore-quality water were added. The material was digested at 200°C and 15 bar for 1.5 h in a MARS 5 microwave (CEM, Kamp-Lintford, Germany). The volume of the extract was adjusted to 12 ml and Ca, K, Mg, P, S, Fe, B, Cu, Mn, Mo, Co, Ni, and Zn concentrations were measured in an IRIS Advantage Duo ER/S ICP spectroscope (Thermo Jarrell Ash, Franklin, MA, USA).

3 RESULTS

3.1 Root hair patterns of the Arabidopsis wildtype adapted to the Fe and P availability

Iron- and phosphate-deficient plants increased the number of root hairs (Fig. 2, a-c). Under P starvation, root hairs were also markedly elongated; their length increased from 0.2 ± 0.01 up to 0.6 ± 0.02 mm (Fig. 2c). For a more detailed phenotypic analysis of root hairs, which are developed in adaptation to the Fe and P availability, root hair patterns were analyzed in cross-sections (Fig. 2, d-f; Fig. 3).

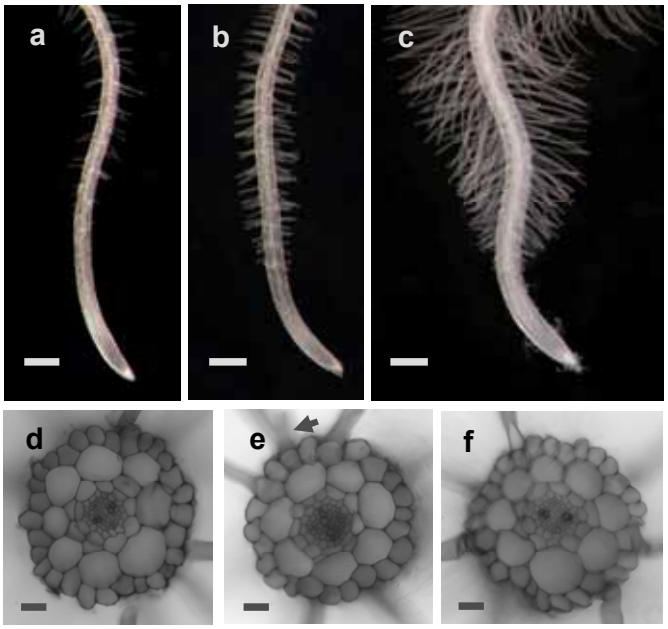

Figure 2: Root tips (a-c) and hand-cut sections (d-f) of 18-day-old Col-0 plants grown under sufficient nutrient supply (a, d), Fe deficiency (b, e), or P deficiency (c, f). Bar = 250 µm (a-c) and 20 µm (d-e). The arrow head indicates a branched root hair out of focus.

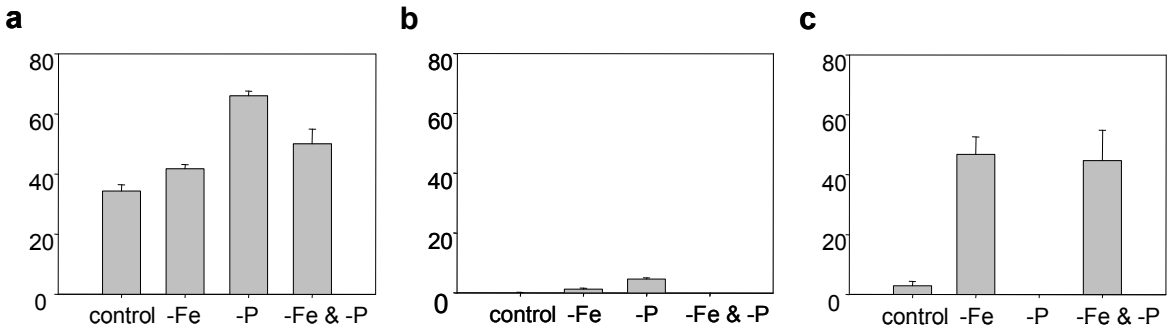

Figure 3: Root hair patterns of the primary roots of 18-day-old Arabidopsis plants grown under sufficient nutrient supply (control), without Fe (-Fe) or P (-P) for seven days, or without both nutrients for four days (-Fe & -P). (a) % of root hairs in the H position. 100% correspond to the total number of epidermal cells that had contact to two underlying cortical cells. (b) % of root hairs in the N position. 100% correspond to all epidermal cells with contact to one underlying cortical cell. (c) % of branched root hairs. 100% corresponds to the sum of root hairs in the H and N position. n = 20 plants.

In contrast to seedling roots, in which nearly all epidermal cells in the H position develop a root hair (Galway *et al*. 1994, Masucci *et al*. 1996; Table 5), in the aging primary root and in laterals this number was considerably reduced (Fig. 3a; Table 5). Under sufficient nutrient supply, only 34% of the H positions formed a root hair (Fig. 3a). This proportion was slightly increased under Fe deficiency (P value = 0.1 with n = 10 plants, $P = 0.005$ with n = 20). However, P-deficient plants nearly doubled their root hair number in the H position (Fig. 3a). In the N position of sufficient plants, no root hairs were formed (Fig. 3b). Under Fe and P deficiency, a significant increase of root hairs in this position occurred, which was more pronounced in plants grown without P ($P \leq 0.05$; Fig. 3b). In Fe-limited plants, nearly one-half of all root hairs were branched at their base. Branching was never observed in P-starved plants (Fig. 3c; Fig. 4, b-c). Thus, it appears that the increase in the absorptive surface area is realized by different developmental programs in response to Fe and P deficiency, either by the formation of branched root hairs as in the case of -Fe plants or by an increase in the number of root hairs as in the case of –P plants. Lateral roots behaved in the same manner (Table 5). If the plants were cultivated in the absence of both Fe and P, the root hair frequency is intermediate between the individual Fe or P deficiencies, indicating a contrasting effect of the two deficiency signals on the modulation of the root hair number (Fig. 3a). The rate of root hair branching was as high as under Fe-limitation alone, suggesting the stimulation of root hair branching under Fe deficiency abolishes the suppression of branching in P-deficient plants (Fig. 3c). The branched root hairs exhibited a regular shape. Always two branches of the same length developed that were arranged in the transversal layer (Fig. 2e; Fig. 4c).

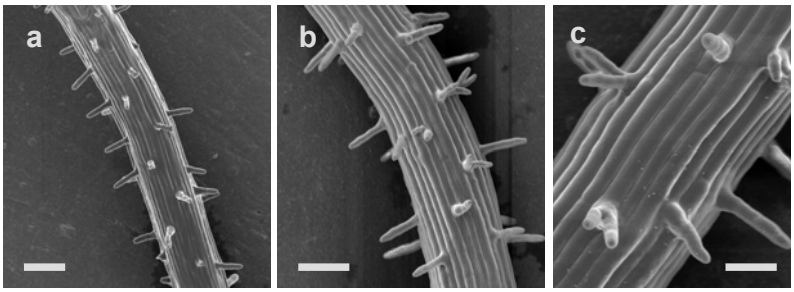

Figure 4: Cryo-scanning electron microscope images of Fe-sufficient (a) and Fe-deficient (b, c) Arabidopsis roots. Bar = 20 µm.

3.2 Split-root experiments

To determine whether the root hair phenotype of Fe- or P-deficient plants is controlled by a local or a systemic signaling pathway, we conducted split-root experiments, in which the root system of adult Arabidopsis plants was divided into two nearly equal parts. One-half of the root system was exposed to control medium and the other half to Fe- or P-deficient medium. A reaction of the deficient part of the root system is indicative of a local control, while a response on both halves of the root system points to a systemic regulation. In the case of both nutrients, the root hair phenotype of different experimental variations was investigated. Initially, plants with a sufficient shoot were treated for two or seven days; time points corresponding to the state of early or late adaptation to nutrient shortage. Subsequently, plants with an Fe- or P-deficient shoot and plants without a shoot were analyzed for root hair development. The nutrient-deficient shoot was achieved by utilizing mutants with reportedly disrupted xylem loading of either Fe or P. In the case of Fe, we made use of the *frd3* mutant (Green & Rogers 2004). In *frd3*, all components following the xylem loading (Fig. 1) suffer from a lack of iron, and a systemic deficiency response is triggered. An analougous mutant defective in the xylem loading of P is *pho1* (Poirier *et al*. 1991).

Regulation of root hair development under Fe deficiency

As a control for the induction of the root Fe deficiency response, the ferric-chelate reductase activity in the roots was measured (Fig. 5). The enzyme showed a 24-fold induction in -/-Fe plants; the activity in both split-root halves of +/-Fe plants was equal to the +/+Fe controls. This finding indicated the existence of a systemic signal that represses the Fe deficiency responses.

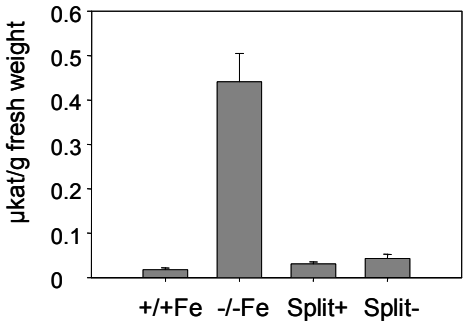

Figure 5: Ferric-chelate reductase activity in the roots of plants that were split two days on +/+Fe, -/-Fe, or +/-Fe agar media. The reductase was measured as an end-point determination. Results are an average of three independent experiments, each with 10 plants. Treatment for three days gave the same results.

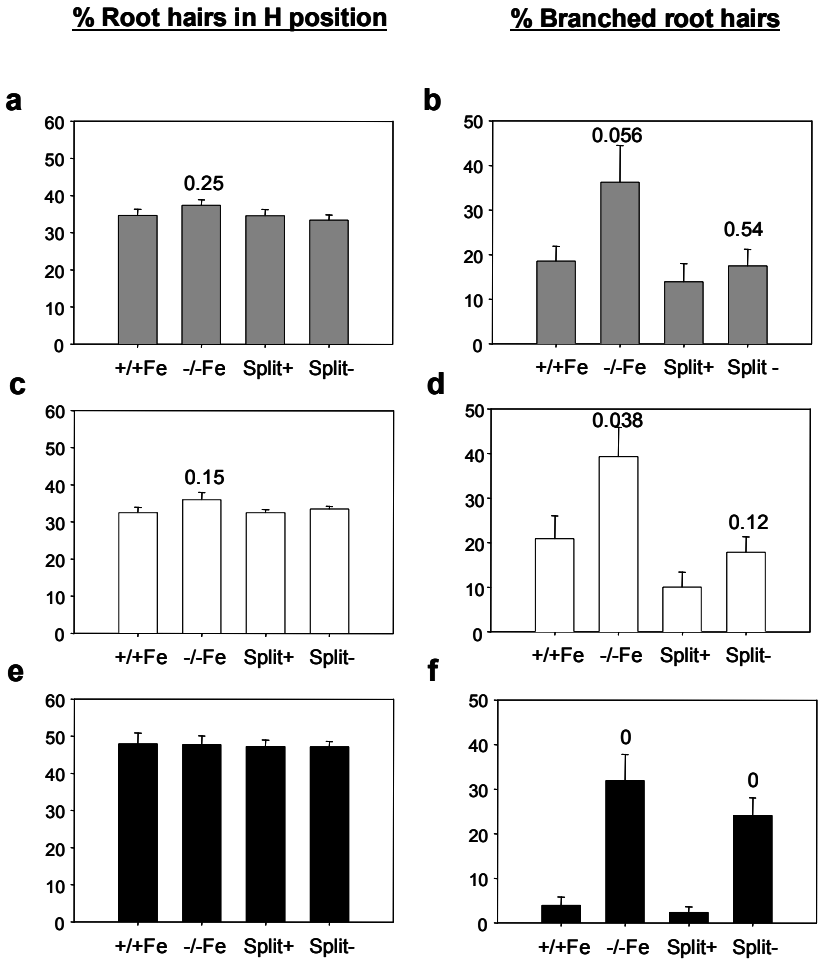

Figure 6: Split-root experiments related to Fe nutrition. Roots of 25-day-old Arabidopsis were divided into two approximately equal parts and grown on +/+Fe, -/-Fe, or +/-Fe agar medium as indicated in the x-axis of each bar graph. The mean percentage ± standard error of root hairs in the H position and of branched root hairs was determined after two (a, b) and seven days (c, d). The split-root experiment was also conducted with the *frd3-1* mutant that has an Fe-deficient shoot (e, f). The occurrence of root hairs in the N position was below 1% in all treatments. Numbers above the bars in the charts indicate the *P* value that results from the respective t-test comparing either +/+Fe with -/-Fe or the split+ with the split- halves of the root. n = 10.

In the roots of -/-Fe split plants, the frequency of root hair branching increased compared to +/+Fe split plants (Fig. 6, b, d) as in the case of non-split plants (Fig. 3c). A slight increase in the root hair number was not statistically significant (Fig. 6, a, c). In the +/-Fe wildtype, the frequency of branched root hairs was low and did not differ significantly in both split-root halves after two and seven days (Fig. 6, b, d). Because the branching frequency in -/+ split-root plants was similar to that in +/+Fe controls, a systemic repression of root hair branching caused by a sufficient shoot can be assumed. The formation of branched root hairs in +/+Fe split-root plants (Fig. 6, b, d) was higher than in Fe-sufficient non-split control plants (Fig. 3c) and might have been caused by wounding stress resulting from the splitting procedure.

Split-root plants with an Fe-deficient shoot like in the case of the *frd3-1* mutant revealed a marked increase in the frequency of branched root hairs under -/-Fe conditions compared to +/+Fe split plants (Fig. 6f). If the systemic Fe deficiency signal of *frd3-1* was combined with a local +Fe signal in +Fe halves of +/-Fe plants, a local repression on root hair branching was observed (Fig. 6f). In addition, root hairs in the H position were increased compared to the wildtype under all conditions (Fig. 6e). Together, the root hair branching typical of Fe-deficient plants only occurred if both a local and a systemic Fe deficiency signal were present. In other words, any Fe sufficiency signal was able to repress the response, regardless of its local or systemic origin and acted, thus, dominantly.

Regulation of root hair development under P deficiency

The most significant effect of P deficiency (-/-P) on the enlargement of the root surface was an increase in the number of root hairs in the H position (Fig. 7, a, d) and N position (Fig. 7e). Additionally, a significant decrease of the root hair branching frequency was observed (Fig. 7, c, f). In the +/-P split wildtype, root hairs in the H position were significantly increased in the –P halves compared to the +P halves after a treatment for two and seven days (Fig. 7, a, d). The suppression of root hair branching also followed a local –P signal (Fig. 7, c, f).

Plants with a P-deficient shoot resulting from the *pho1-2* mutation showed a P deficiency response with regard to the frequency of root hairs in the H position under all treatments (Fig. 7g). The systemic P deficiency signal was not suppressed by a sufficient local P concentration, indicating a dominant role for a systemic P deficiency signal over a signaling pathway perceiving a local abundance of the nutrient. Furthermore, the number of root hairs in the N position was significantly increased in –P root-halves of +/-P *pho1-2* (Fig. 7h), pointing to a local effect in combination with a systemic P deficiency signal. The frequency of branched root hairs was similar to the wildtype, indicating that a local suppression by low P was independent of the systemic P status (Fig. 7, c, f, i, l, o).

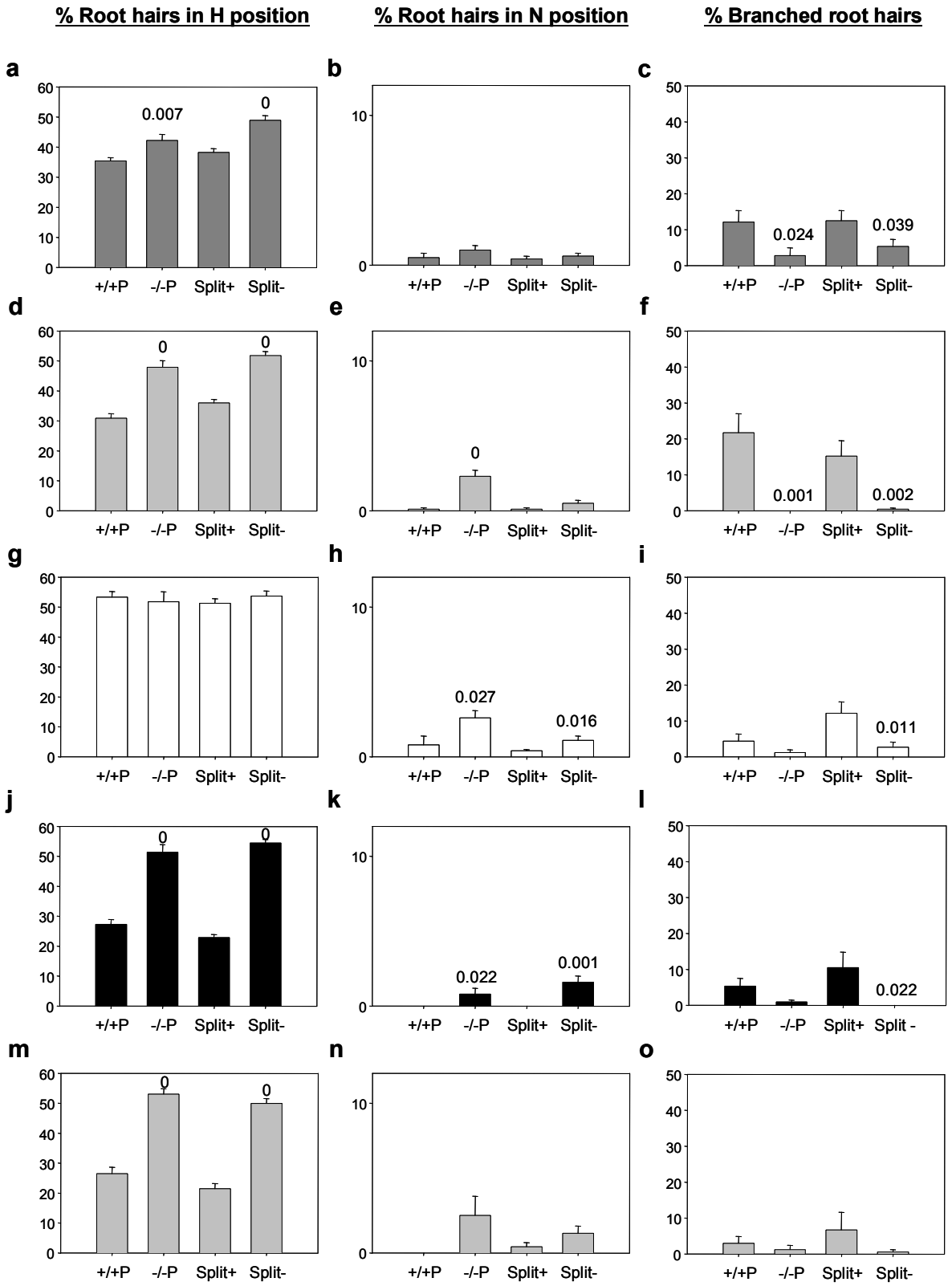

Figure 7: Split-root experiments related to P nutrition. Plants were grown on +/+P, -/-P, or +/-P agar media. +/+P is the same as +/+Fe in Fig. 2, but was determined separately. The mean percentage ± standard error of root hairs in the H position root hairs in the N position, and branched root hairs was determined after two (a, b, c) and seven days (d, e, f). (g, h, i) Split-root experiments with the *pho1* mutant that had a P-deficient shoot and (j, k, l) with wildtype plants and (m, n, o) *pho1* whose shoot was removed. Numbers above the bars in the graph indicate the *P* values that results from the respective *t*-test comparing either +/+P with -/-P or the split+ with the split- halves of the root.

A local –P signal in wildtype roots without a shoot caused a significant increase of root hairs (Fig. 7j). The *pho1-2* mutant without a shoot reacted similarly to the wildtype, providing evidence that the behavior of the mutant was the result of a shoot-born signal, communicating the P status of the shoot to the root (Fig. 7m). Together, the increase in the root hair number of P-depleted plants was triggered by the presence of a P deficiency signal, regardless of its local or systemic origin. In other words, the P deficiency signal acted in a dominant way.

3.3 The influence of Fe and P availability on the stages of root hair development

Mutants with defects in the root hair developmental pathway have been investigated mainly in 3-5-day-old roots (Table 2). At this seedling stage, nearly all epidermal cells in the H position form a root hair in the wildtype (Dolan *et al*. 1994, Galway *et al*. 1994, Lee & Schiefelbein 2001). This was also observed in the present study when the plants were germinated on P-sufficient or P-deficient media (Table 5). However, if the plants were germinated on Fe-depleted medium no root hairs developed (Table 5). This result was similar to 2-week-old plants that also formed no root hair during the first 3 days after transfer to -Fe medium. Thereafter, root hairs developed in both cases. To determine whether defects in seedling root hair development also affect root hair formation of aging plants during the response to nutrient starvation, 19 mutants harboring defects in different stages of seedling root hair development were grown in the presence and absence of Fe and P. Mutants affected in different processes of root hair specification, initiation, bulge formation and tip growth were included in this study (Table 5).

Analysis of mutants with defects in root hair specification

The *ERH1* and *ERH3* genes are required for correct differentiation of hair and non-hair cells in positions corresponding to the underlying cortex (Schneider *et al.*, 1997). *ERH3* encodes a katanin-p60 protein involved in the regulation of microtubules and cell wall biosynthesis (Burk *et al*. 2001, Webb *et al*. 2002). Under all conditions, both mutants formed more root hairs than did wildtype plants in the H position (Table 5). This might in part be due to a significantly higher number of cortex cells in both mutants, increasing the epidermal cell number in the H position. However, if this were taken into account, the root hair number would also be higher. In the N position, more root hairs were formed as well. This indicates that the *ERH* genes might be involved in rhizodermal cell differentiation also of elder plants. An increase in root hair frequency in response to Fe and P deficiency was, however, apparent when compared to the sufficient control, but the factor was slightly lower than in the wildtype suggesting the response to the nutrient supply was only slightly influenced in *erh1* and *erh3*. The number of branched root hairs formed in response to Fe deficiency was significantly lower in *erh* plants.

Table 5: The effect of Fe and P deficiency on root hair formation in the primary roots of 3-week-old Arabidopsis wildtype and mutant plants. Values represent the number (mean ± S_E) of the indicated cell type per cell layer. Ten roots were scored for each genotype and treatment.

	Root hairs in H position			**Root hairs in N position**			**Branched root hairs**			**Cortical cell number**			**Epidermal cell number**		
Gene	Control	-Fe	-P	Control	-Fe	-P	Control	-Fe	-P	Control	-Fe	-P	Control	-Fe	-P
primary root	3.0 ± 0.2	3.5 ± 0.1	5.0 ± 0.2	0.1 ± 0.03	0.4 ± 0.1	1.2 ± 0.2	0.1 ± 0.1	1.3 ± 0.2	0	8.1 ± 0.1	8.4 ± 0.3	8.2 ± 0.1	27.7 ± 0.6	26.3 ± 0.3	28.8 ± 0.6
lateral root	2.6 ± 0.2	3.8 ± 0.2	5.1 ± 0.1	0.02 ± 0.02	0.2 ± 0.1	0.6 ± 0.1 [a]	0.07 ± 0.04	0.8 ± 0.2	0	9.4 ± 0.4	8.3 ± 0.3	8.8 ± 0.2	22.9 ± 0.5 [a]	21.7 ± 0.5 [a]	24.7 ± 1 [a]
seedling root	7.8 ± 0.2 [a]	0 [a]	7.9 ± 0.1 [a]	0	0	0.3 ± 0.1 [a]	0.1 ± 0.1	0	0	8.3 ± 0.1	8.2 ± 0.1	8.3 ± 0.2	23.6 ± 0.4	22.5 ± 0.4	22.8 ± 0.6
erh1 [d]	3.7 ± 0.2 [a]	4.6 ± 0.2 [a]	5.2 ± 0.3	0.6 ± 0.1 [a]	1.7 ± 0.2 [a]	2.2 ± 0.2 [a]	0.06 ± 0.03	0.5 ± 0.1 [a]	0.04 ± 0.04	9.4 ± 0.3 [a]	9.6 ± 0.3	9.1 ± 0.3 [a]	32.3 ± 0.5 [a]	31.0 ± 0.4 [a]	30.7 ± 0.8
erh3	4.3 ± 0.2 [a]	4.8 ± 0.3 [a]	5.9 ± 0.2 [a]	0.8 ± 0.1 [a]	1.0 ± 0.2 [a]	1.7 ± 0.3	0	0.1 ± 0.1 [a]	0	9.5 ± 0.4 [a]	9.9 ± 0.4 [a]	9.9 ± 0.3 [a]	28.3 ± 0.5	26.5 ± 0.9	27.9 ± 0.4
wer	0.2 ± 0.1 [a,b]	3.9 ± 0.3	3.8 ± 0.2 [a]	0	4.6 ± 0.6 [a]	5.3 ± 0.3 [a]	0	1.3 ± 0.5	0	8.4 ± 0.4	8.2 ± 0.2	8.4 ± 0.2	27.3 ± 1.7	26.9 ± 0.5	27.9 ± 0.6
cpc [d]	0.6 ± 0.1 [a]	2.6 ± 0.2 [a]	2.9 ± 0.2 [a]	0	0.1 ± 0.03	0 [a]	0.05 ± 0.03	0.3 ± 0.1 [a]	0.02 ± 0.02	8.6 ± 0.2	8.4 ± 0.2	8.3 ± 0.1	26.6 ± 0.4	25.8 ± 0.4	27.9 ± 0.6
ttg [d]	3.5 ± 0.5	4.2 ± 0.4	5.6 ± 0.3	3.2 ± 0.5 [a]	4.5 ± 0.8 [a]	9.2 ± 0.4 [a]	0.04 ± 0.04	0.1 ± 0.1 [a]	0	8.6 ± 0.2	8.9 ± 0.3	8.9 ± 0.2	29.4 ± 0.5	28.1 ± 0.8	30.8 ± 0.6 [a]
gl2-1 [d]	5.2 ± 0.3 [a]	4.6 ± 0.4	5.8 ± 0.2 [a]	4.1 ± 0.5 [a]	2.8 ± 0.8 [a]	6.3 ± 0.4 [a]	0.02 ± 0.02	0.3 ± 0.2 [a]	0	8.7 ± 0.2	8.5 ± 0.2	8.7 ± 0.3	30.8 ± 0.6 [a]	27.9 ± 0.9	30.0 ± 0.4
rhl1 [d]	0 [a]	0 [a]	0 [a]	0	0 [a]	0 [a]	0	0 [a]	0	n.d.	n.d.	n.d.	n.d.	n.d.	n.d.
rhl2-1	0 [a]	0 [a]	0 [a]	0	0 [a]	0 [a]	0	0 [a]	0	n.d.	n.d.	n.d.	n.d.	n.d.	n.d.
rhl3-1	0 [a]	0 [a]	0 [a]	0	0 [a]	0 [a]	0	0 [a]	0	n.d.	n.d.	n.d.	n.d.	n.d.	n.d.
rhd6	0 [a]	0 [a]	0 [a]	0	0 [a]	0 [a]	0	0 [a]	0	8.2 ± 0.3	8.4 ± 0.2	8.4 ± 0.2	31.2 ± 0.5 [a]	30.7 ± 0.9 [a]	30.4 ± 0.5 [a]
trh1 [d]	0.2 ± 0.1 [a,b]	0.04 ± 0.04 [a,b]	4.5 ± 0.3	0	0 [a]	1.7 ± 0.2	0	0 [a]	0.06 ± 0.04	8.6 ± 0.4	8.0 ± 0	8.7 ± 0.2	27.0 ± 0.5	25.2 ± 0.3	28.6 ± 0.3
tip1-2	3.1 ± 0.2	3.8 ± 0.3	5.5 ± 0.3	0.09 ± 0.03	0.7 ± 0.2	0.8 ± 0.2	2.8 ± 0.2 [a]	3.5 ± 0.4 [a]	4.1 ± 0.3 [a]	9.6 ± 0.3 [a]	8.5 ± 0.2	9.9 ± 0.2 [a]	33.0 ± 0.7 [a]	26.6 ± 0.4	31.7 ± 0.6 [a]
rhd2	2.2 ± 0.3	4.5 ± 0.3	5.5 ± 0.3 [c]	0.06 ± 0.03	0.9 ± 0.3	0.6 ± 0.1 [c]	0.06 ± 0.04	1.0 ± 0.3	0.04 ± 0.03	8.5 ± 0.3	9.1 ± 0.3	9.0 ± 0.3	27.3 ± 0.5	26.9 ± 0.4	26.9 ± 0.3
rhd3	3.4 ± 0.1	4.4 ± 0.3	5.1 ± 0.3	0.04 ± 0.04	0.1 ± 0.04	1.1 ± 0.2	0.4 ± 0.3	1.3 ± 0.3	0.04 ± 0.03	9.1 ± 0.4	8.4 ± 0.2	8.6 ± 0.3	25.3 ± 0.8	25.4 ± 0.2	25.8 ± 0.6
rhd4	3.3 ± 0.2	4.3 ± 0.1 [a]	5.8 ± 0.2	0.2 ± 0.1	1.2 ± 0.3	0.9 ± 0.1	0.08 ± 0.03	0.8 ± 0.2	0.08 ± 0.07	8.6 ± 0.2	8.3 ± 0.2	8.3 ± 0.1	28.5 ± 0.5	25.7 ± 0.3	27.6 ± 0.6
kjk [d]	0.6 ± 0.2 [a]	2.9 ± 0.6	5.1 ± 0.3	0	0.2 ± 0.1	1.0 ± 0.2	0	0.1 ± 0.1 [a]	0.04 ± 0.03	8.4 ± 0.2	8.8 ± 0.2	8.5 ± 0.2	28.8 ± 0.7	30.2 ± 0.5 [a]	30.3 ± 0.2 [a]
rhd1	0 [a]	0 [a]	0.07 ± 0.05 [a]	0	0 [a]	0.06 ± 0.04 [a]	0	0 [a]	0	n.d.	n.d.	8.7 ± 0.3	n.d.	n.d.	26.1 ± 0.7
lrx	2.5 ± 0.1	3.6 ± 0.2	4.0 ± 0.3 [a]	0.02 ± 0.02	0.3 ± 0.2	0.3 ± 0.1 [a]	0.7 ± 0.1 [a]	3.1 ± 0.4 [a]	0	8.1 ± 0.1	8.0 ± 0	8.0 ± 0	26.7 ± 0.6	26.0 ± 0.5	28.0 ± 0.5

[a] A comparison with the primary roots of the wildtype under the respective growth condition resulted in a *P* value ≤ 0.01. In addition, these data are marked in blue. [b] Only small bulges appeared that were not visible in the cross-sections. The value represents root hairs that were elongated. [c] Under P deficiency, the *rhd2* mutant also developed small bulges, but in cross-sections, distinct rhizodermal cells showed a strong toluidine blue staining. These cells were counted as root hair cells. [d] mutant background is not Col-0. n.d. = not determined.

WER is a negative regulator of root hair development in the N position. *WER* encodes a MYB-related protein that is preferentially expressed in non-hair cells and is required for the appropriate level and pattern of *CPC* and *GL2* transcription. In *wer* seedling roots, nearly all rhizodermal cells differentiate into root hairs cells (Lee and Schiefelbein 1999, 2002). In this study, the root hair number of *wer* was not as high as described for the seedling roots. The typical phenotype was only observed a few days after germination. Thereafter, under control conditions the aging primary root and newly formed laterals formed only bulges under control conditions that did not elongate. When grown in media lacking either Fe or P, a high number of hairs was formed in *wer* plants. The number of hairs in H position was similar to that of the wildtype under Fe-deficient conditions and was slightly reduced in P-deficient roots, but the frequency of hairs in N position was considerably enhanced under both Fe- and P deficiency (Table 5). Thus, the *WER* gene function seemed to be involved in the root hair development of aging plants: although, the effect of the *wer* mutation was not as strong as in seedling roots.

CPC is a positive regulator of root hair development in the H position. *CPC* encodes a MYB-like protein that is expressed in the N position due to positive regulation by WER. CPC moves from the N cells into the neighboring H cells, where it represses its own expression and the expression of *WER* and *GL2* (Wada *et al*. 1997, 2002, Lee & Schiefelbein 2002). Under control conditions, roots of the *cpc* mutants formed only a few root hairs that were randomly distributed along the root. The appearance of the phenotypes of *cpc* roots under –Fe and -P conditions were similar to the wildtype: although, the number of hairs was lower ($P < 0.01$; Fig. 8, a-c; Table 5). Ectopic root hairs were not produced in *cpc* roots.

TTG encodes a small protein with WD40 repeats (Walker *et al*. 1999). The root hair pattern of *ttg* seedlings is abolished in H and N positions (Galway *et al*. 1994). Under all three growth conditions, the frequency of root hairs in the H position was not significantly different from the wildtype (Table 5). The number of hairs in the N position was drastically enhanced. In P-deficient roots, 30% of the epidermal cells in N position were developed into root hairs. This indicated that *TTG* might be more important for non-hair cell development in the N position than for the specification of non-hair cells in the H position that occurs in older plants in adaptation to the nutrient supply. In addition, roots of P-deficient *ttg* plants produced root hairs which were clearly longer than those of the wildtype under similar conditions (1.0 ± 0.02 mm, Fig. 8f).

GL2 inhibits root hair development in the N position (Masucci *et al*. 1996). *GL2* encodes a homeobox-containing transcription factor and is preferentially expressed in atrichoblasts (Wada *et al.* 1997, Masucci *et al.* 1996). The root hair density of *gl2* mutant plants was increased in the H and N position and differed between the growth types (Table 5).

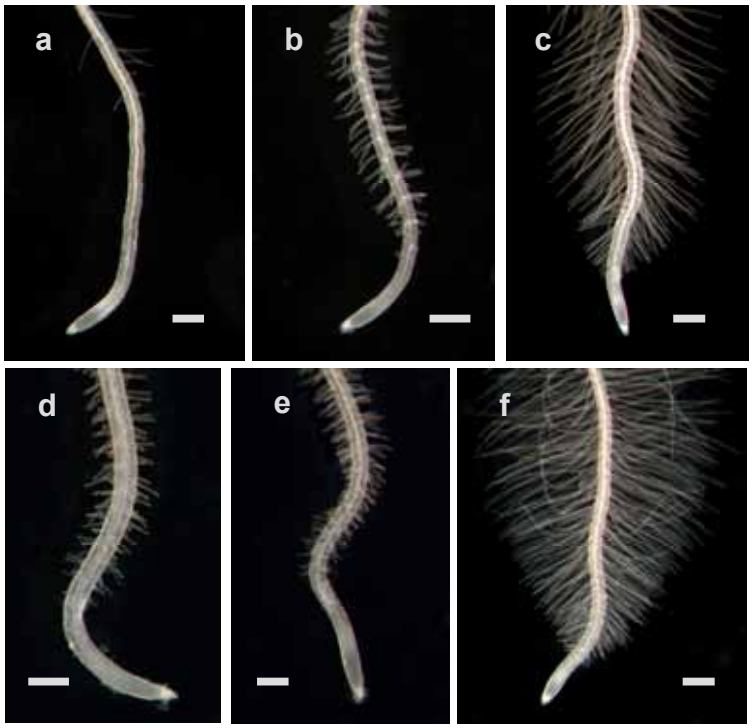

Figure 8: Root tips of the *cpc* and *ttg* mutants grown under control conditions or in the absence of Fe or P. (a) *cpc* control, (b) *cpc* –Fe, (c) *cpc* –P, (d) *ttg* control, (e) *ttg* –Fe, (f) *ttg* –P. Bar = 250 µm.

Despite marked changes in the root hair frequency in the H and N position among the *wer*, *ttg*, *gl2*, and *cpc* mutants compared to the wildtype under all growth conditions, the number of root hairs was increased in response to Fe or P starvation. Thus, the nutritional signal can be perceived and translated in this group of mutants. Interestingly, in *wer* mutants branched root hairs with a frequency typical of –Fe wildtype plants were induced by Fe deficiency. In contrast, *cpc*, *ttg*, and *gl2* had a significant lower number of branched hairs.

RHL1, RHL2, and RHL3 are subunits of the topoisomerase VI complex involved in endoreduplication, a process in which one to several rounds of DNA replication take place without mitosis. Endoreduplication is important during cell differentiation and expansion (Sugimoto-Shirasu *et al*. 2005, Joubès & Chevalier 2000). Under the present conditions, *rhl1*, *rhl2*, and *rhl3* were dwarf and their roots remained hairless when grown on standard medium or under either Fe or P deficiency, suggesting an essential function of endoreduplication in root hair development during adaption to the Fe and P supply (Table 5).

Analysis of mutants with defects in root hair initiation and tip growth

The *RHD6* gene promotes root hair initiation and is associated with the establishment of epidermal cell polarity (Masucci & Schiefelbein 1994). In roots of the *rhd6* mutant, no hairs were formed under all three growth conditions indicating that the gene was necessary for root hair development independent of the nutrient supply.

TRH1 is required for root hair initiation and tip growth. TRH1 is a potassium transporter that accelerates auxin efflux in the root cap (Rigas *et al*. 2004, Vincente-Agullo *et al*. 2004). Plants lacking the *TRH1* gene function only formed bulges that did not elongate under control and -Fe conditions (Fig. 9, a, b). The *trh1* mutant produced normal root hairs under -P conditions in a frequency and positional pattern that did not differ from the wildtype (Fig. 4c; Table 5). Thus, TRH1 is possibly not essential for the formation of root hairs in response to P deficiency.

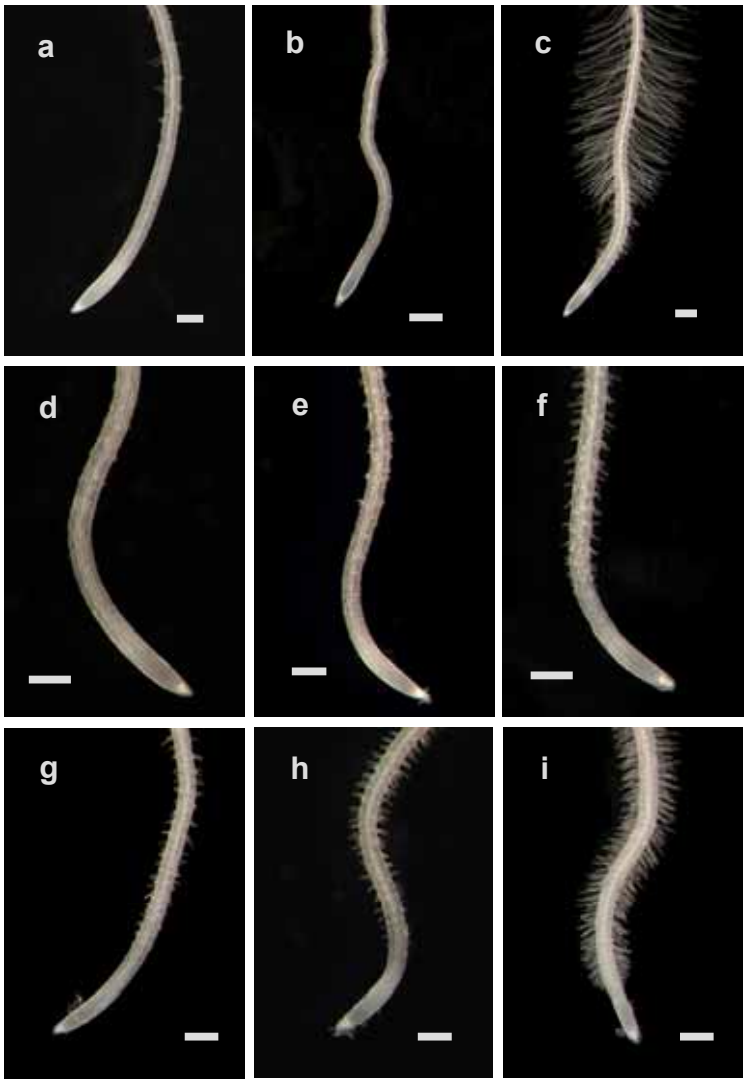

Figure 9: Root tips of the *trh1*, *tip1*, and *rhd3* mutants grown under control conditions or in the absence of Fe or P. (a) *trh1* control, (b) *trh1* -Fe, (c) *trh1* –P, (d) *tip1* control, (e) *tip1* –Fe, (f) *tip1* –P, (g) *rhd3* control, (h) *rhd3* -Fe, (i) *rhd3* –P. Bar = 250 µm.

The *S*-acyl transferase, TIP1, is important for vesicle traffic during root hair initiation and tip growth. In *tip1* roots, only short root hairs are formed that are often branched (Ryan *et al*. 1998, Parker *et al*. 1998, Hemsley *et al*. 2005). The frequency of these short root hairs did not differ markedly from the wildtype under all growth conditions. Root hairs of -P plants were longer than those of the control plants (Fig. 9, d-f; Table 5). Under control and -P conditions

but not in medium lacking Fe, *tip1* plants produced significantly more cortical and epidermal cells (Table 5). Independent of the growth conditions, the majority of the hairs was branched. Under control conditions, nearly all hairs had two tips (87.5%); the percentage of branched hairs was slightly lower in -Fe and -P plants (Table 5). The phenotype of *tip1* suggests that *TIP1* function is important for the proper initiation of only one root hair tip and for tip growth independent of the Fe or P availability. Since the number of cortical and epidermal cells was increased in the *tip1* mutant, the gene might also be involved in early developmental stages of these tissues.

RHD2 is an NADPH oxidase important for root hair tip growth (Foreman *et al*. 2003, Schiefelbein & Somerville 1990). The *rhd2* mutant produced short root hairs under control and Fe-deficient conditions that had a normal degree of branching. When grown in P-deficient medium, only bulges were produced that did not elongate. The number of these bulges was similar to the root hair frequency of the wildtype (Table 5). *RHD3* encodes a small G protein which is required for ER and golgi vesicle trafficking (). The rhd3 mutation causes short and wavy root hairs (Schiefelbein & Somerville 1990). In the present study, *rhd3* mutants also produced short root hairs under all conditions (Fig. 9, g-i). The number of root hairs was similar to the wildtype. As no other characteristics were altered in the *rhd2* and *rhd3* mutants, both genes may be required for root hair elongation after the appropriate position and number of root hairs in response to the Fe and P supply has been established and after a proper bulge has been formed in the correct position of the epidermal cell.

RHD4 is a further gene active in the maintenance of root hair elongation (Schiefelbein & Somerville 1990). Root hair density under –Fe and –P conditions in *rhd4* mutants did not deviate significantly from the wildtype except for the number of root hairs in H position under Fe deficiency, which was significantly higher than in the wildtype. Root hairs of the *rhd4* mutant were generally shorter than in the wildtype.

Analysis of root hair mutants with defects linked to the cell wall

A mutation in the cellulose synthase-like protein KJK/CSLD3 causes a burst of the root hairs after swelling formation (Favery *et al*. 2001, Wang *et al*. 2001). When grown under either Fe or P deficiency, *kjk* mutants displayed a phenotype almost similar to the wildtype with respect to the root hair number, but most of the hairs were ruptured at their tip and had irregular lengths. A considerably lower frequency of root hairs in the H positions was found under control conditions. In contrast to the wildtype, only few branched root hairs developed in response to Fe starvation (Table 5). In contrast to the *kjk* mutation, bulges of *csld3-1* mutants did not elongate. The frequency of the bulges did not significantly deviate from the wildtype under all growth conditions (Table 6). Thus, KJK/CSLD seems to be involved in root hair tip growth independent of the nutrient supply.

Defects in the *RHD1* locus lead to larger bulges at the base of root hairs (Schiefelbein & Somerville 1990). RDH1 is a UDP-D-glucose-4-epimerase that galactosylates xyloglucan and arabinogalactan, which are pectin and cell wall structural protein constituents, respectively (Seifert *et al*. 2002). Under the present conditions, the primary root of *rhd1* plants was completely devoid of hairs (Fig. 10a), with the exception of –P plants, in which some hairs were occasionally observed (Table 5). In laterals, root hair density of *rhd1* roots was not significantly different from the wildtype under all growth conditions, when only those trichoblasts were considered that succeeded in initiating root hairs (Table 6). The non-hair cells were characterized by wide bulges that comprised the entire epidermal cell wall (Fig. 10b). This phenotype suggests that *RHD1* is important for proper epidermal cell development but that root hair initiation and tip growth of laterals might not strictly depend on *RHD1* function.

Table 6: The number of root hairs or root hair bulges per mm. The plants were cultivated under sufficient nutrient supply (control) or in media without Fe (-Fe) or P (-P). Root hairs were counted in the root hair zone of root tip within the 2nd mm behind the apex. n = 20.

Genotype	Control	-Fe	-P
Col-0	34.8 ± 1.4	50.3 ± 2.4	66.5 ± 3.1
csld	32.7 ± 1.2	47.7 ± 2.1	62.8 ± 2.2
rhd1 laterals	37.8 ± 2.7	59.3 ± 2.4	71.2 ± 4.0

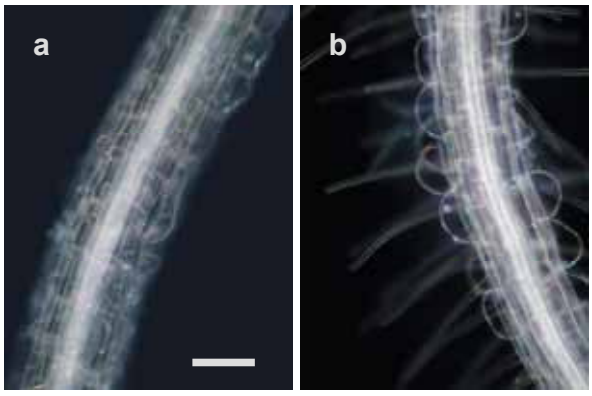

Figure 10: Roots of the *rhd1* mutant grown in P deficient medium. (a) The primary root did not form root hairs. (b) Epidermal cells of lateral roots exhibited large bulges and normally shaped root hairs. Bar = 100 μm.

The chimeric leucine-rich repeat/extensin protein, LRX1, is localized in the cell wall of root hairs. LRX is a possible regulator for proper cell wall assembly (Baumberger *et al*. 2001). The *lxr* mutants show an irregular root hair length with hairs often being shorter, and with swellings either at the basis or along the stalk. Root hairs of *lrx* roots were often ruptured at their tips. The mutant responded to Fe and P depletion with an increase in the number of root hairs. However, fewer hairs than in the wildtype were formed in response to P deficiency. Under –Fe conditions, most of the hairs (80%) in the *lrx* mutant were branched. A significant higher number of branched hairs was also formed under control conditions (Table 5). *LRX*

may, thus, be involved in root hair initiation and elongation after the proper number of root hairs in the correct position has been determined.

Differential cytoplasmic staining of rhizodermal cells in adaptation to Fe and P supply

In 5-day-old seedlings, nearly all epidermal cells in the H positions form a root hair (Dolan *et al*. 1994, Galway *et al*. 1994, Lee & Schiefelbein 2001; Table 5; Fig. 11a). In the late meristematic region of the root, nearly all H positions show a more intense cytoplasmic staining and lower degree of vacuolization (Dolan *et al*. 1994, Galway *et al*. 1994, Masucci *et al*. 1996). In the aging primary root and in laterals, however, only three of eight rhizodermal cells in the H position develop a root hair under sufficient nutrient supply or Fe starvation. The majority of cells in the hair position had, therefore, no root hair (Table 5, Fig. 11b). Under P deficiency, five of eight H positions possess a root hair (Table 5, Fig. 11c). This raised the question, if the root hair patterning in mature, sufficient and Fe- or P-deficient plants was also reflected in the spatial distribution of the differential cytoplasmic staining and degree of vacuolization in the meristematic region. However, similar to seedlings, nearly all epidermal cells in the H position exhibited a stronger staining with toluidine blue than epidermal cells in the N position (Fig. 11, d-f). The same observation held true for the lower degree of vacuolization (Fig. 11, d-f). Therefore, the Fe or P nutritional status did not alter the differential cytoplasmic staining and lower degree of vacuolization.

Adaptation of GL2-GUS and CPC-GUS activities to Fe and P supply

The *GL2* gene, which is a negative regulator of root hair development, and the *CPC* gene, a positive regulator, are expressed in nearly all N positions of 5-day-old seedling roots (Masucci *et al*. 1996, Wada *et al*. 2002). The lack of *GL2* and *CPC* expression in the H positions of seedlings is correlated with the occurrence of root hairs (Masucci *et al*. 1996). Thus, it remains to be clarified, if the non-hair cells in the H position occurring in plants older than 5 days are correlated with an expression of *CPC* or *GL2* in the H position. To determine the expression pattern of *CPC* and *GL2*, plants carrying GUS transgenes were cultivated in the presence and absence of either Fe or P. Both GL2-GUS and CPC-GUS plants showed vertical stripes of stained cells as previously described by Masucci *et al.* (1996) and Wada *et al.* (2002) in primary and lateral root tips. No difference in the intensity of staining was visible between nutrient sufficiency and Fe or P deficiency in GL2-GUS and CPC-GUS plants. Cross-sections revealed that GL2-GUS and CPC-GUS were expressed under all conditions in nearly all N positions, whereas nearly all H positions showed no GUS staining (Fig. 11, g-l; Table 7). Thus, the expression pattern was the same as that described for 5-day-old seedlings. The root hair patterning of GL2-GUS and CPC-GUS plants did not deviate from the wildtype (not shown). Therefore, root hairs in the H position (Fig. 11, b-c) were not correlated with the expression patterns of GL2-GUS and CPC-GUS (Fig. 11, d-i; Table 7).

The spatial expression of *CPC* and *GL2* was independent of age and nutrient status of the plants.

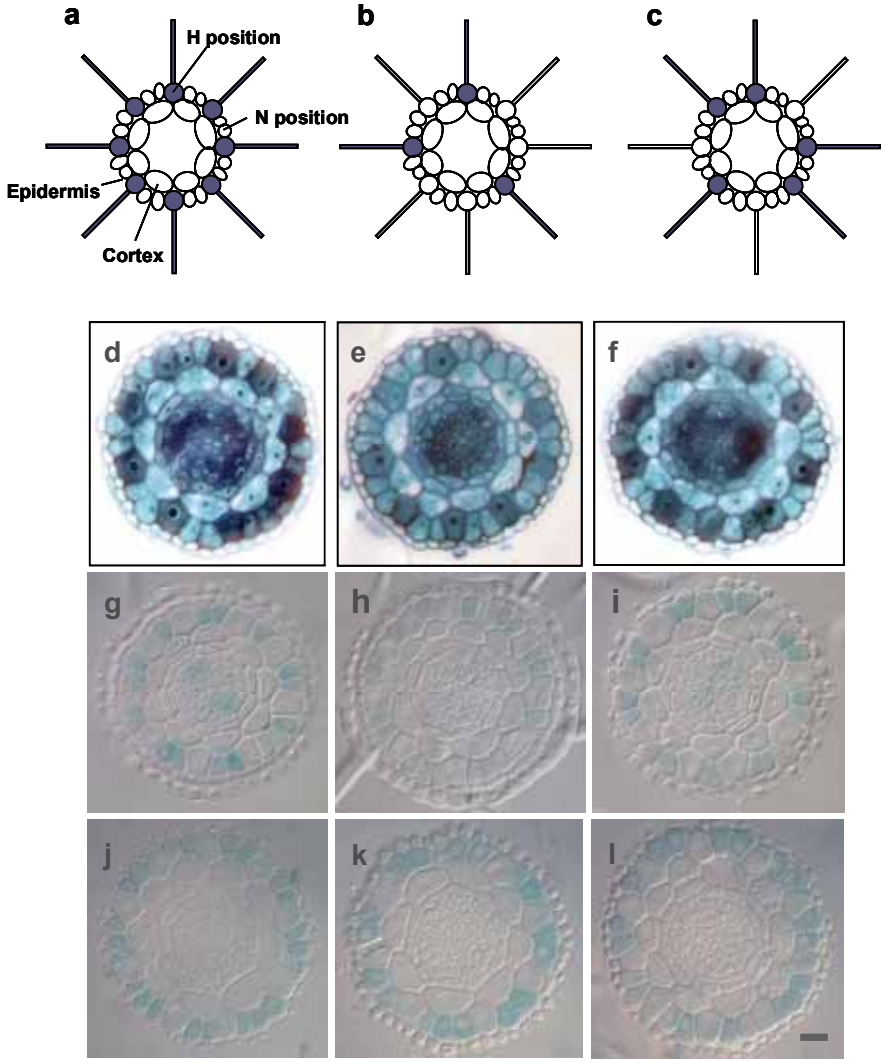

Figure 11: (a-c) Schematic representation of one transverse cell layer from the *Arabidopsis* root hair zone with only cortical and epidermal cells. Root hairs in the H position are marked in blue. (a) In five-day-old seedlings nearly all eight epidermal cells in the H position form a root hair. (b) In roots older than five days that are cultivated under sufficient nutrient supply or Fe deficiency, only three of eight H positions develop a root hair in a randomly distributed manner. (c) P-deficient roots older than five days have on average five root hairs in the H position per cell layer. (d-f) Differential cytoplasmic staining with toluidine blue is shown in cross-sections from the late meristematic region of three-week-old *Arabidopsis*. (d) control, (e) Fe-deficient, and (f) P-deficient roots. The differential cytoplasmic staining is visible in the epidermis, which is surrounded by cells of the lateral root cap. The lower intensity of staining in (e) is due to a lower thickness of the cross-section (2µm). (g-l) Shown are cross-sections from the late meristematic region of three-week-old GL2-GUS and CPC-GUS plant roots adapted to Fe and P nutrition. (g) control GL2-GUS, (h) Fe-deficient GL2-GUS, (i) P-deficient GL2-GUS, (j) control CPC-GUS, (k) Fe-deficient CPC-GUS, and (l) P-deficient CPC-GUS plants. Bar = 20 µm.

Table 7: The percentage of H and N cells showing GUS staining. Twelve-day-old GUS plants were cultivated in the presence and absence of either Fe or P. The spatial GUS expression was analyzed in cross-sections from the late meristematic region of the root. n = 6.

Genotype	Treatment	% H positions +GUS	% N positions +GUS
GL2-GUS	control	1.9	98.9
	-Fe	3.5	92.2
	-P	0.6	97.9
CPC-GUS	control	2.1	93.8
	-Fe	2.2	89.8
	-P	0.5	95.3

3.4 Screening of the *per2* mutant and phenotypical and genetical characterization

Mutant screening and genetic analysis

To identify potentially new genes that are involved in the root hair development under P limitation, a mutant screening was performed. Mutants were searched for that were not able to develop root hairs when the plants were germinated on –P medium but formed normal root hairs after the plants were transfered to +P medium. An EMS-mutagenized and a T-DNA mutant population were screened. Putative mutants were propagated. After retesting the progeny of putative mutants, 4 EMS and 2 T-DNA mutants were considered to be clearly impaired in the root hair development under P starvation, which was abolished in the presence of P (Table 8). One of the EMS mutants was characterized in more detail. The mutant was called *per2* (*phosphate deficiency root hair defective2*).

Table 8: The statistical data from the primary and secondary mutant screening.

Type of mutagenesis	No. of M2 plants screened	% chlorotic [a]	% albinos [a]	No. of putative mutants	No. of mutants after retest
EMS	39,266	0.5	0.16	205	4
T-DNA	31,326	0.1	0.01	13	2

[a] For estimation of the mutant rate, chlorotic and albino plants were counted.

The F1 offspring of a cross between the *per2* mutant and the Col-0 wildtype developed normal root hairs under P deficiency. The F2 generation segregated in a ratio of 23% plants exhibiting the *per2* phenotype and of 77% plants appearing normal; a 1:3 ration that is consistant with a single recessive nuclear mutation.

The F1 progeny of crosses between the *per2* mutant and the 5 remaining mutants from the screening also displayed the wildtype phenotype indicating none of the mutants was allelic to *per2* and all mutations were recessive.

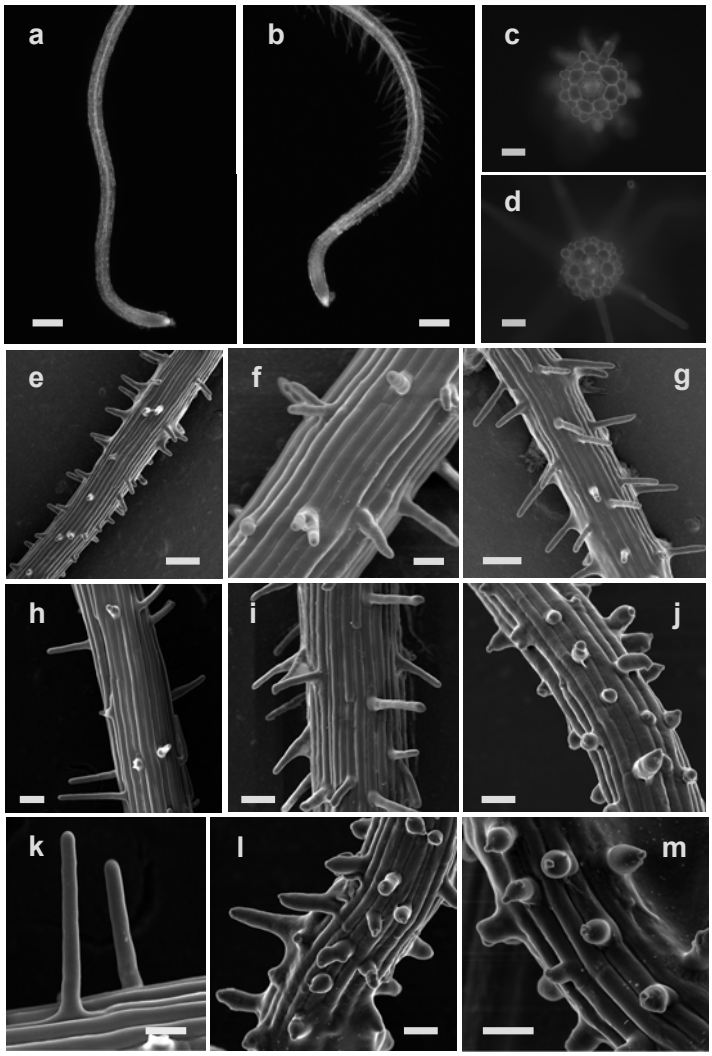

Figure 12: The root hair phenotype of the *per2* mutant. (a, b) Stereo microscope images (a) *per2*, -P, (b) *per2* +P. (c, d) Micrographs of hand-cut sections from the root hair zone. (c) *per2*, -P, (d) Col-0, -P. (e-m) Cryo-SEM images. (e) Col-0, control, (f) Col-0, -Fe, (g) Col-0, -P, (h) *per2*, control, (i) *per2*, -Fe, (j) *per2*, -P, (k) *per2*, control, (l, m) *per2*, -P. Bars = 250 µm (a, b), 100 µm (e, g), 50 µm (c, d, h, i, j, l, m), and 30 µm (f, k).

Microscopic analysis of the *per2* root hair phenotype

Under the stereo microscope, only small bulges or short root hairs that did not elongate were visible in P-deficient *per2* plants. In the presence of P, the root hairs appeared to be nearly normal, although a bit elongated (Fig. 12, a, b). In cross-sections, the bulges were located in the H positions and did not differ in their frequency from the wildtype (Fig. 12, c, d; Fig. 13). However, the epidermal cells of *per2* seemed to be slightly enlarged (Fig. 12, c, d). A more detailed analysis of the root surface with the scanning electron microscope revealed a regular shape of the root hairs formed in *per2* under sufficient nutrient supply or Fe starvation (Fig. 12, h, i, k). In P-deficient *per2* plants, the root hairs were shorter, thicker, and deformed. Nearly all root hairs showed material accumulations at their tips. These accumulations could results from improperly secreted or assembled cell wall constituents. Occasionally, two growth points were visible in one root hair indicating the direction of vesicle transport could be altered in *per2* (Fig. 12, j, l, m).

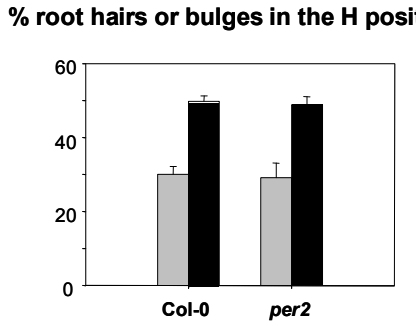

Figure 13: The percentage of wildtype root hairs and *per2* bulges in the H position. 14-day-old plants were germinated in the presence of P (grey bars) or without P (black bars).

The *per2* mutation lead to a constitutively high lateral root number

To determine, if in addition to the impaired root hair development also other P starvation responses are affected in the *per2* mutant, the length of the primary root and the number of lateral roots were measured (Fig. 14). The primary root length of the *per2* mutant was not altered (Fig. 14a). In contrast, the lateral root number was increased under sufficient P supply ($P \leq 0.01$). Also P-deficient *per2* showed an increased number of lateral roots, but this was not significant ($P = 0.08$; Fig. 14, b-c). Thus, the *per2* mutation seemed to affect also other P deficiency responses in addition to root hair development. To test, if the impaired root hair formation and the increased lateral root development of the *per2* mutant were caused by the same mutation, F2 plants from a backcross to Col-0 were selected for the *per2* phenotype. Plants with an impaired root hair development on –P medium were allowed to self. The progeny were then checked for the frequency of lateral roots. Also these backcross plants exhibited an increased lateral root development (Fig. 14b), which could be a first indication for a genetic linkage of the impaired root hair development and the increased lateral root frequency of the *per2* mutant.

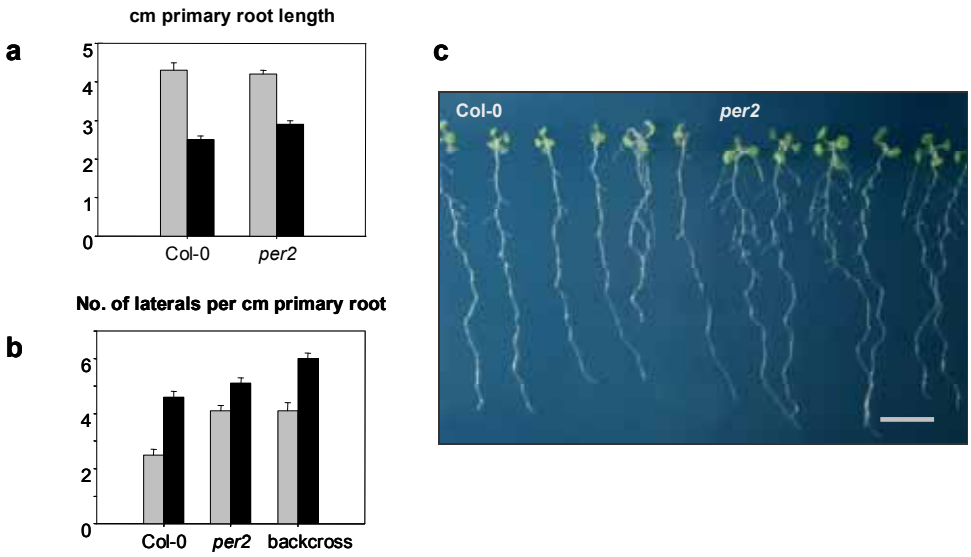

Figure 14: The root system architecture of the *per2* mutant. The primary root length (a) and the number of lateral roots (b) of *per2* and the Col-0 wildtype grown in vertical culture for 15 days in the presence (grey bars)

or absence (black bars) of P. Any lateral root outgrowth that was visible without magnification was counted as a lateral. Also included in the experiment were F3 plants that were the progeny of F2 lines from a backcross with Co-0 that had been selected for the *per2* root hair phenotype. (c) The increased lateral root development of the *per2* mutant on +P medium is shown in an image of 16-day-old plants. Bar = 1 cm. Two repetitions of the experiment gave the same results.

The *per2* mutant showed and increased anthocyanin accumulation under P deficiency

One of the classical features of P deprivation is the accumulation of anthocyanins in the leaves (Poirier & Bucher 2002). To test if this response was altered in *per2*, the absorbance of anthocyanins extracted from the leaves of *per2* and Col-0 was measured (Fig. 15). No differences were obvious in the P-sufficient mutant. When cultivated under P deficiency, an increase in the anthocyanin absorbance in *per2* was observed. Allthough this increase was not significant ($P > 0.05$), it was apparent in two independent experiments. Plants from a backcross that exhibit the *per2* root hair phenotype also showed an increased anthocyanin absorbance indicating the reaction could be linked with the same mutation that causes the impaired root hair phenotype.

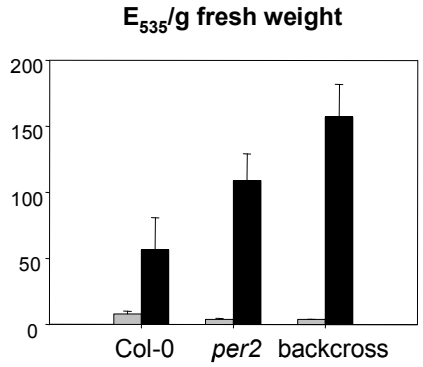

Figure 15: The anthocyanin content of the *per2* mutant grown vertical culture for 20 days in the presence (grey bars) or absence (black bars) of P. Also included in the experiment were F3 plants that were the progeny of F2 lines from a backcross with Co-0 that had been selected for the *per2* root hair phenotype. Repetition of the experiment gave the same result.

The *per2* mutantion did not influence the phosphorus content or biomass production

To test wether the *per2* mutation affects the uptake of phosphate or of other elements from the medium, an element analysis with ICP was conducted (Fig. 16). The content of none of the elements investigated was changed in the root and shoot material of *per2*. Thus, only the phophorus content is shown (Fig. 16, a-b). Unfortunately, the climate conditions were changed by others during repetition of the experiment. Allthough the experiments could not be repeated under the same growth conditions, no effect of the *per2* mutation on the phosphorus content or on the content of other elements was obvious under the different growth conditions. Also the shoot fresh weight of *per2* was not altered in the different experiments ($P > 0.05$). Thus, under growth conditions tested, the *per2* mutation had no impact on the phosphorus accumulation or biomass production of the plants.

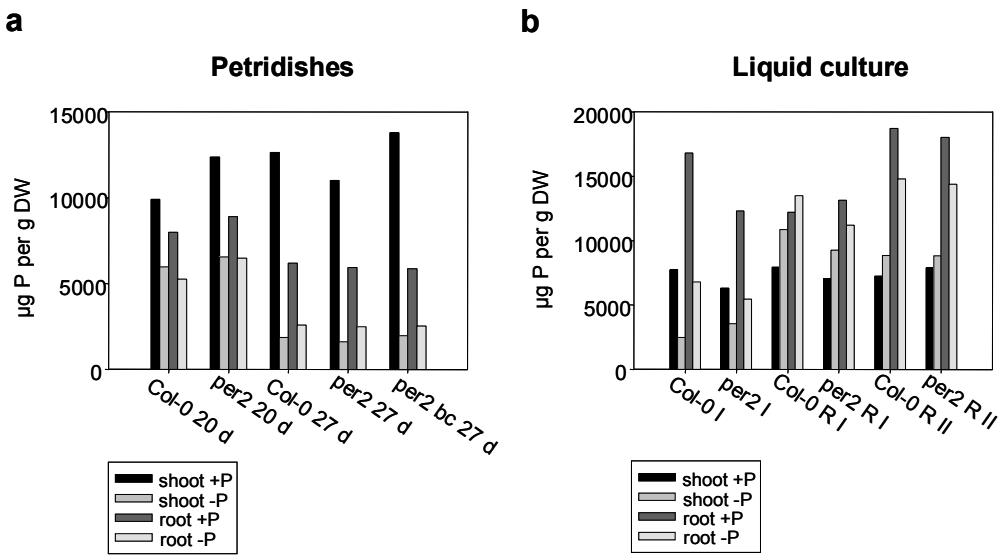

Figure 16: (a, b) The phosphorus content of *per2* and Col-0 that had been cultivated on Petri dishes (a) or in liquid culture medium (b). (a) Two independent experiments were conducted. In the first experiment, *per2* and Col-0 were treated for 20 days. The second experiment includes also the backcross (bc). During this repetition, the climate conditions had been changed by others to a continuous light period and 23°C. Because direct competion of the replicas was not impossible, the culture period was then extended to 27 days to increase potential effects of P deficiency on the P content of the mutant. (b) The plants were also grown in liquid culture. Also a replenishment study was included. One part of the plants were harvested after 7 days of treatment with P deficiency together with the sufficient controls. The remaining plants were replenished with medium containing sufficient amounts of P and were harvested after one day. Two experimental replicas were conducted. During the second experiment, plant material was limiting and was only sufficient to conduct the replenishment experiment.

The impaired root hair elongation of *per2* was rescued by the phosphate analogon phosphite

As the *per2* root hair phenotype could be repressed by a sufficient P supply (Fig. 12), it was tested if this suppression is mediated by a systemic or a local signal. A local abundance of phosphate can be mimicked by phosphite (Phi), the reduced but metabolically inert form of phosphate, which is readily taken up by plant cells (Carswell *et al*. 1996). Phi specifically suppresses anthocyanin accumulation, expression of *At4* and nucleolytic enzymes, and high affinity transport while the phosphate content decreases and growth is inhibited (Carswell *et al*. 1997, Ticconi *et al*. 2001). When the *per2* mutant and Col-0 were grown on medium containing Phi instead of phosphate, both showed a severely inhibited root and shoot growth, as it was described by Ticconi *et al*. (2001). However, the root hair elongation of *per2* was the same as in the wildtype (Fig. 17). Thus, the impaired root hair elongation of *per2* can be overcome by mimicking a local P abundance indicating the *PER2* gene might belong to a local rather than to a systemic signaling pathway.

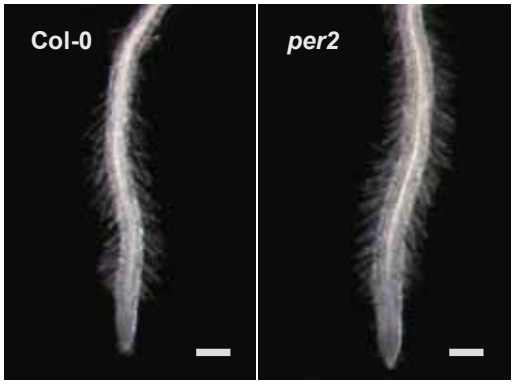

Figure 17: The effect of the phosphate analogon phosphite on the root hair elongation of *per2*. The plants were germinated on medium containing phosphite instead of phosphate and were analyzed after 14 days. Bar = 250 µm.

The *per2* mutation showed an additive genetic interaction with *gl2* and *erh3*

To characterize the interaction between *per2* and genes involved in root hair specification, double mutants with *gl2* and with *erh3* were generated. In both cases, the F2 offspring was analyzed for the root hair phenotype on –P medium (Fig. 18). The segregation ratio was 9:3:3:1. The *per2gl2* and the *per2erh3* double mutants both showed the phenotype of either parent. This additive interaction indicated that *per2* acts in a pathway that is independent of *gl2* or *erh3*.

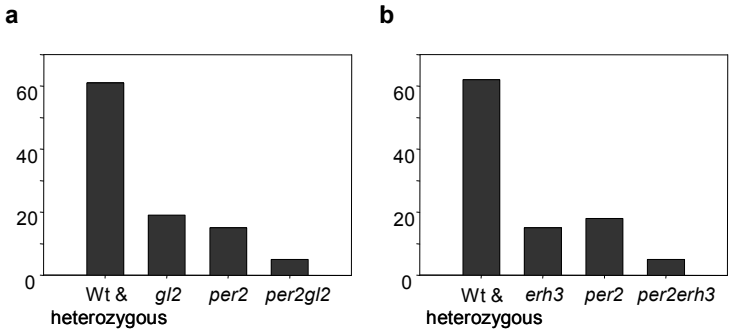

Figure 18: The characterization of a potential genetic interaction of the *per2* mutation with mutations in genes regulating epidermal cell specification. The *per2* mutant was crossed with *gl2* (a) or *erh3* (b). The F2 progeny was germinated on –P medium and the phenotype was analyzed after 14 days. The percentage of plants exhibiting the indicated phenotype is given. (a) The F2 offspring of a cross between *per2* and *gl2* segregated into 4 different phenotypes. Plants that showed many and elongated root hairs represented the homozygous wildtype and the heterozygous mutant genotypes. The recessive *gl2* mutation is phenotypically linked with the lack of trichomes (Koornneef *et al*. 1982). Thus, plants that showed many root hairs but no trichomes represented the homozygous *gl2* mutants. One-quarter of the plants showing the *per2* root hair phenotype also had no trichomes indicating that those mutants carrying a homozygous mutation in both loci have an additive phenotype. n = 910 plants. (b) The root system of the recessive *erh3* mutant is stunted and the roots are radially expanded (Schneider *et al*. 1997, Burk *et al*. 2001). The F2 progeny of a cross between *per2* and *erh3* also segregated in four phenotypical groups. Those plants that exhibited the *per2* phenotype segregated into plants with normal root growth and plants, which showed the *erh3* root morphology. Thus, the homozygous *per2erh3* genotypes showed both the *per2* and the *erh3* phenotypes suggesting an additive interaction. n = 684 plants.

Map-based cloning of the *per2* locus

Low resolution mapping of the *per2* mutation was performed by linkage analysis with the SNP marker set described by Törjek *et al*. (2003). F2 plants from a mapping population with C24 that displayed the *per2* root hair phenotype were analyzed with a subset of of these markers spanning the whole Arabidopsis genome (Fig. 19a). The *per2* penotype was linked with the markers MASC02947 and MASC02841 located on the upper arm of chromosome 3 (Fig. 19a). Analysis with further markers located in that region revealed the highest recombination frequencies with MASC04279 and MASC02841. The genetic map distances between *per2* and the markers were 9.2 and 9.8 cM, respectively (Fig. 19b).

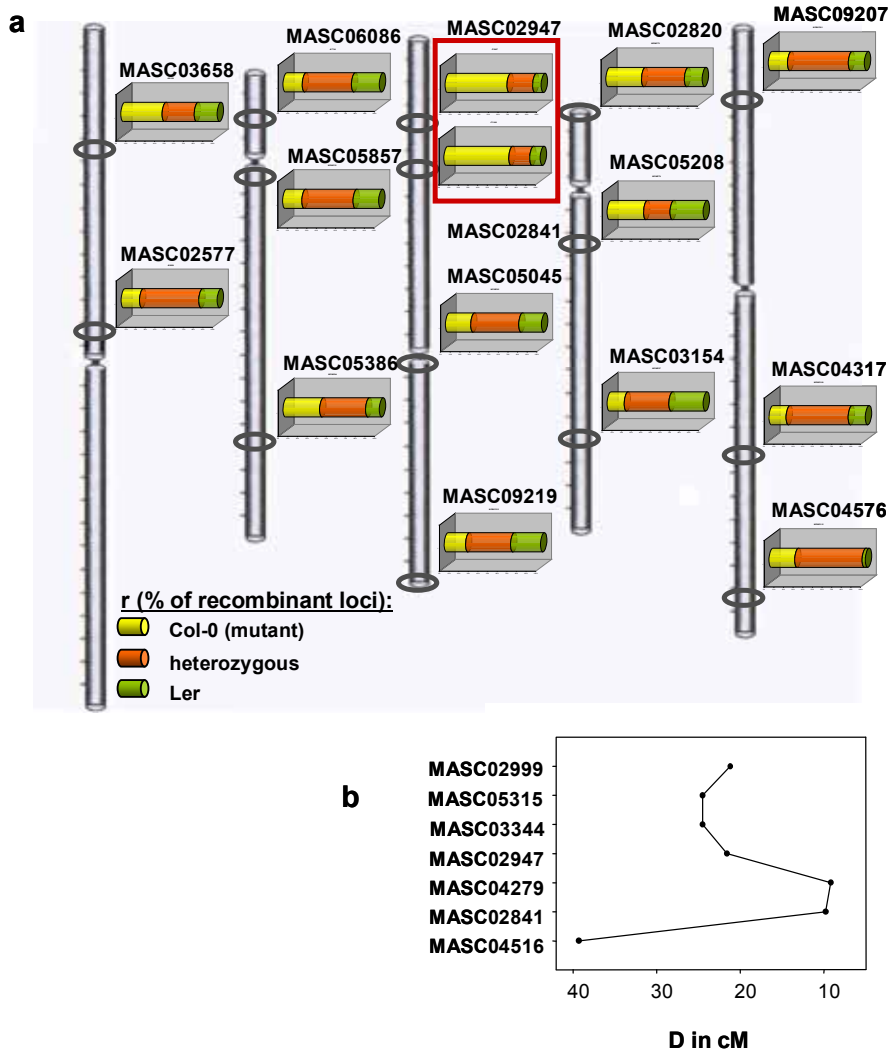

Figure 19: The low resolution mapping of the *per2* mutation with the SNP marker set described by Törjek *et al.* (2003). The SNPs were detected with the SNaPshot method. (a) Analysis of 213 F2 plants from a mapping population derived from a cross between *per2* (Col-0 background) and C24 that showed the *per2* root hair phenotype revealed a co-segregation with markers on the upper arm of chromosome 3. (b) Genetic map distances in cM between *per2* and markers from the upper arm of chromosome 3 calculated with the Kosambi function.

For fine mapping, further F2 plants displaying the *per2* phenotype from a mapping population with Cvi were tested for recombination events between the markers MASC04279 and

MASC02841. Recombinant lines were then analyzed by closer SNP markers (Fig. 20). Newly identified SNPs are listed in Table 9.

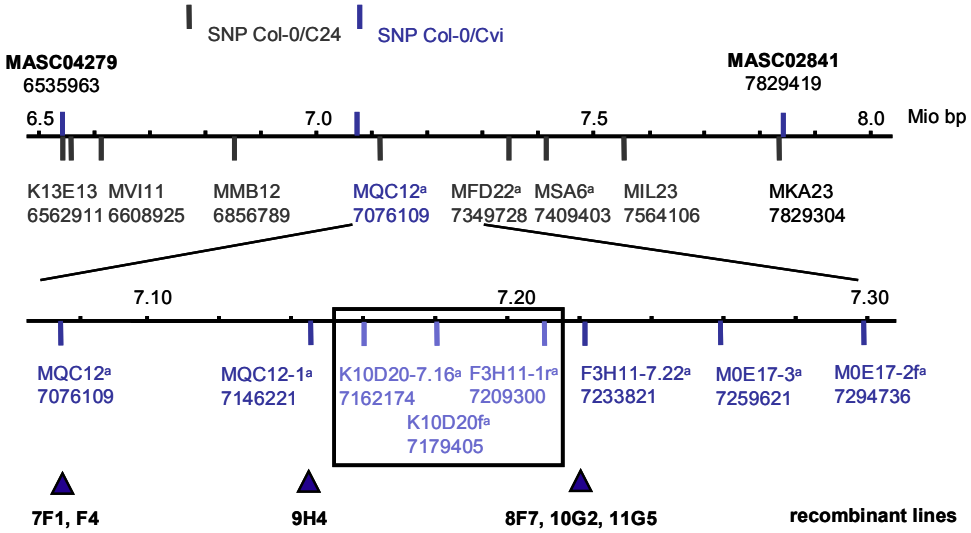

Figure 20: The fine mapping of *per2*. The upper arm of chromosome 3 is shown ranging from nucleotide no. 6,500,000 to 8,000,000. The F2 plants from the low resolution mapping and 987 further plants exhibiting the *per2* phenotype from a mapping population with Cvi were analyzed for recombinations between the markers MASC04279 and MASC02841. The location of these recombinations was then analyzed with a higher resolution of SNP markers that were either obtained from the NASC SNP database (http://www2.mpiz-koeln.mpg.de/masc/search_masc_snps.php) or identified by sequence analysis ([a]). The name of the markers was chosen according to the BAC clone they were located on. The numbers below the SNP marker names indicate the chromosomal location of the polymorphic nucleotide. Three lines were heterozygous at the marker location F3H11-7.22 and homozygous at F3H11-1r, two lines were heterozygous at MQC12 and homozygous at MQC12-1, and one line was heterozygous at MQC12-1 and homozygous at K10D20-7.16. The frame indicates markers where no recombination was found.

Table 9: The SNPs between Cvi and Col-0 identified by sequence analysis.

Marker	Cvi/Col-0	Marker	Cvi/Col-0
MQC12	C/T	F3H11-7.22	T/C
MQC12-1	C/T	M0E17-3	A/G
K10D20-7.16	A/T	M0E17-2f	A/G
K10D20f	T/A	MFD22[a]	T/C
F3H11-1r	T/C	MSA6[a]	G/C

[a] The indicated polymorphism was between C24 and Col-0 and not between Cvi and Col-0.

No recombinations were found between nucleotide 7162174 and 7209300, inclusively. In conclusion, a location of *per2* outside this area is unlikely since only plants with the recessive *per2* phenotype had been selected for the marker analysis. The *per2* phenotype of the recombinant lines was confirmed in the F3 progeny. Candidate genes that are located between nucleotide 7162174 and 7209300 are listed in Table 10.

Table 10: The candidate genes for the *per2* mutation.

Gene	Biological Process	Location	Molecular Function
At3g20475	DNA mismatch repair protein, putative, 3' partial		
At3g20480	lipid A biosynthesis	membrane	tetraacyldisaccharide 4'kinase activity
At3g20490	unknown	unknown	unknown
At3g20520	glycerol metabolism	anchored to membrane	glycerophosphodiester phosphodiesterase activity
At3g20530	protein amino acid phosphorylation,	mitochondrion	ATP binding, serine/threonine kinase activity, tyrosine kinase activity
At3g20540	DNA replication	chloroplast, mitochondrion	3'-5' exonuclease activity, DNA binding, DNA-directed DNA polymerase activity
At3g20560	unknown protein	unknown	electron carrier activity, protein disulfide oxidoreductase activity
At3g20570	electron transport	predicted GPI-anchored protein	copper ion binding, electron carrier activity
At3g20580	unknown	predicted GPI-anchored protein	unknown, phytochelatin synthase related
At3g20600	defence response to bacteria and fungi,	membrane	non-race specific disease resistance protein (NDR1), signal transduction activity
At3g20620	unknown protein	mitochondrion	F-box protein interaction domain, F-box family protein-related
At3g20640	putative bHLH transcription factor (bHLH123)	chloroplast	transciption factor activity

The genes At3g20550 and At20630 could be excluded as candidates for *per2* since their mutation causes curly leaves or an embryo-lethal phenotype, respectively, which was both not observed in *per2*. By comparing the sequences of *per2* and Col-0, no SNPs were found in the genes At3g20500, At3g20510, At3g20555, At3g20590, and At3g20610. Thus, these genes could also be excluded as possible candidates.

4 DISCUSSION

Ferric iron and phosphate both are highly immobile in the soil and among others form insoluble iron phosphate precipitates. In adaptation to this, plants evolved common responses for mobilization of the nutrients. In both cases, the rhizosphere is acidified by H^+-ATPases. Substantial amounts of organic acids and phenolics are secreted; responses that require a

continuing supply of carbohydrates that are transported from the shoot to the root. Iron and phosphate starvation both inhibit primary root growth and stimulate lateral root development, and both lead to an increase in the number of root hairs. However, differences exist between the iron and phosphate homeostasis in plants. While phosphate is highly mobile within the plants, iron transport through the plant is costly. In addition, Fe is toxic. In this work, an examination was conducted to identify further differences that may exist between root hairs of iron- and phosphate-deficient Arabidopsis plants. To this end, root hair patterns of iron- and phosphate-deficient Arabidopsis plants were analyzed. The influence of local and systemic signals on the respective root hair phenotype was investigated in split-root experiments. To determine at which stage of root hair development was influenced by iron and phosphate, mutants with defects in different stages of root hair development were analyzed for their root hair patterns in response to Fe and P starvation. Finally, to identify potentially novel genes involved in root hair formation in adaptation to P limitation, mutants were screened that did not form root hairs under P deficiency but developed normal, when the plants were transferred to P-sufficient medium. One of these mutants, *per2*, was characterized phenotypically and genetically.

4.1 Root hair patterns of the Arabidopsis wildtype adapted to Fe and P availability

The development of additional root hairs in response to iron and phosphate limitation was analyzed in cross-sections of the wildtype. The root hair phenotypes of Fe- and P-deficient plants differed markedly. Under P starvation, the number of cells in the H position that develop a root hair was increased (Fig. 2a). The number of root hairs in the N position was also increased but was below 5%. Of all root hairs formed, 85% were in the H position indicating root hair development adapted to P limitation was still position-dependent. An increase of the root hair number has been observed before (Foehse & Jungk 1983, Bielenberg *et al*. 2001). Root hair development of Fe-deficient plants was also position-dependent. The elevated root hair number of Fe-starved plants was predominantly caused by the formation of root hairs that were branched from their base (Fig. 3c; Fig. 4, b-c). Two branches of the same length were always formed that were arranged transversally (Fig. 2e; Fig. 4c). Branched root hairs also occur in several mutants with defects in different processes of root hair formation, such as *gl2-5*, *axr2*, the *aux1ein2* double mutant, *hydra*, *tip1*, *rpa*, *rhd3*, *exo70A1*, *cow1*, and *rdh4* (Ohashi *et al*. 2003, Wilson *et al*. 1990, Fischer *et al*. 2006, Souter *et al*. 2002, Hemsley *et al*. 2005, Song *et al*. 2006, Schiefelbein & Somerville 1990, Synek *et al*. 2006, Böhme *et al*. 2004). Treated with microtubule stabilizing or destabilizing drugs also leads to root hair branching (Bibikova *et al*. 1999). However, in contrast to the branched root hairs of Fe-deficient plants, in the mutants, root hair branching was often correlated with an overall deformed appearance, the development of more than two tips, or with a nontransverse branching layer. The branching of the hairs of leaves, trichomes, also occurs in distinct layers (Hülskamp 2000). The pattern of trichome initiation in the epidermis of leaves is regulated by

a similar transcription factor cascade that establishes the *GL2* expression pattern in the epidermis of the root (Scheres 2000, 2002, Schiefelbein 2003, Pesch & Hülskamp 2004). Thus, the branching of root hairs could be regulated by a similar mechanism to that involved in the branching of trichomes. In trichomes, the microtubule cytoskeleton plays an important role in the regulation of branch formation (Hülskamp 2000, Schnittger & Hülskamp 2002). During trichome development, four cycles of endoreduplication are proceeded. The first endoreduplication cycle is completed prior to trichome outgrowth and the second and third cycle take place concomitantly with the first and second branching event, respectively (Hülskamp *et al*. 1994). The *siamese* mutation results in the formation of multicellular trichomes suggesting trichomes are evolutionary derived from multicellular forms (Walker *et al*. 2000). Thus, the spatial information underlying branching in the unicellular Arabidopsis trichomes is based on the cell division machinery. More than 15 genes that affect branch number have been identified; most of them act in separate genetic pathways (Schnittger & Hülskamp 2002). Endoreduplication is also essential for the development of root hairs (Sugimoto-Shirasu *et al*. 2005). During root hair initiation, a new direction of polar cell growth is established. It is, thus, possible that a mechanism similar to the one regulating trichome initiation and branching could also be involved in root hair initiation and branching.

Together, root hair formation adapted to Fe and P supply was also position-dependent. Different strategies appeared to be used for increasing the root surface area during iron and phosphate limitation. P-deficient plants increased the number of root hairs, while in Fe-starved plants root hairs were branched.

4.2 Split-root experiments: local or systemic control?

A local or systemic Fe sufficiency signal is dominant in regulating root hair branching

The physiological and morphological iron deficiency responses are likely under the control of local and systemic signaling pathways. Bienfait (1987) found a local induction of ferric-chelate reductase, acidification, and root hair and transfer cell formation in potato tubers without sprouts. The first evidence of a shoot-derived signal controlling the Fe uptake system in the root was supplied by the grafting experiments of Grusak and Pezeshgi (1996) with the Fe hyperaccumulating pea mutant *dgl*. The mutant has a constitutively elevated ferric reductase activity in the root, which depends on the genotype of the shoot. In tobacco overexpressing the iron storage protein ferritin, van Wuytswinkel *et al*. (1999) found an increase of the root ferric-chelate reductase, which normally occurs under Fe deficiency. Further indication of an as yet unidentified systemic Fe deficiency signal addressing the root is provided by the phenotype of the *frd3* mutant, former designated as *man1* (*manganese accumulator1*). As a consequence of the Fe undersupply within the leaf cells, *frd3* shows a constitutively induced strategy I response in the root (Delhaize 1996, Rogers & Guerinot

2002). Also *chloronerva*, which shows intercostal chlorosis as an Fe deficiency symptom due to a lack of NA synthesis, has a constitutively upregulated ferric-chelate reductase in the root (Ling *et al*. 1999).

Morphological changes of the root are also controlled by the iron status of the shoot. Foliar application of an iron-chelate to plants grown on Fe-deficient medium suppresses the formation of extra lateral roots in addition to the ferric-chelate reductase (Moog *et al*. 1995). Because down-regulation after replenishment showed a different kinetic response, Moog *et al*. (1995) concluded the morphological and physiological iron deficiency responses are differentially regulated. This hypothesis was corroborated by Schikora & Schmidt (2001) who showed that the iron-overaccumulating pea mutants *brz* and *dgl*, which have constitutively high ferric-chelate reductase, are able to down-regulate their transfer cell frequency under sufficient iron supply. With split-root experiments in tomato, Schmidt and Schikora (2001) found that transfer cells are increased on the Fe-deficient half of the split-root; leading them to propose a local control of transfer cell development by iron.

To determine if the root hair branching of Fe-starved plants is under local or systemic control, we conducted split-root experiments combined with a sufficient or deficient shoot. The presence of a sufficient shoot of +/-Fe split wildtype plants was supported by the fact that the activity of the Fe deficiency marker ferric-chelate reductase, which is reportedly induced by a systemic signal, was not elevated in either split-root halves over the +/+Fe control (Fig. 6). This indicates that the plant is able to meet its Fe demand via the Fe-sufficient part of the root system. Both split-root halves of +/-Fe Col-0 wildtype plants displayed a frequency of root hair branching similar to +/+Fe plants (Fig. 5, b, d). Therefore, the root hair branching typical of Fe-deficient plants is not induced by a local Fe limitation if the shoot is Fe-sufficient (Fig. 21a). The induction of root hair branching requires, however, the combination of both a systemic Fe deficiency signal and local Fe depletion, as –Fe-halves of the +/-Fe *frd3* mutant showed a significantly increased frequency of branched root hairs (Fig. 5f, Fig. 21b). Local Fe deficiency leads to branched root hairs only if the availability of Fe in the leaf cells is decreased. The ferric-chelate reductase is also systemically activated, but in contrast to root hair branching, the reductase is not downregulated by a local Fe abundance (Fig. 21b). Schmidt and Steinbach (2000) observed rather an upregulation of the enzyme activity by a local presence of Fe when the shoot is Fe-deficient due to lowering the root zone temperature. In split-root experiments, Vert *et al*. (2003) found an upregulation of *FRO2* and *IRT1* transcripts in the sufficient part of the root, and Schmidt *et al*. (1996) observed a slight increase of ferric-chelate reductase activity that declines after three days of treatment. However, an increased enzyme activity on the +Fe half of the split-root system was not found in this study. Perhaps, the plants in the experiments of Schmidt *et al*. (1996) and Vert *et al*. (2003) had a deficient shoot resulting from the transfer from Fe-sufficient medium to +/-Fe conditions, which has already been overcome in this study.

Together, root hair branching is triggered only by a combination of both a local and a systemic deficiency signal. This is in contrast to the ferric-chelate reductase that is induced also in the presence of a high local Fe abundance. Thus, root hair branching and ferric-chelate reductase may share the systemic signal but they differ in the mechanism responding to the local supply.

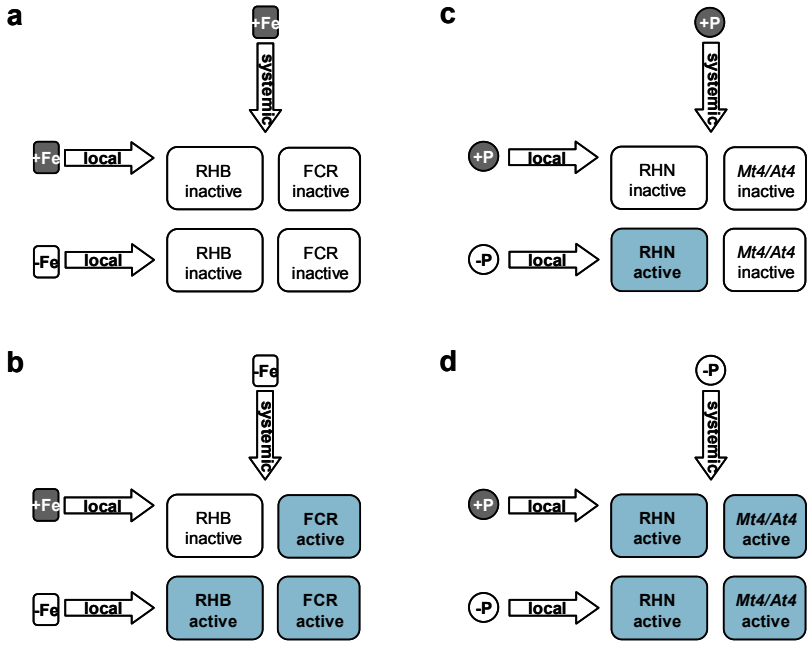

Figure 21: Influence of local and systemic signals related to iron (a, b) and phosphate homeostasis (c, d) on root hair development and deficiency markers. (a) If the shoot is Fe sufficient, a local Fe limitation can not activate root hair branching (RHB). Also the Fe-deficiency marker ferric-chelate reductase (FCR) is inactive. (b) Only if a systemic Fe deficiency signal is combined with a local deficiency signal, RHB is induced. FCR is active also in the presence of local Fe. (c) Also in the presence of a sufficient shoot local P depletion leads to an increase in the root hair number (RHN). The P starvation markers *Mt4/At4* are not induced under these conditions. (d) If the shoot is P deficient, RHN is increased and *Mt4/At4* induced.

Noteworthy is the constitutively high number of root hairs in the H position observed in the *frd3* mutant (Fig. 5e), which was not found in Fe-deficient wildtype roots (Fig. 5, a, c) and, therefore, could not be attributed solely to Fe deficiency. The influenced root hair number could have originated from additional effects caused by the *frd3* mutation. Accordingly, Delhaize (1996) showed that the *man1* mutant mainly accumulates manganese, but also copper, zinc, magnesium, and sulphur, and He *et al.* (2005) found a stimulating effect of Mn and Zn on the root hair density. Thus, the elevated root hair number of *frd3* might rather be due to a defective Mn or Zn homeostasis.

A local or systemic P deficiency signal is dominant in regulating the root hair number

The increased root hair number of P-deficient plants is induced by a local signal even if the shoot is sufficient, as the number of H cells in the H position was significantly higher in the -P-halves of +/-P split wildtype plants than in the +P-halves, which were equal to the +/+P

controls (Fig. 7, c, h, Fig. 21c). This finding is consistent with Bates & Lynch (1996) who found a similar local control of the root hair elongation under P depletion. Using a geometric model, Ma *et al.* (2001b) calculated a synergistic effect of root hair length and density on P acquisition efficiency and argued for a coordinated regulation. A sufficient shoot of +/-P wildtype plants is presumed basing on the fact that the expression of the phosphate starvation marker *Mt4*, and the P starvation-inducible phosphate transporters *LePT1* and *LePT2* in the roots are systemically suppressed (Burleigh & Harrison 1999, Liu *et al*. 1998, Fig. 21c). In the present study, it was, moreover, shown that a long-distance -P signal cannot be overruled by a sufficient local P supply (Fig. 21d). Support for this statement comes from the *pho1* mutant that exhibited a constitutively elevated root hair number under all treatments similar to -/-P Col-0 (Fig. 7g). This increased root hair number was not apparent when the shoot was removed (Fig. 7m). The shoot-derived P deficiency signal is, therefore, dominant to a local sufficiency signal, which might allow the plant to meet an increased P demand, e.g. during seed maturation from nutrient-rich patches. Also *At4* can not be downregulated in the *pho1* mutant (Burleigh & Harrison 1999, Fig. 21d). The increase of the root hair number and of *At4* induction may be regulated by a common systemic signal. In addition, a local P depletion was able to trigger root hair formation. Because the same phenotype was induced by a systemic or a local deficiency signal both pathways may discharge into the same target.

Together, this study established further differences between Fe and P regulated root hairs. Root hair branching of Fe starved plants is repressed by either a local or a systemic sufficiency signal, while the increase in the root hair number of P depleted plants is triggered by a systemic or a local deficiency signal. In both cases, root hair development may share common systemic signaling components with physiological starvation markers, but are differentially regulated from them with respect to a local signaling mechanism.

4.3 Which stage of root hair development is influenced by Fe and P?

In contrast to seedlings that develop a root hair in nearly all H positions, in the aging primary root the number of root hairs in the H position was markedly reduced (Fig. 3; Table 5). The components involved in seedling root hair development are likely also involved in the Fe- and P-sensitive root hair development of older plants. To test this and to address the question which stage of root hair development is influenced by the Fe or P supply, the root hair patterns of 19 Arabidopsis mutants with defects in different processes of root hair specification, initiation, bulge formation, or tip growth were investigated in plants that had been grown under sufficient nutrient supply or Fe or P starvation. Figure 22 summarizes those genes whose dysfunction lead to a significantly different root hair phenotype compared to the wildtype in the respective developmental stage under Fe or P deficiency.

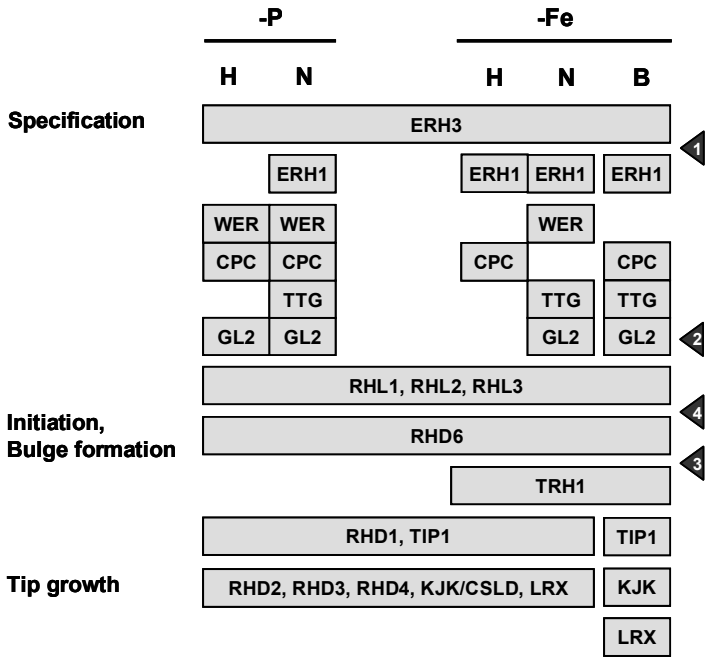

Figure 22: The involvement of genes from the root hair developmental pathway in root hair formation in Arabidopsis adapted to P- or Fe-deficient conditions (-P or -Fe). In the group of genes from the root hair specification, those are mentioned, whose dysfunction caused a different root hair frequency in the H or N position or in the degree of branching (B) compared to the wildtype ($P \leq 0.01$). The *ERH3* gene product is required in all cell types independent of the Fe or P supply. The need for *ERH1*, *WER*, *CPC*, *TTG*, and *GL2* gene function is different in the particular cell types of P- or Fe-deficient plants. The *RHL* genes and *RHD6* are required for H cell specification and root hair initiation, irrespective of the Fe or P supply. *TRH1* is only essentiell for root hair initiation and tip growth of Fe-deficient plants but is not required under P starvation. From the gene products required for root hair initiation, bulge formation, and tip growth, those are mentioned that differed in root hair length and shape. *RHD1, TIP1, RHD2, RHD3, RHD4, KJK/CSLD,* and *LRX* are required for root hair development independent of the nutrient supply. A different frequency of root hair branching during Fe deficiency is caused by mutation of *ERH3, ERH1, CPC, TTG, GL2, TIP1, KJK,* and *LRX*. The arrowheads mark possible entries of the Fe- or P-nutritional signal into the root hair developmental pathway.

Analysis of mutants with defects in root hair specification

The *erh1* and *erh3* mutants formed more root hairs in H and N position than the wildtype (Table 5) indicating that the *ERH1* and *ERH3* genes are important for proper epidermal cell development also in older plants. The increase in the root hair number under Fe and P deficiency was similar to the wildtype; although, the size of the increase was slightly lower (Table 5). This suggests the genes may not directly be involved in the nutrient-sensitive changes of the root hair number. ERH3 is a katanin-p-60 protein involved in microtubule organization and cell wall biosynthesis. In the *erh3* mutant, the identities of H and N cells and the cell identities of other root tissues are changed (Burk *et al*. 2001, Webb *et al*. 2002). Thus, the *ERH3* gene may be required at an early developmental stage, which is mainly independent of the nutrient status. The nutritional signal may enter the root hair developmental pathway downstream of *ERH3* action (Fig. 22, arrowhead 1).

The H and N cell identities are determined by a transcription factor cascade in the late meristematic region involving a MYB protein, which is either WER or CPC, the WD40 repeat

protein TTG, and the bHLH proteins GL3 and EGL3. Activation of this cascade leads to *GL2* expression in the N position whereby inhibiting root hair formation (Schiefelbein & Lee 2006). Under the tested growth conditions, the root hair patterning of the *wer*, *cpc*, *ttg*, and *gl2* mutants differed from the wildtype in H and N positions. With the exception of *ttg*, the Fe and P deficiency-specific increase in the root hair number in the H position was also different in this group of mutants. These observations could be interpreted in two ways. One possibility is that the formation of root hair cells adapted to the Fe and P supply is directly linked with the action of the transcription factor cascade leading to *GL2* expression (Fig. 22, arrowhead 2). However, all these mutants were able to increase their root hair frequency in response to Fe or P starvation; although, not to the same degree as the wildtype. This observation indicates that the WER/CPC/GL2 pathway may not be a direct target of the nutritional signals.

With the exception of *wer*, the *erh1*, *erh3*, *cpc*, *ttg*, and *gl2* mutants were not able to develop branched root hairs. These genes could be a prerequisite for the branching procedure or be directly involved in branching. Ohashi *et al*. (2003), in contrast, observed the formation of branched root hairs in the *gl2-5* mutant, but these root hairs were formed rather irregular and not in a transversal layer. The difference between the *gl2-1* phenotype in this study and the *gl2-5* phenotype observed by Ohashi *et al.* (2003) could have resulted from using different mutant alleles or growth conditions.

The *RHL* genes are part of the topoisomerase VI complex and are important for ploidy-dependent cell growth. All the *rhl* mutants all did not develop root hairs under the conditions described (Table 5), indicating endoreduplication is required for root hair formation independent of age or nutrient supply (Fig. 22).

Analysis of mutants with defects in root hair initiation and tip growth

RHD6 is involved in positioning the root hair initiation site near the apical end of the epidermal cell (Masucci & Schiefelbein 1994). In the present study, *RHD6* gene function was essential for root hair initiation independent of age or nutrient status. Under all conditions, the *rhd6* mutant was devoid of root hairs (Table 5). The nutritional signal could be a prerequisite for RHD6 action or act together with or downstream of RHD6.

TRH1 is a potassium transporter that accelerates auxin transport in the root cap (Rigas *et al*. 2001, Vincente-Agullo *et al*. 2004). Under control and –Fe growth conditions, root hair initiation and tip growth were dependent on *TRH1* function (Fig. 9, a-b; Table 5). In contrast, when grown under P deficiency, the *trh1* mutant developed normal root hairs (Fig. 9c; Table 5). Thus, TRH1 is important for root hair initiation and tip growth in sufficient and Fe-deficient but not of P-deficient plants (Fig. 22). The behavior of *trh1* is similar to the response of the *axr1*, *axr2*, and *ein2* mutants under the same growth conditions (Schmidt & Schikora 2001). This supports the hypothesis of Schmidt and Schikora (2001) that root hair

development of Fe- and P-deficient plants is regulated by different pathways and that root hairs formed under P starvation are at least partially regulated independent of components belonging to the auxin signaling pathway.

The *tip1*, *rhd2*, *rhd3*, and *rhd4* mutants developed short root hairs under all growth conditions at a frequency that did not deviate from the wildtype (Fig. 9; Table 5). The *S*-acyl-transferase TIP1, the NADPH oxidase RHD2, and the small G protein RHD3 are assumed to be involved in different processes of vesicle traffic during the tip growth of root hairs (Hemsley *et al*. 2005, Foreman *et al*. 2003, Hu *et al*. 2003). *KJK/CSLD*, *RHD1*, and *LRX* are involved in proper cell wall assembly during root hair initiation and tip growth (Wang *et al*. 2001, Favery *et al*. 2001, Schiefelbein & Somerville 1990, Seifert *et al*. 2002, Baumberger *et al*. 2001). Also in this group of mutants, the number of root hairs was unaltered (Table 5, Table 6), but the root hair shape was impaired as previously described. Hence, it appears that after the proper position and frequency of root hairs in response to the nutrient supply has been determined, the same root hair-specific vesicle transport and cell wall synthesis machinery performs the elongation of the root hairs. This suggests that the nutritional signal enters the root hair developmental pathway upstream of root hair tip growth (Fig. 22, arrowhead 3).

Together, the data indicate that Fe and P influence root hair development at the stage of root hair specification or root hair initiation upstream of components involved in tip growth.

Fe or P deficiency did not affect the pattern of early cell characteristics in the late meristematic region

Root epidermal cells originate from the epidermal initials in the meristem. A periclinal division initially forms two daughter cells, of which one remains an initial and the other undergoes a second periclinal division producing two cells, one outside the other. Each of these daughter cells then divides anticlinally to produce cell files, the outer one generates the lateral root cap and the inner one the epidermis (Dolan *et al*. 1993). Dependent on the underlying cortical cells, trichoblast and atrichoblast files are formed. The trichoblasts are shorter than the atrichoblasts and divide more often. They have a denser cytoplasm and a lower degree of vacuolization. Occasionally, the trichoblasts divide longitudinally; thereby the daughter cell in the N position switches its identity into an atrichoblast (Dolan *et al*. 1994, Berger *et al*. 1998a). These studies have been performed with 5-day-old seedlings that develop a root hair in nearly all H positions (Dolan *et al*. 1994, Galway *et al*. 1994, Lee & Schiefelbein 2001). In plants older than 5 days, only about one-half of epidermal cells in the H position developed a root hair and this frequency was sensitive to the Fe and P supply (Fig. 3a; Table 5). It was, therefore, determined if the root hair cells in the H position can already be distinguished from the non-hair cells in the H position by a stronger cytoplasmic staining and lower degree of vacuolization in the late meristematic region. However, both features did not reflect the root hair patterning in adaptation to the Fe or P supply

(Fig. 11, b-f). The non-hair cells in the H position showed the same cytological features as the root hair cells and they have not completely been converted from H cells into N cells. The differential cytoplasmic staining and the degree of vacuolization reflect, therefore, more a developmental state unaffected by nutrient signals rather than an early indication of future root hair outgrowth. Thus, the nutritional signal enters the root hair developmental pathway after cell characteristics like a denser cytoplasm and a lower degree of vacuolization have been established.

ERH3 is required for the correct positioning of cells with a denser cytoplasm in the H position. Because this feature is not altered under the investigated conditions, the nutritional signal may enter the developmental pathway downstream of *ERH3* action (Fig. 22, arrowhead 1).

In seedlings, the *gl2* mutant develops root hairs in the N position, as do mutations in its upstream regulators *WER* and *TTG*, but displays, in contrast to them, the differential cytoplasmic staining of the wildtype. Thus, the *gl2* mutation alters only a subset of N cell differentiation processes and does not cause the complete conversion of N into H cells (Masucci *et al.*, 1996). In this study, the *gl2* mutant showed an increased number of root hairs in H and N position when compared to the wildtype under all growth conditions (Table 5). Under Fe and P starvation, the root hairs in the H position were not increased to the same degree in the *gl2* mutant as in the wildtype suggesting an involvement of *GL2* in the nutrient-sensible root hair development. Using GUS plants, we determined if the non-hair cells in the H position are linked with *GL2* expression in the H position. Additionally, we investigated the GUS expression pattern of *CPC*, a negative regulator of *GL2* (Wada *et al.* 2002). Similar to the situation in the postembryonic root, nearly all H positions showed no *CPC-GUS* or *GL2-GUS* staining (Fig. 11, g-l; Table 7). Fe or P had, thus, no impact on the spatial expression pattern of *CPC* and *GL2*. The data indicate that the CPC- and GL2-related pathway primarily controls the non-hair specification in the N position as discussed by Masucci *et al.* (1996) and not the development of non-hair cells in the H position observed in this study. It is possible that the transcription factor cascade leading to *GL2* expression is part of a common mechanism that specifies the positional information irrespective of age or nutrient status. The nutritional signal rather modulates the abundance of hair or non-hair cells in the H position. However, it is also possible that the root hairs in Arabidopsis might be regulated by fine tuning the level of GL2 or CPC in the N position that was not visible with the GUS staining.

In the *rhl* mutants, *GL2* is correctly expressed leading Sugimoto-Shirasu *et al*. (2005) to conclude that *RHL* function is independent of the *GL2* activity. Since the *rhl* mutants are not able to induce a denser cytoplasm and lower degree of vacuolization (Schneider *et al*. 1997), as did Fe- and P-deficient plants in the present study, *RHL* function may be a prerequisite for Fe- and P-dependent root hair development, which would than act downstream of RHL (Fig. 22, arrowhead 4).

In summary, the Fe and P nutritional status did not affect the spatial distribution of *GL2*, *CPC*, and the mechanism causing the differential cytoplasmic staining in the late meristematic region of the root. Thus, Fe and P may influence root hair development after these characteristics have been established. Together with the mutant analysis (Table 5), the results indicate that the nutritional signal may modulate root hair development at the stage of root hair initation (Fig. 22, between arrowhead 3 and arrowhead 4).

4.4 The *per2* mutant

To identify potentially novel genes involved in root hair development under P starvation, 6 mutants were screened that did not develop root hairs under P deficiency but displayed the wildtype phenotype in the presence of P. One of these mutants, *per2*, was characterized in further detail. The *per2* mutant had a single recessive nuclear mutation. The mutant developed only small bulges or short root hairs that were deformed and this behaviour was restricted to P deficiency (Fig. 12). The position-dependent pattern or the frequency of the *per2* bulges was not altered indicating the *PER2* gene is involved in the P-sensitive root hair elongation rather than in root hair cell specification (Fig. 13). At the tips of the *per2* bulges, material accumulations were visible (Fig. 12). Material accumulations at root hair tips have also been observed in the *lrx* mutant, which is a regulator of cell wall assembly during root hair tip growth (Baumberger *et al*. 2001). The material accumulation at the tips of *per2* bulges could also caused by a defect in a similar component, but none of which is under the candidate genes listed in Table 10. In addition to the impaired root hair growth, *per2* developed a constitutively increased number of laterals, and this phenotype was genetically linked with the root hair phenotype (Fig. 14). In this study, only laterals were counted that were visible without magnification. Thus, a stimulation of lateral root elongation in *per2* is more likely than the induction of more primordia. A visualization of primordia by the expression of cell cycle markers could prove this hypothesis. Under P starvation, *per2* accumulated also higher amounts of anthocyanine, which was also genetically linked with the root hair phenotype (Fig. 15). Thus, *PER2* seemed to be a regulator involved in at least three different P starvation responses. In the case of the impact on root hair development and anthocyanine accumulation, *PER2* acted, thereby, as a positive regulator, in the case of the lateral root development, *PER2* appeared to be a negative regulator. Next, an analysis of P starvation marker genes would be of importance. No other of the 6 mutants was allelic to *per2*. But from their similar phenotype, an involvement in the same pathway could be assumed. Among the mutants impaired in P signalling, none has been described that is similar to *per2*. Also none of the mutants from the root hair developmental pathway did exhibit a phenotype similar to *per2*. Thus, *PER2* could represent a novel gene involved in P signalling. The phosphate content of the mutant was unaltered (Fig. 16) indicating that *per2* did not impact phosphate acquisition under the tested conditions, and that the mutant phenotype was not an effect of the internal P status. A local abundance of the phosphate analogon phosphite rescued the impaired root hair

elongation of *per2* (Fig. 17) suggesting the *PER2* gene belongs to a local signalling pathway. The *per2gl2* and *per2erh3* double mutants displayed an additive phenotype. This indicates that the *PER2* gene acts independent of the root hair specification genes *GL2* and *ERH3*. This is consistant with the result that early cell characteristics in the late meristematic region, which are regulated by *GL2* and *ERH3*, were not altered in response to P starvation (Fig. 11).

The *per2* mutation was mapped to a 87.6 kbp region on the upper arm of chromosome 3. This region contains 19 genes (Fig. 19; Fig: 20; Table 10). The most interesting candidates for the *PER2* gene are the unknown proteins At3g2049 and At3g20620, the protein kinase At3g20530, the defence response protein At3g20600, and the glycerol metabolism related protein At3g20520, since all these genes could be involved in signal transduction. During the mapping procedure, a phenotype is linked with a certain genotype. Only one recombinant line has been identified to be heterozygous in marker MQC12-1 (Fig. 20) Thus, it is possible that the *per2* phenotype of this line is mimicked by another effect resulting from the cross of the two different accessions Col-0 and Cvi. This effect could be a QTL or an epiallelic influence. However, a complementation with cosmids could be the best strategy for the identification of the *PER2* gene.

Together, the *PER2* gene is a potentially new gene involved in root hair development under phosphate deficiency and possibly also in the regulation of lateral root development and anthocyanin synthesis.

LITERATURE

Abadía J, López-Millán A-N, Rombolà A, Abadía A (2002) Organic acids and Fe deficiency: a review. Plant and Soil **241**: 75-86

Abel S, Nürnberger T, Ahnert V, Krauss G-J, Glund K (2000) Induction of an extracellular cyclic nucleotide phosphodiesterase as an accessory ribonucleolytic activity during phosphate starvation of cultured tomato cells. Plant Physiology **122**: 543-52

Ae N, Arihara J, Okada K, Yoshihara T, Johansen C (1990) Phosphorus uptake by pigeon pea and its role in cropping systems of the Indian subcontinent. Science **248**: 477-80

Anthony RG, Henriques R, Helfer A, Mészáros T, Rios G, Testerink C, Munnik T, Deák M, Koncz C, Bögre L (2004) A protein kinase target of a PDK1 signaling pathway is involved in root hair growth in Arabidopsis. The EMBO Journal **23**: 572-81

Arahou M, Diem HG (1997) Iron deficiency induces cluster (proteoid) root formation in *Casuarina glauca*. Plant and Soil **196**: 71-9

Aung K, Lin S, Wu C-C, Huang Y-T, Su C, Chiou T-J (2006) pho2, a phosphate overaccumulator, is caused by a nonsense mutation in a microRNA399 target gene. Plant Physiology **141**: 1000-11

Bagnat M, Simons K (2002) Lipid rafts in protein sorting and cell polarity in budding yeast *Saccharomyces cerevisiae*. Biological Chemistry **383**: 1475-80

Baluška F, Salaj J, Mathur J, Braun M, Jasper F, Šamaj J, Nam-Hai C, Barlow PW, Volkmann D (2000) Root hair formation: F-actin-dependent tip growth is initiatied by local assembly of profilin-supported F-actin meshworks accumulated within expansin-enriched bulges. Developmental Biology **227**: 618-32

Bariola PA, Howard CJ, Taylor CB, Verburg MT, Jaglan VD, Green PJ (1994) The Arabidopsis ribonuclease gene *RNS1* is tightly controlled in response to phosphate limitation. The Plant Journal **6**: 673-85

Bates TR, Lynch JP (2000) Plant growth and phosphorus accumulation of wild type and two root hair mutants of *Arabidopsis thaliana* (Brassicaceae). American Journal of Botany **87**: 958-63

Bates TR, Lynch JP (1996) Stimulation of root hair elongation in *Arabidopsis thaliana* by low phosphorus availability. Plant, Cell and Environment **19**: 529-38

Baumberger N, Ringli C, Keller B (2001) The chimeric leucin-rich repeat/extensin cell wall protein LRX1 is required for root hair morphogenesis in *Arabidopsis thaliana*. Genes and Development **15**: 1128-39

Baumberger N, Steiner M, Ryser U, Keller B, Ringli C (2003) Synergistic interaction of the two paralogus Arabidopsis genes *LRX1* and *LRX2* in cell wall formation during root hair development. The Plant Journal **35**: 71-81

Berger F, Haseloff J, Schiefelbein J, Dolan L (1998b) Positional information in root epidermis is defined during embryogenesis and acts in domains with strict boundaries. Current Biology **8**: 421-30

Berger F, Hung C-Y, Dolan L, Schiefelbein J (1998a) Control of cell division in the root epidermis of *Arabidopsis thaliana*. Developmental Biology **194**: 235-45

Bernhardt C, Tierney ML (2000) Expression of AtPRP3, a proline-rich structural cell wall protein from Arabidopsis, is regulated by cell-type-specific developmental pathways involved in root hair formation. Plant Physiology **122**: 705-14

Bernhardt C, Zhao M, Gonzalez A, Lloyd A, Schiefelbein J (2005) The bHLH genes *GL3* and *EGL3* participate in an intracellular regulatory circuit that controls cell patterning in the Arabidopsis root epidermis. Development **132**: 291-8

Bibikova TN, Blancaflor EB, Gilroy S (1999) Microtubules regulate tip growth and orientation in root hair of *Arabidopsis thaliana*. The Plant Journal **17**: 657-65

Bibikova TN, Jacob T, Dahse I, Gilroy S (1998) Localized changes in apoplastic and cytoplasmatic pH are associated with root hair development in *Arabidopsis thaliana*. Development **125**: 2925-34

Bieleski RL (1973) Phosphate pools, phosphate transport, and phosphate availability. Annual Reviews in Plant Physiology **24**: 225-52

Bienfait HF, De Weger LA, Kramer D (1987) Control of the development of iron-efficiency reactions in potato as a response to iron deficiency is located in the roots. Plant Physiology **83**: 244-7

Bischoff F, Vahlkamp L, Molendijk A, Palme K (2000) Localization of AtROP4 and AtROP6 and interaction with the guanine nucleotide dissociation inhibitor AtRhoGDI1 from Arabidopsis. Plant Molecular Biology **42**: 515-30

Bonser AM, Lynch JP, Snapp S (1996) Effect of phosphorus deficiency on growth angle of basal roots in *Phaseolus vulgaris*. The New Phytologist **132**: 281-8

Braun M, Baluška F, von Witsch M, Menzel D (1999) Redistribution of actin, profilin and phosphatidylinositol-4,5-bisphosphate in growing and maturing root hairs. Planta **209**: 435-43

Brown JC, Chaney RL, Ambler JE (1971) A new mutant inefficient in the transport of iron. Physiologica Plantarum **25**: 48-53

Brown JC, Foy CD, Bennett JH, Christiansen MN (1979) Two light sources differentially affect ferric iron reduction and growth of cotton. Plant Physiology **63**: 692-5

Brumbarova T, Bauer P (2005) Iron-mediated control of the basic helix-loop-helix protein FER, a regulator of iron uptake in tomato. Plant Physiology **137**: 1018-26

Bucher M, Schroeer B, Willmitzer L, Riesmeier JW (1997) Two genes encoding extensin-like proteins are predominantly expressed in tomato root hair cells. Plant Molecular Biology **35**: 497-508

Bünning E (1951) Über die Differenzierungsvorgänge in der Cruziferenwurzel. Planta **39**: 126-53

Burk DH, Liu B, Zhong R, Morrison WH, Ye Z-H (2001) A katanin-like protein regulates normal cell wall biosynthesis and cell elongation. The Plant Cell **13**: 807-27

Burleigh SH, Harrison MJ (1997) A novel gene whose expression in *Medicago trunculata* roots is suppressed in response to colonization by vesicular-arbuscular mycorrhizal (VAM) fungi and to phosphate nutrition. Plant Molecular Biology **34**: 199-208

Burleigh SH, Harrison MJ (1999) The down-regulation of *Mt4*-like genes by phosphate fertilization occurs systemically and involves phosphate translocation to the shoots. Plant Physiology **119**: 241-8

Carol RJ, Takeda S, Linstead P, Durrant MC, Kakesova H, Derbyshire P, Drea S, Zarsky V, Dolan L (2005) A RhoGDP dissociation inhibitor spatially regulates growth in root hair cells. Nature **438**: 1013-6

Carpita NC, Gibeaut DM (1993) Structural models of primary cell walls in flowering plants: consistency of molecular structure with the physical properties of the walls during growth. The Plant Journal **3**: 1-30

Carswell C, Grant BR, Theodorou ME, Harris J, Niere JO, Plaxton WC (1996) The fungicide phosphonate disrupts the phosphate-starvation response in *Brassica nigra* seedlings. Plant Physiology **110**: 105-10

Carswell MC, Grant BR, Plaxton WC (1997) Disruption of the phosphate-starvation response of oilseed rape suspension cells by the fungicide phosphonate. Planta **203**: 67-74

Casimiro I, Marchant A, Bhalerao RP, Beeckman T, Dhooge S, Swarup R, Graham N, Inzé D, Sandberg G, Casero PJ, Bennett M (2001) Auxin transport promotes Arabidopsis lateral root initiation. The Plant Cell **13**: 843-52

Cassab GI (1998) Plant cell wall proteins. Annual Reviews of Plant Physiology and Plant Molecular Biology **49**: 281-309

Chen DL, Delatorre CA, Bakker A, Abel S (2000) Conditional identification of phosphate-starvation-response mutants in *Arabidopsis thaliana*. Planta **211**: 13-22

Chiou T-J, Aung K, Lin S, Wu C-C, Chiang S-F, Su C-L (2006) Regulation of phosphate homeostasis by microRNA in Arabidopsis. The Plant Cell **18**: 412-21

Cho H-T, Cosgrove DJ (2002) Regulation of root hair initiation and expansin gene expression in Arabidopsis. The Plant Cell **14**: 3237-53

Ciereszko I, Johansson H, Hurry V, Kleezkowski LA (2001) Phosphate status affects the gene expression, protein content and enzymatic activity of UDP-glucose pyrophosphorylase in wildtype and *pho* mutants of Arabidopsis. Planta **212**: 598-605

Cohen CK, Garvin DF, Kochian LV (2004) Kinetik properties of a micronutient transporter from *Pisum sativum* indicate a primary function in Fe uptake from the soil. Planta **218**: 784-92

Colangelo EP, Guerinot ML (2004) The essential basic helix-loop-helix protein FIT1 is required for the iron deficiency response. The Plant Cell **16**: 3400-12

Connolly EL, Campbell NH, Grotz N, Prichard CL, Guerinot ML (2003) Overexpression of the FRO2 ferric-chelate reductase confers tolerance to growth on low iron and uncovers posttranscriptional control. Plant Physiology **133**: 1102-10

Connolly EL, Fett JP, Guerinot ML (2002) Expression of the IRT1 metal transporter is controlled by metals at the levels of transcript and protein accumulation. The Plant Cell **14**: 1347-57

Cosgrove DJ (2000) Loosening of plant cell walls by expansins. Nature **407**: 321-6

Costa S, Shaw P (2006) Chromatin organization and cell fate switch respond to positional information in Arabidopsis. Nature **439**: 493-6

Cruz-Ramírez A, Oropeza-Aburto A, Razo-Hernánez F, Ramírez-Chávez E, Herrera-Estrella L (2006) Phospholipase DZ2 plays an important role in extraplastidic galactolipid biosynthesis and phosphate recycling in Arabidopsis roots. PNAS **103**: 6765-70

Curie C, Alonso JM, Le Jean M, Ecker JR, Briat J-F (2000) Involvement of *NRAMP1* from *Arabidopsis thaliana* in iron transport. Biochemical Journal **347**: 749-55

Daram P, Brunner S, Rausch C, Steiner C, Amrhein N, Bucher M (1999) Pht2;1 encodes a low-affinity phosphate transporter from Arabidopsis. The Plant Cell **11**: 2153-66

del Pozo JC, Allona I, Rubio V, Leyva A, de la Peña A, Aragoncillo C, Paz-Ares J (1999) A type 5 acid phosphatase gene from *Arabidopsis thaliana* is induced by phosphate starvation and by some other types of phosphate mobilising/oxidative stress conditions. The Plant Journal **19**: 579-89

Delhaize E (1996) A metal-accumulator mutant of *Arabidopsis thaliana*. Plant Physiology **111**: 849-55

Delhaize E, Randall PJ (1995) Characterization of a phosphate-accumulator mutant of *Arabidopsis thaliana*. Plant Physiology **107**: 207-13

DerMardirossian C, Bokoch GM (2005) GDIs: central regulatory molecules in Rho GTPase activation. Trends in Cell Biology **15**: 356-63

Desbrosses G, Josefsson C, Rigas S, Hatzopoulos P, Dolan L (2003) *AKT1* and *TRH1* are required during root hair elongation in Arabidopsis. Journal of Experimental Botany **54**: 781-8

DiDonato R Jr, Roberts LA, Sanderson T, Eisley RB, Walker EL (2004) Arabidopsis *Yellow Stripe-Like2* (*YSL2*): a metal-regulated gene encoding a plasma membrane transporter of nicotianamine-metal complexes. The Plant Journal **39**: 403-14

Diet A, Brunner S, Ringli C (2004) The *enl* mutants enhance the lrx root hair mutant phenotype of *Arabidopsis thaliana.* Plant and Cell Physiology **45**: 734-41

Diet A, Link B, Seifert GJ, Schellenberg B, Wagner U, Pauly M, Reiter W-D, Ringli C (2006) The Arabidopsis root hair cell wall formation mutant lrx1 is suppressed by mutantions in the *RHM1* gene encoding a UDP-L-rhamnose synthase. The Plant Cell **18**: 1630-41

Dittmer HJ (1937) A quantitative study of the roots and root hairs of a winter rye plant (*Secale cereale*). American Journal of Botany **24**: 417-20

Dolan L (2006) Positional information and mobile transcriptional regulators determine cell pattern in the Arabidopsis root epidermis. Journal of Experimental Botany **57**: 51-54

Dolan L, Duckett MD, Grierson C, Linstead P, Schneider K, Lawson E, Dean C, Poethig S, Roberts K (1994) Clonal relationships and cell patterning in the root epidermis of Arabidopsis. Development **120**: 2465-74

Dolan L, Janmaat K, Willemsen V, Linstead P, Poethig S, Roberts K, Scheres B (1993) Cellular organization of the *Arabidopsis thaliana* root. Development **119**: 71-84

Donaldson JG, Cassel D, Kahn RA, Klausner RD (1992a) ADP-ribosylation factor, a small GTP-binding protein, is required for binding of the coatomer protein β-COP to Golgi membranes. PNAS **89**: 6408-12

Donaldson JG, Finazzi D, Klausner RD (1992b) Brefeldin A inhibits Golgi membrane-catalyzed exchange of guanine nucleotide onto ARF protein. Nature **360**: 350-2

Dong B, Rengel Z, Delhaize E (1998) Uptake and translocation of phosphate by pho2 mutant and wildtype seedlings of *Arabidopsis thaliana*. Planta **205**: 251-6

Drew MC, Saker LR (1984) Uptake and long-distance transport of phosphate, potassium and chloride in relation to internal ion concentrations in barley: evidence of non-allosteric regulation. Planta **60**: 500-7

Duff SMG, Plaxton WC, Lefebvre DD (1991) Phosphate-starvation response in plant cells: *de novo* synthesis and degradation of acid phosphatases. PNAS **88**: 9538-42

Durrett T, Gassmann W, Rogers E (2006) Functional characterization of FRD3, a novel organic acid effluxer involved in iron homeostasis. Abstract No. S4-O-7 edited by: 13th International Symposium of Iron Nutrition and Interaction in Plants,, Montpellier

Duy D, Wanner G, Soll J, Philippar K (2006) PIC1: an ancient permease in Arabidopsis chloroplasts mediates transport of metal ions. Abstract No. S4-O-4 edited by: 13th International Symposium of Iron Nutrition and Interaction in Plants, Montpellier

Eckhardt U, Buckhout TJ (1998) Iron assimilation in *Clamydomonas reinhardtii* involves ferric reduction and is similar to strategy I higher plants. Journal of Experimental Botany **49**: 1219-26

Eckhardt U, Mas Marques A, Buckhout TJ (2001) Two iron-regulated cation transporter from tomato complement metal uptake-deficient yeast mutants. Plant Molecular Biology **45**: 437-48

Eide D, Broderius M, Fett J, Guerinot ML (1996) A novel iron-regulated metal transporter from plants identified by functional expression in yeast. PNAS **93**: 5624-8

Eliás M, Drdova E, Ziak D, Bavlnka B, Hala M, Cvrckova F, Soukupova H, Žárský V (2003) The exocyst complex in plants. Cell Biology International **27**: 199-201

Estelle MA, Somerville C (1987) Auxin-resistant mutants of *Arabidopsis thaliana* with an altered morphology. Molecular and General Genetics **206**: 200-6

Evans ML, Ishikawa H, Estelle MA (1994) Response of Arabidopsis roots to auxin studied with high resolution: comparison of wild type and auxin-response mutants. Planta **194**: 215-22

Favery B, Ryan E, Foreman J, Linstead P, Boudonck K, Steer M, Shaw P, Dolan L (2001) *KOJAK* encodes a cellulose synthase-like protein required for root hair cell morphogenesis in Arabidopsis. Genes and Development **15**: 79-89

Fischer U, Ikeda Y, Ljung K, Serralbo O, Singh M, Heidstra R, Palme K, Scheres B, Grebe M (2006) Vectorial information for Arabidopsis planar polarity is mediated by combined *AUX1*, *EIN2*, and *GNOM* activity. Current Biology **16**: 2143-9

Foehse D, Jungk A (1983) Influence of phosphate and nitrate supply on root hair formation of rape, spinach, and tomato plants. Plant and Soil **74**: 359-68

Forde B, Lorenzo H (2001) The nutritional control of root development. Plant and Soil **232**: 51-68

Foreman J, Demidchik V, Bothwell JHF, Mylona P, Miedema H, Torres MA, Linstead P, Costa S, Brownlee C, Jones JDG, Davies JM, Dolan L (2003) Reactive oxygen species produced by NADPH oxidase regulate plant cell growth. Nature **422**: 442-6

Foreman J, Dolan L (2001) Root hairs as a model system for studying plant cell growth. Annals of Botany **88**: 1-7

Foyer C, Spencer C (1986) The relationship between phosphate status and photosynthesis in leaves. Planta **167**: 369-75

Franco-Zorilla JM, González E, Bustos R, Linhares F, Leyva A, Paz-Ares J (2004) The transcriptional control of plant responses to phosphate limitation. Journal of Experimental Botany **55**: 285-93

Franco-Zorrilla JM, Martín AC, Solano R, Rubio V, Leyva A, Paz-Ares J (2002) Mutations at *CRE1* impair cytokinin-induced repression of phosphate starvation responses in Arabidopsis. The Plant Journal **32**: 353-60

Fredeen AL, Rao IM, Terry N (1989) Influence of phosphorus nutrition on growth and carbon partitioning in *Glycine max*. Plant Physiology **89**: 225-30

Fujii H, Chiou T-J, Lin S, Aung K, Zhu J-K (2005) A miRNA involved in phosphate-starvation response in Arabidopsis. Current Biology **15**: 2038-43

Gahoonia TS, Nielsen NE (1998) Direct evidence on participation of root hairs in phosphorus (^{32}P) uptake from soil. Plant and Soil **198**: 147-52

Gahoonia TS, Nielsen NE (1997) Variation in root hairs of barley cultivars doubled soil phosphorus uptake. Euphytica **98**: 177-82

Galway ME, Heckman JW Jr., Schiefelbein JW (1997) Growth and ultrastructure of Arabidopsis root hairs: the *rhd3* mutation alters vacuole enlargement and tip growth. Planta **201**: 209-18

Galway ME, Lane DC, Schiefelbein JW (1999) Defective control of growth rate and cell diameter in tip-growing root hairs of the *rhd4* mutant of *Arabidopsis thaliana*. Canadian Journal of Botany **77**: 494-507

Galway ME, Masucci JD, Lloyd AM, Walbot V, Davis RW, Schiefelbein JW (1994) The *TTG* gene is required to specify epidermal cell fate and cell patterning in the Arabidopsis root. Developmental Biology **166**: 740-54

Gardner WK, Barber DA, Parbery DG (1983) The acquisition of phosphorus by *Lupinus albus* L. III. The probable mechanism by which phosphorus movement in the soil/root interface is enhanced. Plant and Soil **70**: 107-24

Ge Z, Rubio G, Lynch JP (2000) The importance of root gravitropism for inter-root competition and phosphorus acquisition efficiency: results from a geometric simulation model. Plant and Soil **218**: 159-71

Gilbert GA, Knight JD, Vance CP, Allan DL (2000) Proteoid root development of phosphorus deficient lupin is mimicked by auxin and phosphonate. Annals of Botany **85**: 921-8

González E, Solano R, Rubio V, Leyva A, Paz-Ares J (2005) PHOSPHATE TRANSPORTER TRAFFIC FACILITATOR1 is a plant-specific SEC12-related protein that enables the endoplasmatic reticulum exit of a high-affinity phosphate transporter in Arabidopsis. The Plant Cell **17**: 3500-12

Grebe M (2004) Ups and downs of tissue and planar polarity in plants. BioEssays **26**: 719-29

Grebe M, Friml J, Swarup R, Ljung K, Sandberg G, Terlou M, Palme K, Bennett MJ, Scheres B (2002) Cell polarity signaling in Arabidopsis involves a BFA-sensitive auxin influx pathway. Current Biology **12**: 329-34

Green LS, Rogers EE (2004) *FRD3* controls iron localization in Arabidopsis. Plant Physiology **136**: 1-9

Grierson PF (1992) Organic acids in the rhizosphere of *Baksia integrifolia* L.f. Plant and Soil **144**: 259-65

Grusak MA (1995) Whole-root iron(III)-reductase activity throughout the life-cycle or iron-grown *Pisum sativum* L. (Fabaceae): Relevance to the iron nutrition of developing seeds. Planta **197**: 111-7

Hamburger D, Rezzonico E, MacDonald-Comber Petétot J, Somerville C, Poirier Y (2002) Identification and characterization of the Arabidopsis PHO1 gene involved in phosphate loading of the xylem. The Plant Cell **14**: 889-902

Hammond JP, Broadley MR, White PJ (2004) Genetic responses to phosphorus deficiency. Annals of Botany **94**: 323-32

Harada T, Matsuzaki O, Hayashi H, Sugano S, Matsuda A, Nishida E (2003) AKRL1 and AKRL2 activate the JNK pathway. Genes to Cells **8**: 493-500

Harrison PM, Arosio P (1996) The ferritins: molecular properties, iron storage function, and cellular regulation. Biochemica Biophysica Acta **1275**: 161-203

He Z, Ma Z, Brown KM, Lynch JP (2005) Assessment of inequality of root hair density in *Arabidopsis thaliana* using the Gini coefficient: a close look at the effect of phosphorus and its interaction with ethylene. Annals of Botany **95**: 287-93

Hell R, Stephan UW (2003) Iron uptake, trafficking and homeostasis in plants. Planta **216**: 541-51

Hellmann H, Estelle M (2002) Plant development: regulation by protein degradation. Science **297**: 793-7

Helms JB, Rothman JE (1992) Inhibition by brefeldin A of a Golgi membrane enzyme that catalyzes exchange of guanine nucleotide bound to ARF. Nature **360**: 352-4

Hemsley PA, Kemp AC, Grierson CS (2005) The TIP GROWTH DEFECTIVE1 *S*-acyl transferase regulates plant cell growth in Arabidopsis. The Plant Cell **17**: 2554-63

Hepler PK, Vidali L, Cheung AY (2001) Polarized cell growth in higher plants. Annual Review of Cell and Developmental Biology **17**: 159-87

Herbik A, Bölling C, Buckhout TJ (2002) The involvement of a multicopper oxidase in iron uptake by the green algae *Chlamydomonas reinhardtii*. Plant Physiology **130**: 2039-48

Himanen K, Boucheron E, Vanneste S, de Almeida Engler J, Inzé D, Beeckman T (2002) Auxin-mediated cell cycle activation during early lateral root initiation. The Plant Cell **14**: 2339-51

Hobbie L, Estelle M (1995) The *axr4* auxin-resistant mutants of *Arabidopsis thaliana* define a gene important for root gravitropism and lateral root initiation. The Plant Journal **7**: 211-20

Horgan JM, Wareing PF (1980) Cytokinins and the growth responses of seedlings of *Betula pendula* Roth and *Acer pseudoplatanus* L. to nitrogen and phosphorus deficiency. Journal of Experimental Botany **31**: 525-32

Hu Y, Zhong R, Morrison H, Ye Z-H (2003) The Arabidopsis *RHD3* gene is required for cell wall biosynthesis and actin organization. Planta **217**: 912-21

Hülskamp M (2000) Cell morphogenesis: how plants split hairs. Current Biology **10**: 308-10

Hülskamp M, Misera S, Jürgens G (1994) Genetic dissection of trichome cell development in Arabidopsis. Cell **76**: 555-66

Hung C-Y, Lin Y, Zhang M, Pollock S, Marks MD, Schiefelbein J (1998) A common position-dependent mechanism controls cell-type patterning and GLABRA2 regulation in the root and hypocotyl epidermis of Arabidopsis. Plant Physiology **117**: 73-84

Inoue T, Higuchi M, Hashimoto Y, Seki M, Kobayashi M, Kato T, Tabata S, Shinozaki K, Kakimoto T (2001) Identification of CRE1 as a cytokinin receptor from Arabidopsis. Nature **409**: 1060-3

Ivashuta S, Liu J, Liu J, Lohar DP, Haridas S, Bucciarelli B, VandenBosch KA, Vance CP, Harrison MJ, Gantt JS (2005) RNA interference identifies a calcium-dependent protein kinase involved in *Medicago trunculata* root development. The Plant Cell **17**: 2911-21

Jacoby M, Wang H-Y, Reidt W, Weisshaar B, Bauer P (2004) *FRU (bHLH029)* is required for induction of iron mobilization genes in *Arabidopsis thaliana*. FEBS letters **577**: 528-534

Jeschke WD, Kirkby EA, Peuke AD, Pate JS, Hartung W (1997) Effects of P deficiency on assimilation and transport of nitrate and phosphate in intact plants of castor bean (*Ricinus communis* L.). Journal of Experimental Botany **48**: 75-91

Jeschke WD, Peuke A, Kirkby EA, Pate JS, Hartung W (1996) Effects of P deficiency on the uptake, flows and utilization of C, N, and H_2O within intact plants of *Rhicinus communis* L. Journal of Experimental Botany **47**: 1737-54

Johnson JF, Vance CP, Allan D (1996) Phosphorus deficiency in *Lupinus albus*. Altered lateral root development and enhanced expression of phosphoenolpyruvate carboxylase. Plant Physiology **112**: 31-41

Jones M, Raymond MJ, Smirnoff N (2006) Analysis of the root hair morphogenesis transcriptome reveals the molecular identity of six genes with roles in root hair development in Arabidopsis. The Plant Journal **45**: 83-100

Jones MA, Shen J-J, Fu Y, Li H, Yang Z, Grierson CS (2002) The Arabidopsis Rop2 GTPase is a positive regulator of both root hair initiation and tip growth. The Plant Cell **14**: 763-76

Joubès J, Chevalier C (2000) Endoreduplication in higher plants. Plant Molecular Biolgy **43**: 735-45

Kai M, Masuda Y, Kikuchi Y, Osaki M, Tadano T (1997) Isolation and characterization of a cDNA from *Catharanthus roseus* which is highly homologous with phosphate transporter. Soil Science and Plant Nutrition **43**: 227-35

Karandashov V, Bucher M (2004) Symbiotic phosphate transport in arbuscular mycorrhizas. Trends in Plant Science **10**: 22-9

Kiiskinen M, Korhonen M, Kangasjärvi J (1997) Isolation and characterization of cDNA for a plant mitochondrial phosphate translocator (*Mpt1*): ozone stress induces *Mpt1* mRNA accumulation in birch (*Betula pendula* Roth). Plant Molecular Biology **35**: 271-9

Kim DW, Lee SH, Choi S-B, Won S-K, Heo Y-K, Cho M, Park Y-I, Cho H-T (2006) Functional conservation of a root hair cell-specific *cis*-element in angiosperms with different root hair distribution patterns. The Plant Cell **18**: 2958-70

Kim SA, Punshon T, Lanzirotti A, Li L, Alonso JM, Ecker JR, Kaplan J, Guerinot ML (2006) Localization of iron in Arabidopsis seed requires the vacuolar membrane transporter VIT1. Science **314**: 1295-8

Kim WT, Silverstone A, Yip WK, Dong JG, Yang SF (1992) Induction of 1-aminocyclopropane-carboxylate synthase mRNA by auxin in mung bean hypocotyls and cultured apple shoots. Plant Physiology **98**: 465-71

Koornneef M, Dellaert LWM, van der Veen JH (1982) EMS- and radiation-induced mutation frequencies at individual loci in *Arabidopsis thaliana* (L.) Heynh. Mutation Research **93**: 109-123

Koshino-Kimura Y, Wada T, Tachibana T, Tsugeki R, Ishiguro S, Okada K (2005) Regulation of *CAPRICE* transcription by MYB proteins for root epidermis differentiation in Arabidopsis. Plant and Cell Physiology **46**: 817-26

Koyama H, Kawamura A, Kihara T, Hara T, Takita E, Shibata D (2000) Overexpression of mitochondrial citrate synthase in *Arabidopsis thaliana* improved growth on a phosphorus-limited soil. Plant and Cell Physiology **41**: 1030-7

Kramer D, Römheld V, Landsberg E-C, Marschner H (1980) Induction of transfer-cell formation by iron deficiency in the root epidermis of *Helianthus annuus* L. Planta **147**: 335-9

Kristensen I, Larsen PO (1974) Azetidine-2-carboxylic acid derivates from seeds of *Fagus silvativa* L. and a revised structure for nicotianamine. Phytochemistry **13**: 2791-8

Krüger C, Berkowitz O, Stephan UW, Hell R (2002) A metal-binding member of the late embryogenesis abundant protein family transports iron the phloem of *Rhicinus communis* L. The Journal of Biological Chemistry **277**: 25062-9

Kuiper D (1988) Growth responses of *Plantago major* L. ssp. *pleiosperma* (Pilger) to changes in mineral supply. Evidence for regulation by cytokinins. Plant Physiology **87**: 555-7

Kuiper D, Schuit J, Kuiper PJC (1988) Effects of internal and external cytokinin concentrations on root growth and shoot to root ratio of *Plantago major* ssp *pleiosperma* at different nutrient conditions. Plant and Soil **111**: 231-6

Kurata T, Ishida T, Kawabata-Awai C, Noguchi M, Hattori S, Sano R, Nagasaka R, Tominaga R, Koshino-Kimura Y, Kato T, Sato S, Tabata S, Okada K, Wada T (2005) Cell-to-cell movement of the CAPRICE protein in Arabidopsis root epidermal cell differentiation. Development **132**: 5387-98

Kwak S-H, Shen R, Schiefelbein J (2005) Positional signaling mediated by a receptor-like kinase in Arabidopsis. Science **307**: 1111-3

Lamont BB (2003) Structure, ecology and physiology of root clusters - a review. Plant and Soil **248**: 1-19

Landsberg E-C (1996) Hormonal regulation of iron stress response in sunflower roots: a morphological and cytological investigation. Protoplasma **194**: 69-80

Landsberg E-C (1984) Regulation of iron-stress-response by whole plant activity. Journal of Plant Nutrition **7**: 609-21

Landsberg E-C (1986) Function of rhizodermal transfer cells in the Fe stress response mechanism of *Capsicum annuum* L. Plant Physiology **82**: 511-7

Lanquar V, Lelievre F, Bolte S, Hames C, Alcon C, Neumann D, Vansuyt G, Curie C, Schroeder A, Krämer U, Barbier-Brygoo H, Thomine S (2005) Mobilization of vacuolar iron by AtNRAMP3 and AtNRAMP4 is essential for seed germination on low iron. EMBO Journal **24**: 4041-51

Le Jean M, Schikora A, Briat J-F, Curie C (2005) A loss-of-function mutation in AtYSL1 reveals its role in iron and nicotianamine seed loading. The Plant Journal **44**: 769-

Lee MM, Schiefelbein J (1999) WEREWOLF, a MYB-related protein in Arabidopsis, is a position-dependent regulator of epidermal cell patterning. Cell **99**: 473-83

Lee MM, Schiefelbein J (2002) Cell pattern in the Arabidopsis root epidermis determined by lateral inhibition with feedback. The Plant Cell **14**: 611-8

Lefebvre DD, Duff SMG, Fife CA, Julien-Inalsingh C, Plaxton WC (1990) Response to phosphate deprivation in *Brassica nigra* suspension cells. Enhancement of intracellular, cell surface, and secreted phosphatase activities compared to increases in P_i-absorption rate. Plant Physiology **93**: 504-11

Leggewie G, Willmitzer L, Riesmeier JW (1997) Two cDNAs from potato are able to complement a phosphate uptake-deficient yeast mutant: identification of phosphate transporters from higher plants. The Plant Cell **9**: 381-92

Ling H-Q, Bauer P, Bereczky Z, Keller B, Ganal M (2002) The tomato *fer* gene encoding a bHLH protein controls iron-uptake responses in roots. PNAS **99**: 13938-43

Ling H-Q, Koch G, Bäumlein H, Ganal MW (1999) Map-based cloning of *chloronerva*, a gene involved in iron uptake of higher plants encoding nicotinanamine synthase. PNAS **96**: 7098-103

Linkohr BI, Williamson LC, Fitter AH, Leyser HMO (2002) Nitrate and phosphate availability and distribution have different effects on root system architecture of Arabidopsis. The Plant Journal **29**: 751-60

Lipton GS, Blanchar RW, Blevins DG (1987) Citrate, malate and succinate concentration in exudates from P sufficient and P-stressed *Medicago sativa* L. seedlings. Plant Physiology **85**: 315-7

Liu C, Muchhal US, Raghothama KG (1997) Differential expression of TPSI1, a phosphate starvation-induced gene in tomato. Plant Molecular Biology **33**: 867-74

Lobréaux S, Briat J-F (1991) Ferritin accumulation and degradation in different organs of pea (*Pisum sativum*) during development. Biochemical Journal **274**: 601-6

Löffler A, Abel S, Jost W, Beintema JJ, Glund K (1992) Phosphate-regulated induction of intracellular ribonucleases in cultured tomato (*Lycopersicon esculentum*) cells. Plant Physiology **98**: 1472-8

López-Bucio J, Cruz-Ramírez A, Herrera-Estrella L (2003) The role of nutrient availability in regulating root architecture. Current Opinion in Plant Biology **6**: 280-7

López-Bucio J, Hernández-Abreu E, Sánchez-Calderón L, Nieto-Jacobo MF, Simpson J, Herrera-Estrella L (2002) Phosphate availability alters architecture and causes changes in hormone sensitivity in the Arabidopsis root system. Plant Physiology **129**: 244-56

López-Bucio J, Hernández-Abreu E, Sánchez-Calderón L, Pérez-Torres A, Rampey RA, Bartel B, Herrera-Estrella L (2005) An auxin transport independent pathway is involved in phosphate stress-induced root architectural alterations in Arabidopsis. Identification of *BIG* as a mediator of auxin in pericycle cell activation. Plant Physiology **137**: 681-91

López-Milán AF, Morales F, Abadía A, Abadía J (2000) Effects of iron deficiency on the composition of the leaf apoplastic fluid and xylem sap in sugar beet. Implications for iron and carbon transport. Plant Physiology **124**: 873-84

Lynch JP, Brown KM (2001) Topsoil foraging - an architectural adaptation of plants to low phosphorus availability. Plant and Soil **237**: 225-237

Ma Z, Baskin TI, Brown KM, Lynch JP (2003) Regulation of root elongation under phosphorus stress involves changes in ethylene responsiveness. Plant Physiology **131**: 1-10

Ma Z, Bielenberg DG, Brown KM, Lynch JP (2001a) Regulation of root hair density by phosphorus availability in *Arabidopsis thaliana*. Plant, Cell and Environment **24**: 459-67

Maas FM, van de Wetering DAM, van Beusichem ML, Bienfait HF (1988) Characterization of phloem iron and its possible role in the regulation of Fe-efficiency reactions. Plant Physiology **87**: 167-71

Mähönen AP, Bonke M, Kauppinen L, Riikonen M, Benfey PN, Helariutta Y (2000) A novel two-component hybrid molecule regulates vascular morphogenesis of the Arabidopsis root. Genes and Development **14**: 2938-43

Marschner H (1995) Mineral nutrition of higher plants. 2nd edition, Academic Press, London

Masaoka Y, Kojima M, Sugihara S, Yoshihara T, Koshino M, Ichihara A (1993) Dissolution of ferric phosphate by alfalfa (*Medicago stiva* L.) root exudates. Plant and Soil **155/156**: 75-8

Masucci JD, Rerie WG, Foreman DR, Zhang M, Galway ME, Marks MD, Schiefelbein JW (1996) The homeobox gene *GLABRA2* is required for position-dependent cell differentiation in the root epidermis of *Arabidopsis thaliana.* Development **122**: 1253-60

Masucci JD, Schiefelbein JW (1994) The *rhd6* mutation of *Arabidopsis thaliana* alters root-hair initiation through an auxin- and ethylene-associated process. Plant Physiology **106**: 1335-46

Masucci JD, Schiefelbein JW (1996) Hormones act downstream of *TTG* and *GL2* to promote root hair outgrowth during epidermis development in the Arabidopsis root. The Plant Cell **8**: 1505-17

McQueen-Mason S, Durachko DM, Cosgrove DJ (1992) Two endogenous proteins that induce cell wall extension in plants. The Plant Cell **4**: 1425-33

Miller SS, Liu J, Allan DL, Menzhuber CJ, Fedorova M, Vance CP (2001) Molecular control of acid phosphatase secretion into the rhizosphere of proteoid roots from phosphorus-stressed white lupin. Plant Physiology **127**: 594-606

Mimura T, Sakano K, Shimmen T (1996) Studies on the distribution, re-translocation and homeostasis of inorganic phosphate in barley leaves. Plant, Cell and Environment **19**: 311-20

Miura K, Rus A, Sharkhuu A, Yokoi S, Karthikeyan AS, Raghothama KG, Baek D, Koo YD, Jin JB, Bressan RA, Yun D-J, Hasegawa PM (2005) The Arabidopsis SUMO E3 ligase SIZ1 controls phosphate deficiency responses. PNAS **102**: 7760-5

Molendijk AJ, Bischoff F, Rajendrakumar CSV, Friml J, Braun M, Gilroy S, Palme K (2001) *Arabidopsis thaliana* Rop GTPases are localized to tips of root hairs and control planar growth. The EMBO Journal **20**: 2779-88

Moog PR, van der Kooij TAW, Brüggemann W, Schiefelbein JW, Kuiper PJC (1995) Response to iron deficiency in *Arabidopsis thaliana*: The turbo iron reductase does not depend on the formation of root hairs and transfer cells. Planta **195**: 505-13

Moorby H, White RE, Nye PH (1988) The influence of phosphate nutrition on H ion efflux from the roots of young rape plants. Plant and Soil **105**: 247-56

Muchhal US, Liu C, Raghothama KG (1997) Ca^{2+}-ATPase is expressed differentially in phosphate-starved roots of tomato. Physiologica plantarum **101**: 540-4

Muchhal US, Pardot JM, Raghothama KG (1996) Phosphate transporters from the higher plant *Arabidopsis thaliana*. PNAS **93**: 10519-23

Mudge SR, Rae AL, Diatloff E, Smith FW (2002) Expression analysis suggests novel roles for members of the Pht1 family of phosphate transporters in Arabidopsis. The Plant Journal **31**: 341-53

Mukherjee I, Campbell NH, Ash JS, Connolly EL (2006) Expression profiling of the Arabidopsis ferric-chelate reductase (FRO) gene family reveals differential regulation by iron and copper. Planta **223**: 1178-90

Müller A, Guan C, Gälweiler L, Tänzler P, Huijser P, Marchant A, Parry G, Bennett M, Wisman E, Palme K (1998) AtPIN2 defines a locus of Arabidopsis for root gravitropism control. The EMBO Journal **17**: 6903-11

Müller R, Nilsson L, Krintel C, Nielsen TH (2004) Gene expression during recovery from phosphate starvation in roots and shoots of *Arabidopsis thaliana*. Physiologica Plantarum **122**: 233-43

Nacry P, Canivenc G, Muller B, Azmi A, Van Onckelen H, Rossignol M, Doumas P (2005) A role for auxin redistribution in the responses of the root system architecture to phosphate starvation in Arabidopsis. Plant Physiology **138**: 2061-74

Norvell WA, Welch RM, Adams ML, Kochian LV (1993) Reduction of Fe(III), Mn(III), and Cu(II) chelates by roots of pea (*Pisum sativum* L.) or soybean (*Glycine max*). Plant and Soil **155/156**: 123-6

Nürnberger T, Abel S, Jost W, Glund K (1990) Induction of an extracellular ribonuclease in cultured tomato cells upon phosphate starvation. Plant Physiology **92**: 970-6

Ohashi Y, Oka A, Rodrigues-Pousada R, Possenti M, Ruberti I, Morelli G, Aoyama T (2003) Modulation of phospholipid signaling by GLABRA2 in root-hair pattern formation. Science **300**: 1427-30

Oyama T, Shimura Y, Okada K (2002) The *IRE* gene encodes a proetin kinase homologue and modulates root hair growth in Arabidopsis. The Plant Journal **30**: 289-99

Palmgren MG (2001) Plant plasma membrane H^+-ATPases: powerhouses for nutrient uptake. Annual Reviews of Plant Molecular Biology **52**: 817-45

Pao SS, Paulsen IT, Saier MH Jr. (1998) Major facilitator superfamily. Microbiology and Molecular Biology Reviews **62**: 1-34

Parker JS, Cavell AC, Dolan L, Roberts K, Grierson CS (2000) Genetic interactions during root hair morphogenesis in Arabidopsis. The Plant Cell **12**: 1961-74

Pesch M, Hülskamp M (2004) Creating a two-dimensional pattern *de novo* during Arabidopsis trichome and root hair initiation. Current Opinion in Genetics and Development **14**: 422-7

Peterson RL (1992) Adaptations of root structure in relation to biotic and abiotic factors. Canadian Journal of Botany **40**: 661-75

Peterson RL (1992) Adaptations of root structure in relation to biotic and abiotic factors. Canadian Journal of Botany **40**: 661-75

Pich A, Hillmer S, Manteuffel R, Scholz G (1997) First immunohistochemical localization of the endogenous Fe^{2+}-chelator nicotianamine. Journal of Experimental Botany **48**: 759-67

Pich A, Manteuffel R, Hillmer S, Scholz G, Schmidt W (2001) Fe homeostasis in plant cells: Does nicotianamine play multiple roles in the regulation of cytoplasmic Fe concentration? Planta **213**: 967-76

Pich A, Scholz G, Stephan UW (1994) Iron-dependent changes of heavy metals, nichotianamine, and citrate in different plant organs and in the xylem exudate of two tomato genotypes. Nicotianamine as possible copper translocator. Plant and Soil **165**: 189-96

Pilbeam DJ, Cakmak I, Marschner H, Kirkby EA (1993) Effect of withdrawal of phosphorus on nitrate assimilation and PEP carboxylase activity in tomato. Plant and Soil **154**: 111-7

Pinton R, Cesco S, De Nobili M, Santi S, Varanini Z (1998) Water and pyrophosphate extractable humic substances fractions as a source of iron for Fe-deficient cucumber plants. Biology and Fertility of Soils **26**: 23-7

Pitts RJ, Cernac A, Estelle M (1998) Auxin and ethylene promote root hair elongation in Arabidopsis. The Plant Journal **16**: 553-60

Poirier Y, Bucher M (2002) Phosphate transport and homeostasis in Arabidopsis. The Arabidopsis Book edited by: Somerville CR, Meyerowitz EM, American Society of Plant Biologists, Rockville

Poirier Y, Thoma S, Somerville C, Schiefelbein J (1991) A mutant of Arabidopsis deficient in xylem loading of phosphate. Plant Physiology **97**: 1087-93

Preuss ML, Schmitz AJ, Thole JM, Bonner HKS, Otegui MS, Nielsen E (2006) A role for the RabA4b effector protein PI-4Kβ1 in polarized expansion of root hair cells in *Arabidopsis thaliana*. The Journal of Cell Biology **172**: 991-8

Preuss ML, Serna J, Falbel TG, Bednarek SY, Nielsen E (2004) The Arabidopsis Rab GTPase RabA4b localizes to the tips of growing root hair cells. The Plant Cell **16**: 1589-603

Raghothama KG (1999) Phosphate acquisition. Annual Reviews of Plant Physiology and Molecular Biology **50**: 665-93

Raghothama KG, Karthikeyan AS (2005) Phosphate acquisition. Plant and Soil **274**: 37-49

Rausch C, Bucher M (2002) Molecular mechanism of phosphate transport in plants. Planta **216**: 23-37

Reed RC, Brady SR, Muday GK (1998) Inhibition of auxin movement from the shoot into the root inhibits lateral root development in Arabidopsis. Plant Physiology **118**: 1369-78

Rentel MC, Lecourieux D, Ouaked F, Usher SL, Petersen L, Okamoto H, Knight H, Peck SC, Grierson CS, Hirt H, Knight MR (2004) OXI1 kinase is necessary for oxidative burst-mediated signaling in Arabidopsis. Nature **427**: 858-61

Reymond M, Svistoonoff S, Loudet O, Nussaume L, Desnos T (2006) Identification of QTL controlling root growth response to phosphate starvation in *Arabidopsis thaliana*. Plant, Cell and Environment **29**: 115-25

Rigas S, Debrosses G, Haralampidis K, Vincente-Agullo F, Feldmann KA, Grabov A, Dolan L, Hatzopoulos P (2001) *TRH1* encodes a potassium transporter required for tip growth in Arabidopsis root hairs. The Plant Cell **13**: 139-51

Ringli C, Baumberger N, Diet A, Frey B, Keller B (2002) ACTIN2 is essential for bulge site selection and tip growth during root hair development of Arabidopsis. Plant Physiology **129**: 1464-72

Robinson NJ, Procter CM, Collony EL, Guerinot ML (1999) A ferric-chelate reductase for iron uptake from soils. Nature **397**: 694-7

Rogers EE, Eide DJ, Guerinot ML (2000) Altered selectivity in an Arabidopsis metal transporter. PNAS **97**: 12356-60

Rogers EE, Guerinot ML (2002) FRD3, a member of the multidrug and protein efflux family controls iron deficiency responses in Arabidopsis. The Plant Cell **14**: 1787-99

Romera FJ, Alcántara E (1994) Iron-deficiency stress responses in cucumber (*Cucumis sativus* L.) roots. A possible role for ethylene? Plant Physiology **105**: 1133-8

Romera FJ, Alcántara E, De la Guardia MD (1999) Ethylene production by Fe-deficient roots and its involvement in the regulation of Fe-deficiency stress responses by strategy I plants. Annals of Botany **83**: 51-5

Romera FJ, Lucena C, Alcántara E 2006 Plant hormones influencing iron uptake in plants. Iron Nutrition in Plants and Rhizospheric Microorganisms. edited by: Barton LL, Abadía J, Springer, Netherlands

Römheld V (1987) Different strategies for iron acquisition in higher plants. Physiologica Plantarum **70**: 231-34

Römheld V, Marschner H (1986) Mobilization of iron in the rhizosphere of different plant species. Advances in Plant Nutrition 155-204 edited by: Tinker B, Läuchli A, Praeger, New York

Römheld V, Marschner H (1986) Evidence for a specific uptake system for iron phytosiderophores in roots of grasses. Plant Physiology **80**: 175-80

Rubio V, Linhares F, Solano R, Martín AC, Iglesias J, Leyva A, Paz-Ares J (2001) A conserved MYB transcription factor involved in phosphate starvation signaling both in vascular plants and in unicellular algae. Genes and Development **15**: 2122-33

Ryan E, Grierson CS, Cavell A, Steer M, Dolan L (1998) TIP1 is required for both tip growth and non-tip growth in Arabidopsis. New Phytologist **138**: 49-58

Sakano K (1990) Proton/phosphate stoichiometry in uptake of inorganic phosphate by cultured cells of *Catharanthus roseus* (L.) G. Don. Plant Physiology **93**: 479-83

Salama AMSE-DA, Wareing PF (1979) Effects of mineral nutrition on endogenous cytokinins in plant of sunflower (*Helianthus annuus* L.). Journal of Experimental Botany **30**: 971-81

Šamaj J, Ovecka M, Hlavacka A, Lecourieuw F, Meskiene I, Lichtscheidl I, Lenart P, Salaj J, Volkmann D, Bögre L, Baluška F, Hirt H (2002) Involvement of the mitogen-activated protein kinase SIMK in regulation of root hair tip growth. The EMBO Journal **21**: 3296-306

Sánchez-Calderón L, López-Bucio J, Chacón-López A, Cruz-Ramírez A, Nieto-Jacobo F, Dubrovsky JG, Herrera-Estrella L (2005) Phosphate starvation induces a determinate developmental program in the roots of *Arabidopsis thaliana*. Plant and Cell Physiology **46**: 174-84

Sánchez-Calderón L, López-Bucio J, Chacón-López A, Gutiérrez-Ortega A, Hernández-Abreu E, Herrera-Estrella L (2006) Characterization of *low phosphorus insensitive* mutants reveals a crosstalk between low phosphorus-induced determinate root development and the activation of genes involved in the adaptation of Arabidopsis to phosphorus deficiency. Plant Physiology **140**: 879-89

Schaaf G, Schikora A, Häberle J, Vert G, Ludewig U, Briat J-F (2005) A putative function for the Arabidopsis Fe-phytosiderophore transporter homolog AtYSL2 in Fe and Zn homeostasis. Plant and Cell Physiology **46**: 762-74

Scheres B (2002) Plant Patterning: TRY to inhibit your neighbors. Current Biology **12**: 804-6

Scheres B (2000) Non-linear signaling for pattern formation? Current Opinion in Plant Biology **3**: 412-7

Schiefelbein J (2003) Cell-fate specification in the epidermis: a common patterning mechanism in the root and shoot. Current Opinion in Plant Biology **6**: 74-8

Schiefelbein J, Galway M, Masucci J, Ford S (1993) Pollen tube and root hair tip growth is disrupted in a mutant of *Arabidopsis thaliana*. Plant Physiology **103**: 979-85

Schiefelbein J, Lee MM (2006) A novel regulatory circuit specifies cell fate in the Arabidopsis root epidermis. Physiologica Plantarum **126**: 503-10

Schiefelbein JW, Shipley A, Rowse P (1992) Calcium influx at the tip of growing root-hair cells of *Arabidopsis thaliana*. Planta **187**: 455-9

Schiefelbein JW, Somerville C (1990) Genetic control of root hair development in *Arabidopsis thaliana*. The Plant Cell **2**: 235-43

Schikora A, Schmidt W (2001) Iron stress-induced changes in root epidermal cell fate are regulated independently from physiological responses to low iron availability. Plant Physiology **125**: 1679-87

Schikora A, Schmidt W (2002) Formation of transfer cells and H^+-ATPase expression in tomato roots under P and Fe deficiency. Planta **215**: 304-11

Schmidt W (1999) Mechanisms and regulation of reduction-based iron uptake in plants. The New Phytologist **141**: 1-26

Schmidt W (2003) Iron solutions: acquisition strategies and signaling pathways in plants. Trends in Plant Science **8**: 188-93

Schmidt W (2006) Iron stress responses in roots of strategy I plants. Iron nutrition in plants and rhizospere microorganisms. 229-50 edited by: Barton LL, Abadia J, Kluwer Academic Publishers, Dordrecht

Schmidt W, Bartels M (1996) Formation of root epidermal transfer cells in *Plantago*. Plant Physiology **110**: 217-25

Schmidt W, Boomgaarden B, Ahrens V (1996) Reduction of root iron in *Plantago lanceolata* during recovery from Fe deficiency. Physiologica Plantarum **98**: 587-93

Schmidt W, Schikora A (2001) Different pathways are involved in phosphate and iron stress-induced alterations of root epidermal cell development. Plant Physiology **125**: 2078-84

Schmidt W, Schikora A, Pich A, Bartels M (2000) Hormones induce an Fe-deficiency-like root epidermal cell pattern in the Fe-inefficient tomato mutant *fer*. Protoplasma **213**: 67-73

Schmidt W, Steinbach S (2000) Sensing iron - a whole plant approach. Annals of Botany **86**: 589-593

Schneider K, Mathur J, Boudonck K, Wells B, Dolan L, Roberts K (1998) The *ROOT HAIRLESS1* gene encodes a nuclear protein required for root hair initiation in Arabidopsis. Genes & Development **12**: 2013-21

Schneider K, Wells B, Dolan L, Roberts K (1997) Structural and genetic analysis of epidermal cell differentiation in Arabidopsis primary roots. Development **124**: 1789-98

Schnittger A, Hülskamp M (2002) Trichome morphogenesis: a cell-cycle perspective. Philosophical Transactions of the Royal Society of London Series B-Biological Science **357**: 823-6

Scholz G (1989) Effect of nicotianamine on iron re-mobilization in de-rooted tomato seedlings. Biometals **2**: 89-91

Seifert GJ, Barber C, Wells B, Dolan L, Roberts K (2002) Galactose biosynthesis in Arabidopsis: genetic evidence for substrate channeling from UDP-D-galctose into cell wall polymers. Current Biology **12**: 1840-5

Shin H, Shin H-S, Chen R, Harrison MJ (2006) Loss of *At4* function impacts phosphate distribution between the roots and the shoots during phosphate starvation. The Plant Journal **45**: 712-26

Shin H, Shin H-S, Dewbre GR, Harrison MJ (2004) Phosphate transport in Arabidopsis: Pht1;1 and Pht1;4 play a major role in phosphate acquisition from both low- and high-phosphate environments. The Plant Journal **39**: 629-42

Sieberer BJ, Ketelaar T, Esseling JJ, Emons AMC (2005) Microtubules guide root hair tip growth. New Phytologist **167**: 711-9

Smith BN (1984) Iron in higher plants: storage and metabolic role. Journal of Plant Nutrition **7**: 759-66

Smith FW, Ealing PM, Dong B, Delhaize E (1997) The cloning of two Arabidopsis genes belonging to a phosphate transporter family. The Plant Journal **11**: 83-92

Song X-F, Yang C-Y, Liu J, Yang W-C (2006) RPA, a class II ARFGAP protein, activates ARF1 and U5 and plays a role in root hair development in Arabidopsis. Plant Physiology **414**: 966-76

Souter M, Topping J, Pullen M, Friml J, Palme K, Hackett R, Grierson D, Lindsey K (2002) *hydra* mutants of Arabidopsis are defective in sterol profiles and auxin and ethylen signaling. The Plant Cell **14**: 1017-31

Spain BH, Koo D, Ramakrishnan M, Dzudzor B, Colicelli J (1995) Truncated forms of a novel yeast protein suppress the lethality of a G protein a subunit deficiency by interacting with the β subunit. The Journal of Biological Chemistry **270**: 25435-44

Spiegel S, Foster D, Kolesnickz R (1996) Signal transduction through lipid second messengers. Current Opinion in Cell Biology **8**: 159-67

Steinmann T, Geldner N, Grebe M, Mangold S, Jackson CL, Paris S, Gälweiler L, Palme K, Jürgens G (1999) Coordinated polar localization of auxin efflux carrier PIN1 by GNOM ARF GEF. Science **286**: 316-8

Stephan UW, Schmidke I, Pich A (1994) Phloem translocation of Fe, Cu, Mn, and Zn in *Ricinus* seedlings in relation to the concentrations of nicotianamine, an endogenous chelator of divalent metal ions, in different seedling parts. Plant and Soil **165**: 181-8

Stephan UW, Schmidke I, Stephan VW, Scholz G (1996) The nicotianamine molecule is made-to-measure for complexation of metal micronutrients in plants. Biometals **9**: 84-90

Stephan UW, Scholz G, Rudolph A (1990) Distribution of nicotianamine, a presumed symplast iron transporter, in different organs of sunflower and of a tomato wild type and its mutant *chloronerva*. Biochemie und Physiologie der Pflanzen **186**: 81-8

Sugimoto-Shirasu K, Roberts GR, Stacey NJ, McCann MC, Maxwell A, Roberts K (2005) RHL1 is an essential component of the plant DNA topoisomerase VI complex and is required for ploidy-dependent cell growth. PNAS **102**: 18736-41

Sunkar R, Zhu J-K (2004) Novel and stress-regulated microRNAs and other small RNAs from Arabidopsis. The Plant Cell **16**: 2001-19

Susín S, Abián J, Peleato ML, Sánchez-Baeza F, Abadía A, Gelpi E, Abadía J (1993) Flavin excretion from roots of iron-deficient sugar beet (*Beta vulgaris* L.). Planta **193**: 514-519

Suzuki T, Miwa K, Ishikawa K, Yamada H, Aiba H, Mizuno T (2001) The Arabidopsis sensor His-kinase, AHK4, can respond to cytokinins. Plant and Cell Physiology **42**: 107-13

Synek L, Schlager N, Eliás M, Quentin M, Hauser M-T, Žárský V (2006) AtEXO70A1, a member of a family of putative exocyst subunits specifically expanded in land plants, is important for polar growth and plant development. The Plant Journal **48**: 54-72

Takabatake R, Hata S, Taniguchi M, Kouchi H, Sugiyama T (1999) Isolation and characterization of cDNAs encoding mitochondrial phosphate transporters in soybean, maize, rice, and Arabidopsis. Plant Molecular Biology **40**: 479-86

Taylor CB, Bariola PA, del Cardayré SB, Raines RT, Green PJ (1993) RNS2: a senescence-associated RNase of Arabidopsis that diverged from the S-RNases before speciation. PNAS **90**: 5118-22

Thomine S, Lelièvre F, Debarbieux E, Schroeder JI, Barbier-Brygoo H (2003) AtNRAMP3, a multispecific vacuolar metal transporter involved in plant responses to iron deficiency. The Plant Journal **34**: 685-95

Thomine S, Wang R, Ward JM, Crawford NM, Schroeder JI (2000) Cadmium and iron transport by members of a plant transporter gene family in *Arabidopsis* with homology to NRAMP genes. PNAS **97**: 4991-6

Ticconi CA, Abel S (2004) Short on phosphate: plant surveillance and countermeasures. Trends in Plant Science **9**: 548-55

Ticconi CA, Delatorre CA, Abel S (2001) Attenuation of phosphate starvation responses by phosphite in Arabidopsis. Plant Physiology **127**: 963-72

Ticconi CA, Delatorre CA, Lahner B, Salt DE, Abel S (2004) Arabidopsis *pdr2* reveals a phosphate-sensitive checkpoint in root development. The Plant Journal **37**: 801-14

Tiffin OL (1966) Iron translocation I. Plant culture, exudate sampling, and iron-citrate analysis. Plant Physiology **41**: 510-4

Törjék O, Berger D, Meyer RC, Müssig C, Schmidt KJ, Sörensen TR, Weisshaar B, Mitchel-Olds T, Altmann T (2003) Establishment of a high-affinity SNP-based framework marker set for Arabidopsis. The Plant Journal **36**: 122-40

Torrey J (1950) The induction of lateral roots by indoleacetic acid and root decapitation. American Journal of Botany **37**: 257-64

Tsugeki R, Fedoroff NV (1999) Genetic ablation of root cap cells in Arabidopsis. PNAS **96**: 12941-6

Ueki K (1978) Control of phosphatase release from cultured tobacco cells. Plant and Cell Physiology **19**: 385-92

Ullrich-Eberius CI, Novacky A, van Bel AJE (1984) Phosphate uptake in *Lemna gibba* G1: energetics and kinetics. Planta **161**: 46-52

van Hengel AJ, Barber C, Roberts K (2004) The expression patterns of arabinogalactan-protein *AtAGP30* and *GLABRA2* reveals a role for abscisic acid in the early stages of root epidermal patterning. The Plant Journal **39**: 70-83

Vance CP, Uhde-Stone C, Allan DL (2003) Phosphorus acquisition and use: critical adaptations by plants for securing a nonrenewable resource. The New Phytologist **157**: 423-47

Vernoud V, Horton AC, Yang Z, Nielsen E (2003) Analysis of the small GTPase gene superfamily of Arabidopsis. Plant Physiology **131**: 1191-205

Vert G, Briat J-F, Curie C (2003) Dual regulation of the Arabidopsis high-affinity root iron uptake system by local and long-distance signals. Plant Physiology **132**: 796-804

Vert G, Grotz N, Dédaldéchamp F, Gaymard F, Guerinot ML, Briat J-F, Curie C (2002) IRT1, an Arabidopsis transporter essential for iron uptake from the soil and for plant growth. The Plant Cell **14**: 1223-33

Very A-A, Davies JM (2000) Hyperpolarization-activated calcium channels at the tip of Arabidopsis root hairs. PNAS **97**: 9801-6

Vincent P, Chua M, Nogue F, Fairbrother A, Mekeel H, Xu Y, Allen N, Bibikova TN, Gilroy S, Bankaitis VA (2005) A Sec14p-nodulin domain phosphatidylinositol transfer protein polarizes membrane growth of *Arabidopsis thaliana* root hairs. The Journal of Cell Biology **168**: 801-12

Vincente-Agullo F, Rigas S, Desbrosses G, Dolan L, Hatzopoulos P, Grabov A (2004) Potassium carrier TRH1 is required for auxin transport in Arabidopsis roots. The Plant Journal **40**:

Vissenberg K, Fry SC, Verbelen J-P (2001) Root hair initiation is coupled to a highly localized increase of xyloglucan endotransglycosylase action in Arabidopsis roots. Plant Physiology **127**: 1125-35

von Wirén N, Klair S, Bansal S, Briat J-F, Khodr H, Shioiri T, Leigh RA, Hider RC (1999) Nicotianamine chelates both FeIII and FeII. Implications for metal transport in plants. Plant Physiology **119**: 1107-14

Wada T, Kurata T, Tominaga R, Koshino-Kimura Y, Tachibana T, Goto K, Marks D, Shimura Y, Okada K (2002) Role of a positive regulator of root hair development, *CAPRICE*, in Arabidopsis root epidermal cell differentiation. Development **129**: 5409-19

Wada T, Tachibana T, Shimura Y, Okada K (1997) Epidermal cell differentiation in Arabidopsis determined by a MYB homolog CPC. Science **277**: 1113-6

Wade VJ, Treffry A, Laulhère JP, Bauminger ER, Cleton MI, Mann S (1993) Structure and composition of ferritin cores from pea seed (*Pisum sativum*). Biochimica Biophysica Acta **1161**: 91-6

Walker AR, Davison PA, Bolognesi-Winfield AC, James CM, Srinivasan N, Blundell TL, Esch JJ, Marks MD, Gray JC (1999) The *TRANSPARENT TESTA GLABRA1* locus, which regulates trichome differentiation and anthocyanin biosynthesis in Arabidopsis, encodes a WD40 repeat protein. The Plant Cell **11**: 1337-49

Walker JD, Oppenheimer DG, Concienne J, Larkin JC (2000) SIAMESE, a gene controlling the endoreduplication cell cycle in *Arabidopsis thaliana* trichomes. Development **127**: 3931-40

Wang H, Lockwood SK, Hoeltzel MF, Schiefelbein JW (1997) The *ROOT HAIR DEFECTIVE3* gene encodes an evolutionarily conserved protein with GTP-binding motifs and is required for regulated cell enlargement in Arabidopsis. Genes and Development **11**: 799-811

Wang X, Cnops G, Vanderhaeghen R, De Block S, Van Montagu M, Van Lijsebettens M (2001) *AtCSLD3*, a cellulose synthase-like gene important for root hair growth in Arabidopsis. Plant Physiology **126**: 575-86

Wasaki J, Yonetani R, Kai M, Osaki M (2003) Expression of the *OsPI1* gene, cloned from rice roots using cDNA microarray, rapidly responds to phosphorus status. New Phytologist **158**: 239-48

Waters BM, Blevins DG, Eide DJ (2002) Characterization of FRO1, a pea ferric-chelate reductase involved in root iron acquisition. Plant Physiology **129**: 85-94

Webb M, Jouannic S, Foreman J, Linstead P, Dolan L (2002) Cell specification in the Arabidopsis root epidermis requires the activity of ECTOPIC ROOT HAIR3 - a katanin-p60 protein. Development **129**: 123-31

Welch RM, Norvell WA, Schaefer SC, Shaft JE, Kochian LV (1993) Induction of iron(III) and copper(II) reduction in pea (*Pisum sativum* L.) roots by Fe and Cu status: Does the root-cell plasmalemma Fe(III)-chelate reductase perform a general role in regulating cation uptake? Planta **190**: 555-61

Wellman CH, Osterloff PL, Mohiuddin U (2003) Fragments of the earliest land plants. Nature **425**: 282-5

White PF, Robson AD (1989) Rhizosphere acidification and Fe^{3+} reduction in lupins and peas: Iron deficiency in lupins is not due to a poor ability to reduce Fe^{3+}. Plant and Soil **119**: 163-75

Willemsen V, Friml J, Grebe M, van den Toorn A, Palme K, Scheres B (2003) Cell polarity and PIN protein positioning in Arabidopsis require *STEROL METHYLTRANSFERASE1* function. The Plant Cell **15**: 612-25

Williamson LC, Ribrioux SPCP, Fitter AH, Leyser HMO (2001) Phosphate availability regulates root system architecture in Arabidopsis. Plant Physiology **126**: 875-82

Wilson AK, Pickett FB, Turner JC, Estelle M (1990) A dominant mutation in Arabidopsis confers resistance to auxin, ethylene and abscisic acid. Molecular and General Genetics **222**: 377-83

Wintz H, Fox T, Wu Y-Y, Feng V, Chen W, Chang H-S, Zhu T, Vulpe C (2003) Expression profiles of *Arabidopsis thaliana* in mineral deficiencies reveal novel transporters involved in metal homeostasis. The Journal of Biological Chemistry **278**: 47644-53

Wykoff DD, Grossman AR, Weeks DP, Usuda H, Shimogawara K (1999) Psr1, a nuclear localized protein that regulates phosphorus metabolism in Clamydomonas. PNAS **96**: 15336-41

Wymer CL, Bibikova TN, Gilroy S (1997) Cytoplasmic free calcium distributions during the development of root hairs of *Arabidopsis thaliana*. The Plant Journal **12**: 427-39

Xu C-R, Liu C, Wang Y-L, Li L-C, Chen W-Q, Xu Z-H, Bai S-N (2005) Histone acetylation affects expression of cellular patterning genes in the Arabidopsis root epidermis. PNAS **102**: 14469-74

Xu J, Scheres B (2005) Dissection of Arabidopsis ADP-RIBOSYLATION FACTOR1 function in epidermal cell polarity. The Plant Cell **17**: 525-36

Yalovsky S, Rodríguez-Concepción M, Gruissem W (1999) Lipid modifications of proteins - slipping in and out of membranes. Trends in Plant Science **4**: 439-45

Yan F, Zhu Y, Müller C, Zörb C, Schubert S (2002) Adaptation of H^+-pumping and plasma membrane H^+ ATPase activity in proteoid roots of white lupin under phosphate deficiency. Plant Physiology **129**: 50-63

Yi K, Wu Z, Zhou J, Du L, Guo L, Wu Y, Wu P (2005) OsPTF1, a novel transcription factor involved in tolerance to phosphate starvation in rice. Plant Physiology **138**: 2087-96

Yu Y-B, Yang SF (1979) Auxin-induced ethylene production and its inhibition by aminoethoxyvinylglycine and cobalt ion. Plant Physiology **64**: 1074-7

Zhang C, Römheld V, Marschner H (1995) Distribution pattern of root-supplied ^{59}iron in iron-sufficient and -deficient bean plants. Journal of Plant Nutrition **18**: 2049-58

Zhang Y-J, Lynch JP, Brown KM (2003) Ethylene and phosphorus availability have interacting yet distinct effects on root hair development. Journal of Experimental Botany **54**: 2351-61

Zheng H, Kunst L, Hawes C, Moore I (2004) A GFP-based assay reveals a role for RHD3 in transport between the endoplasmic reticulum and Golgi apparatus. The Plant Journal **37**: 398-414

Zheng Z-L, Yang Z (2000) The Rop GTPase: an emerging signaling switch in plants. Plant Molecular Biology **44**: 1-9

ACKNOWLEDGMENTS

I thank Wolfgang Schmidt for providing the interesting topic, the money for the material, literature tips, and the interesting scientific discussions. My special thank belongs to Tom Buckhout for giving me the possibility to work in his lab, for supervision, the scientific discussions and all things I could learn from him. Bettina Linke for the seminars in plant development and tips in molecular biology. Susanne Olstowski-Jacoby for sowing out the plants for the fine mapping and for the double mutant analysis, which was a big help. Marion Dewender for running the lab, and Immo Reinhardt, Nadine Jungnick, Franziska Beran, Juliane Wambutt, Sylvia Griese for the scientific exchange. Thomas Altmann for the possibility to map the mutation in his lab and for his useful advices. Ottó Törjek for introducing me into map-based cloning and Maik Zehnsdorf for showing me the SNsPshot analysis. Melanie Teltow for showing me the crossing and the Arabidopsis greenhouse culture. Georg Strompen for and Hanna Wall for their advices in map-based cloning. Bernhardt Grimm for giving be the possibility to use the plant culture root and the greenhouse and for the scientific exchange. Ute Krämer for ICP analysis and Ina Talke for instructing me into ICP digestion. Dörte Boll for her big help with the primary screening. Angelika Pötter for watering the Arabidopsis for fine mapping and double mutant analysis in the greenhouse. Renate Kort for her excellent technical assistance with the cryo-SEM. Günther Scholz for proving the microtome and microscopy facilities. Kurt Zoglauer making the whole-plant photos with his Nikon D 70 camera. Andrea Rupps for coaching and proof reading and, finally, my father for his support.

Lebenslauf

Persönliche Daten

Name	Margarete Müller
Anschrift	Langhansstr. 33
	13086 Berlin
geboren am	13.7.1973 in Leer
Familienstand	ledig

Schulbildung

1980 - 1993	Grundschule, Orientierungsstufe, Altes Gymnasium Oldenburg
1993	Abitur, Fremdsprachen: Englisch, Latinum, Graecum

Studium

1994 - 2001	Biologie an der Carl-von-Ossietzky-Universität Oldenburg
Okt. 1996	Vordiplom, Beginn Hauptstudium
Okt. 1997 – Dez. 2001	Tätigkeiten als studentische Hilfskraft: Tutorien in Grund- und Fortgeschrittenenpraktika der Biochemie und Pflanzenphysiologie, Grundkurs Botanik; Elementanalyse von Bodenproben, Mikropropagation tropischer Baumarten am MPI für Limnologie in Plön
Juli 2001	Diplom mit Note 'ausgezeichnet'
	Thema: *Isolation, Charakterisierung und on-grid Immuno-Lokalisation der Isocitrat-Lyase aus Chlorogonium elongatum*

Tätigkeiten

Jan. 2002 – Nov. 2003	Anstellung als wissenschaftliche Mitarbeiterin and der Carl-von-Ossietzky-Universität Oldenburg im Drittmittelprojekt *Transferzellen II*
1.4.2004 - 31.3.2006	Promotionsstipendium nach dem Gesetz zur Förderung des wissenschaflichen Nachwuchses (NaFöG)
15.4.2006 – 14.8.2006	Anstellung als wissenschaftliche Mitarbeiterin an der Humboldt-Universität zu Berlin im Projekt Kartierung der *per2*-Mutation

Publikationen

Müller M, Schmidt W (2004) Environmentally induced plasticity of root hair development in Arabidopsis. *Plant Physiology* 134, 409-19. Cited by 11

Emanuel C, von Groll U, Müller M, Börner T, Weihe A (2006) Development and tissue-specific expression of the *RpoT* gene family of *Arabidopsis* encoding mitochondrial and plastid RNA polymerases. *Planta* 223, 998-1009. Cited by 2

Schikora A, Thimm O, Linke B, Buckhout TJ, Müller M, Schmidt W 2006. Expression, localization, and regulation of the iron transporter LeIRT1 in tomato roots. *Plant and Soil* 284, 101-8.

Erklärung

Hiermit erkläre ich, dass ich die Arbeit selbständig erarbeitet und verfasst habe und keine anderen als die angegebenen Hilfsmittel verwendet habe.

Berlin, den